THE UNIVERSITY OF CHICAGO

THE ROLE OF NITROGEN IN MEDIATING ALGAL-MICROBIAL INTERACTIONS IN A ROCKY INTERTIDAL ECOSYSTEM

A DISSERTATION SUBMITTED TO

THE FACULTY OF THE DIVISION OF THE BIOLOGICAL SCIENCES

AND THE PRITZKER SCHOOL OF MEDICINE

IN CANDIDACY FOR THE DEGREE OF

DOCTOR OF PHILOSOPHY

DEPARTMENT OF ECOLOGY AND EVOLUTION

BY

ORISSA MERRITT MOULTON

CHICAGO, ILLINOIS

AUGUST 2016

DEDICATION

For Jon, my most encouraging and inspirational colleague,
And for Emerson, who trusts us to explain his world.

TABLE OF CONTENTS

LIST OF TABLES

LIST OF FIGURES

LIST OF PLATES

ACKNOWLEDGEMENTS

First, I must acknowledge my advisor, Cathy Pfister, for trusting me to design and direct my PhD research remotely. As the crow flies, Sekiu and Friday Harbor, WA are close, but as the car drives and the ferries sail, they are not. I thank her for providing patient support and rapid feedback, and for allowing me to make decisions, make mistakes, and persevere to ultimately make sense of my data. Cathy's bravery in tackling really interesting questions with techniques that are foreign to many community ecologists has made her an exceptional role model. I am also thankful to my other committee members, Tim Wootton, Jack Gilbert, Greg Dwyer, and Maureen Coleman. Tim's expertise in ecological analysis has improved my data analysis and figure presentation immensely. Together, Cathy and Tim are generous with their time, their expertise, and their home. With his infectious enthusiasm for cool questions, Jack Gilbert has opened his lab and the world of microbial community ecology to me. Greg Dwyer and Maureen Coleman have provided terrific ecological and broadly scientific support and perceptiveness, from the messy and frustrating early stages of my project through to the conclusion, and I am grateful for their dedication and insight.

I want to thank the many other U. Chicago faculty and staff members who have shaped and supported me. As a repeat TA for Eric Larsen, I was inspired by his ability to incorporate storytelling into biological instruction; I thank him for driving me to always reach for the majors, the nonmajors, and the big picture in my instruction. Bonnie Brown, Connie Homan, Jeff Wisniewski, Melissa Lindberg, Diane Hall, Mary Johnson, Noami Perez, and Julie Steffen have taken care of countless financial and logistical details during my time in the department. Alison Anastasio, Libby Eakin, and Audrey Aronowski have been constantly available and extraordinarily competent with discussions of logistical details related to my PhD path, and I thank them for being wonderful role models and friends in this process. I am grateful to Dean Vicky Prince, who is an

important and supportive advocate for BSD graduate students, and a dedicated fellow equestrian always willing to talk about horses in addition to science.

My Pfister-Wootton lab mates, Aaron Kandur, Will Tyburczy, Sophie McCoy, Sara Jackrel, Courtney Stepien, Amy Henry, Simon Lax, Katherine Silliman, Shelly Stepien, John Park, and Mark Bitter, have provided a lab atmosphere of scientific curiosity and supportive friendship. The Darwinian Cohort of 2010 has provided me with a tremendous support network along the PhD path (e.g. **B**iological **A**colytes **D**iscussing **A**wesome **S**econd-year **S**tuff), but are are also some of the smartest people I've had the privilege to interact with. These many colleagues have driven me to be a better scientist, and I look forward to following their extraordinary careers for many years to come.

I had the good fortune to have hard-working, cheerful, clever, and entertaining field helpers in each summer of my field research. Gregor Siegmund was a tremendously good sport; his field summer corresponded with an extremely messy stage of my early project development, yet he persevered to not only help me advance my research but independently obtained his own data to produce a strong Honors Thesis. Annie Thomson, Karl Biederbeck, and Natalie Rivlin joined me in subsequent summer seasons, and were indispensable as we wrangled a tricky system, collected many samples, and kept a complicated mesocosm experiment running [mostly] smoothly. The University of Washington Friday Harbor Labs community welcomed me with open arms, and I will be forever grateful for the adventures had, friendships grown, and collaborations built in my four summers spent there. Special thanks to Alex Lowe, Hilary Hayford, Connie Sullivan, Misty Paig-Tran, Eric Anderson, Karen Ravensbergen, Tim Dwyer, Katie Dobkowski, Stephanie Crofts, Wendel Raymond, Becca Guenther, Laura Newcomb, Kristy Kull, Pema Kitaeff, Ericka Iyengar, Vik Iyengar, Megan Dethier, Paul Gabrielson, Breck Tyler, Aimee Urata, and Scott Swinge.

My decision to pursue a PhD had a foundation in my overwhelmingly positive experience as a Masters student at Oregon State University. My MS advisor, Sally Hacker, continues to be one of my most cherished professional and personal contacts, and I appreciate her important role in helping me ask good questions and pursue them creatively. Bruce Menge provided a warm welcome to the PNW rocky intertidal zone; he introduced me to the system he's spent decades getting to know, and pointed me towards the questions he still wonders about. The OSU ZoGrads, particularly Sarah Close, Margot Hessing-Lewis, and Phoebe Zarnetske, remain strong role models, colleagues, and friends.

My undergraduate experience at Wheaton College in Norton, MA convinced me that a small liberal arts college is a phenomenal community to be a part of, and that it's possible to make a career out of messing about in nature. I am grateful to the Wheaton College Biology Department, and faculty members in particular, Barbara Brennessel, John Kricher, Scott Shumway, and Shawn McCafferty, who were vitally important in pushing me to pursue field-based ecological research.

I am indebted to my parents for fostering my early explorations by making me play outside and giving me beautiful places to do just that. I thank them for their unwavering support in my eternal student-hood and unconditional pride. And finally, words can't fully capture my love for and gratitude to my husband, Jon Kay. I thank Jon for covering all the bases so many times in these past few years, especially as I traveled for field seasons (and recently in the push to the finish). He is my partner in all pursuits, an incredible father, and an inspiring scientist, and I am so happy to be sharing this adventure with him. Finally, I acknowledge Emerson Moulton Kay as the most significant and meaningful result of this dissertation.

- O. Moulton, 13 May 2016

CHAPTER I

INTRODUCTION

Indirect species interactions via nutrients that can limit productivity (Holt 1984; Miller 1994; Menge 1995) have the potential to affect ecosystems in ways that reverberate across multiple trophic levels (Croll *et al.* 2005). Although it is widely acknowledged that human activities have greatly reduced the biomass of large consumers (Jackson *et al.* 2001; Worm *et al.* 2006; Dirzo *et al.* 2014), we know little about how their loss has affected nutrient cycling and retention, though some calculations suggest a prominent role via lost excretion products. The positive interaction between nitrogen-excreting organisms and the primary producers that utilize nitrogen can be highly influential in community structuring (Bracken 2004; Pfister 2007). In North America's Pacific Northwest coastal areas, increased animal biomass is associated with increased sources of regenerated nitrogen in the form of ammonium (Pfister 2007; Pfister *et al.* 2007), and this animal-excreted nitrogen is also available to microbes. These processes, mediated via nitrogen, thus enhance the variety and types of species interactions we should expect in the nearshore. In this dissertation, I take experimental and observational approaches to determining the relative roles of microbial metabolism and primary productivity in the uptake and assimilation of locally regenerated animal-excreted nitrogen.

Plants require nitrogen (N), yet few can assimilate abundant atmospheric N (N_2). As such, N is a common limiting factor for plant growth in the ocean and on land (Hanisak 1979; Croll *et al.* 2005). In general, nearshore marine algae utilize three forms of N. Ocean subsidies deliver N as nitrate (NO_3^-) via upwelling processes, and this quantitatively dominates the total N-pool. Animals excrete ammonium (NH_4^+), and nitrifying microbial communities associated with animals utilize ammonium to produce nitrite (NO_2^-) and nitrate (Ward 2013). Assembling known interactions

builds a template for unknown interactions. Nitrification is a process that puts microbes in competition with algae for N. Despite the potential for competition between microbes and algae, empirical work suggests that algae benefit from animal-regenerated N (Bracken 2004; Pfister 2007) even in the presence of a rich microbial assemblage (Pfister *et al.* 2010), suggesting that microbes could also serve to facilitate algae via retention of N in a high-energy environment.

Nutrient availability can limit ecosystem productivity (Dugdale and Goering 1967), but ratios between nutrients may also mediate community structure (Sterner *et al.* 1996). Within natural ecosystems, cycling of carbon, nitrogen, and phosphorus are tightly coupled in relatively fixed proportions (C:N:P ~ 106:16:1) (Redfield 1934), and deviations from this ratio suggest biological interactions (Frost and Elser 2002a, b; Sterner and Elser 2002). Anthropogenic activities have altered all of Earth's major biogeochemical cycles; the total amount of circulating atmospheric N has increased by >100% since industrialization (Galloway *et al.* 2008; Elser *et al.* 2009; Fowler *et al.* 2013). Because coastal marine systems are N-limited, this has major implications for the temperate oceans, where atmospheric N deposition is leading to increased abundance in seawater (Kim *et al.* 2011). Increased atmospheric N is associated with anthropogenic activities, and the highest concentrations arise where human population density is high. Approximately 37-60% of the world's population lives within 100 km of the coast (Cohen 1997; Vitousek *et al.* 1997) at densities 2-3 times higher than the global average (Cohen 1997; Small and Nicholls 2003; Small and Cohen 2004).

DISSERTATION OVERVIEW

In this dissertation, I use a combination of laboratory mesocosm experiments, observational field surveys across spatial and temporal scales, and a manipulative field experiment to understand the role of animal-excreted ammonium in driving microbial and algal function in a rocky intertidal ecosystem. By studying the influence of naturally relevant ammonium concentrations on species interactions, I have assembled baseline data against which predicted environmental change can be compared.

Many coastal ecosystems are nitrogen limited. Nitrate is the quantitatively dominant form of dissolved inorganic nitrogen (DIN) delivered to intertidal biota from the oceanic water column but locally regenerated animal-excreted ammonium is another important DIN source. Both primary producers and chemolithotrophic microbes (bacteria and archaea) utilize ammonium. Through a series of outdoor mesocosm experiments (*Chapter II: Context-dependent algal-microbial competition for a shared nitrogen*) I isolated the interaction between marine phototrophs (algae) and benthic microbes in terms of ammonium. Experiments tested the hypothesis that the interaction between benthic microbes and primary producers is bidirectional and context-dependent. Results indicate that phototrophs and microbes compete for the shared resource of ammonium: periphyton blooms limited microbial nitrogen use, and microbial biofilms affected macroalgal growth. Data presented in this chapter provide a baseline for potential range of a simplified natural interaction between algae and microbial biofilms that could be expected in natural systems. Microbial-algal interactions likely play an important role in net community interactions, a link will improve community structuring models.

Determinants of microbial community structure in aquatic environments remain poorly understood. In rocky shore environments, microbes might be influenced by both local abiotic and

biotic factors, as well as larger-scale physical drivers. In *Chapter III: Drivers of variability among NE Pacific rocky intertidal microbial communities,* I used spatially and temporally broad field surveys and characterized microbial community composition and structure from a rocky intertidal benthic biofilm across four sites and two years to address three questions: 1) Within a site (<100m), do benthic surfaces of tidepools and emergent rock host distinct microbial communities? 2) Do intertidal microbial communities vary on a regional scale (>25km), between sites? 3) Are microbial communities temporally stable? I sequenced microbial communities cultured *in situ* on replicated artificial surfaces deployed May-August in 2013 and 2014 at four southwest-facing sites in the San Juan Islands, WA, USA on both emergent rock and in permanent tidepools. Simultaneous with microbial community analysis, I quantified neighboring macrobiota and local environmental variables. Results from this chapter indicate strong local control of microbial community composition. Microbial communities were highly differentiated between habitat types (tidepools, emergent rock). Several phototrophic cyanobacteria were tightly associated with emergent substrate, suggesting that temperature, desiccation, and light are strong drivers of community variability. Despite variation in macroscopic community composition, sites hosted only weakly differentially structured microbial communities. Taken together, these results indicate intersite (>25km) homogeneity of intertidal microbial communities present in biofilm, with overwhelming intrasite (between-habitat; <100m) heterogeneity. I observed community turnover on a coarse annual scale (August 2013 to August 2014), with maintenance of source habitat identity. Although distribution of microbial taxa was broadly regional, microbial community structure in this NE Pacific rocky intertidal system was strongly environmentally selected.

Growth of primary producers is often limited by the single factor necessary for growth that is available in shortest supply; a single limiting factor can limit the distribution and productivity of

an entire guild of organisms. In the nearshore and intertidal environment, nitrogen limitation can be ameliorated by animal regenerated ammonium, but algae and ammonia oxidizing benthic microbes compete for this shared resource. In *Chapter IV*: *Algal-microbial response to rocky intertidal ammonium availability*, I used field dispensers to elevate ammonium several times above ambient levels at sites with measured differences in animal composition, testing the hypothesis that ammonium availability drives algal and microbial function in a temperate rocky intertidal system. I queried whether elevated ammonium gets immediately incorporated into local microbes and phototrophs, and whether a site with elevated animal abundance (and animal-excreted ammonium) leads to a microbial community that utilizes this ammonium, looking at microbial identities and associated genes. Our simulated animal regenerated ammonium drove microbial community structure to resemble that in naturally high ammonium tidepools, but only at our low-animal site. Macroalgae did not utilize our experimentally elevated ammonium, but the photosynthetic biofilm did show an ammonium treatment response that was strongest at the low-animal site. This study contributes to better prediction of the consequences of human-induced changes in nutrient cycles in the productive temperate rocky intertidal habitat.

Understanding the interaction between microbes and algae in systems with varied natural and enhanced levels of N will help guide coastal management. Microbial composition and function has been largely ignored in studies of rocky shore community assembly. Through observational and empirical investigations, this dissertation quantifies how microbes contribute to rocky shore productivity via interactions with ammonium-excreting animals, the microbial potential to retain N in coastal waters, and human impacts (e.g., harvest of marine fauna, terrestrial agriculture).

In *Chapter V: Microbial associations with macrobiota in coastal ecosystems: patterns and implications for nitrogen cycling* (written collaboratively), I (along with my coauthors) present a

broadened view of interactions between macrobiota and associated microbial communities. Although macrobiota can have significant effects on nitrogen cycling via excretion by macrofauna and assimilation by macroflora, many macrobiota also host or facilitate microbial taxa responsible for nitrogen transformations. This is an area of expanding interest in coastal marine systems, where nitrogen is a limiting nutrient. Our understanding of the diversity of microbes associated with coastal marine animals and macrophytes is increasing, and recent studies indicate that the microbiomes of macrobiota may directly contribute to nitrogen cycling. In this chapter, we review the roles that macrobiota play in coastal nitrogen cycling, appraise current understanding of macrobial-microbial associations in terms of nitrogen processing, and suggest implications for coastal ecosystem function as animals are harvested and foundational habitat is lost or degraded. Given the biodiversity of microbial associates of macrobiota, we advocate increased research into the functional consequences of these associations for the coastal nitrogen cycle.

CHAPTER II

CONTEXT-DEPENDENT ALGAL-MICROBIAL COMPETITION FOR A SHARED NITROGEN RESOURCE

ABSTRACT

Many coastal ecosystems are nitrogen limited. Nitrate (NO_3^-) is the quantitatively dominant form of dissolved inorganic nitrogen (DIN) delivered to intertidal biota from the oceanic water column but locally regenerated animal-excreted ammonium (NH_4^+) is another important DIN source. Both primary producers and chemolithotrophic microbes (bacteria and archaea) utilize NH_4^+. Through a series of outdoor mesocosm experiments, this study isolates the interaction between marine phototrophs (algae) and benthic microbes in terms of NH_4^+. Experiments using artificial NH_4^+ elevation and nitrogen isotope tracers tested the hypothesis that the interaction between benthic microbes and primary producers is bidirectional. Phototrophic algal and chemolithotrophic microbial responses indicate that algae and microbes compete for the shared resource of NH_4^+: periphyton blooms limited microbial nitrogen use, and microbial biofilm decreased macroalgal growth, but these competitive interactions were dependent upon the addition of NH_4^+. Our results suggest that competitive interactions between algae and microbial biofilm in natural systems are bidirectional and context-dependent; specifically, each interaction was apparent only under high NH_4^+ resource conditions. Benthic microbes responded competitively to periphyton presence. High light conditions that benefit phototrophic eukaryotes drove the microbial response, and it is possible that phototrophic microbes outcompeted chemolithotrophic genera for the NH_4^+ resource. Though microbial community structure was driven by NH_4^+ availability and periphyton presence interactively, nitrogen-metabolizing gene

counts were not different among NH_4^+ treatments and may reflect the need to query functional responses with other methodologies. Broadly, microbial-algal competitive interactions likely play an important role in net community interactions, the fixation of carbon, and the fate of nitrogen.

INTRODUCTION

In both aquatic (Howarth 1988) and terrestrial (Vitousek 1984) nutrient-limited systems, non-trophic interactions can be strongly influential in community structuring. For example, the positive effect of nitrogen regeneration or excretion by consumers can significantly increase primary productivity (McNaughton 1985; Croll *et al.* 2005). Croll *et al*. (2005) show that introduced predatory foxes, by predation on naïve seabirds, thwart transport of nutrients between marine and terrestrial systems. Seabirds normally shuttle marine nutrients to terrestrial systems, so their reduction transformed native grassland to relatively plant depauperate tundra. The identity and strength of nontrophic forces driving community structure in the marine nearshore, a typically nitrogen-limited system, is an important consideration in our assessment of animal effects in ecosystems (Howarth and Marino 2006).

Nitrogen is delivered to the intertidal via upwelling in the form of nitrate (NO_3^-), and the relationship between NO_3^- availability and the growth of marine algae fluctuates in predictable ways within seasonal upwelling regions like the temperate coastal northeast Pacific Ocean (Fujita *et al.* 1989; Menge *et al.* 1997; Chavez *et al.* 2002; Corwith and Wheeler 2002). However, animal excreta is high in nitrogen, and this localized nutrient recycling process can contribute significantly to the total available nitrogen pool at a given location. Rocky intertidal invertebrates excrete water-soluble NH_4^+ (NH_4^+) and urea ($(NH_2)_2CO$), and excretion rates by

several marine taxa (Jensen and Muller-Parker 1994; Bracken 2004) paired with experimental work within tide pools (Pfister 2007) and on wave-exposed, emergent mussel beds (Aquilino *et al.* 2009) suggest that excreted NH_4^+ can contribute significantly to nitrogen needs of marine algae (Pather *et al.* 2014; Pfister *et al.* 2016). NH_4^+ excretion by animals increases availability of biologically accessible nitrogen, and subsequent primary production at a local scale (Wootton 1991; Asmus and Asmus 1991; Taylor and Rees 1998; Plaganyi and Branch 2000; Bode *et al.* 2004; Bracken 2004; Bracken and Nielsen 2004a).

Though the interactions, including competition, among macrobiota on coastal rocky shores are well-known (Connell 1961a, b; Paine 1966, 1969; Dayton 1971; Menge 1972; Menge and Menge 1974; Hillebrand and Sommer 2000; Worm *et al.* 2000), our understanding of microbial community structure and microbial metabolic capabilities in this environment remain nascent. Marine phototrophs (algae and angiosperms such as seagrasses) require nitrogen, yet cannot fix abundant atmospheric nitrogen (N_2) and are thus often limited by this nutrient (Hanisak 1979; Howarth and Marino 2006) . Although NO_3^- is often relatively abundant in oceanic upwelling regions and quantitatively dominates the coastal nitrogen pool, phototrophs show relative preference for NH_4^+ in nitrogen uptake because it is energetically favorable (Ryther *et al.* 1981; Dortch 1990; Bracken and Stachowicz 2006). Microbial nitrifiers are obligate NH_4^+ consumers (Spencer 1956). Animal-excreted NH_4^+ might thus be a contested resource for both phototrophs and chemolithotrophic microbes. Prior experiments indicate that tide pools with mussels have both higher nitrification rates and higher algal growth rates (Pfister 2007), suggesting that both algae and microbial nitrifiers benefit from increased animal-sourced nitrogen, and that nitrification does not inhibit algal growth. Yet untested is the competitive interaction between

primary producers and N-cycling microbes for the metabolically important NH_4^+ nutrient resource.

Recent studies indicate that microbial utilization of nutrient resources in coastal systems is of high importance. Microbial transformations of nitrogen can equal or exceed contributions of phototrophs (algae and seagrasses) to nitrogen dynamics in coastal marine systems (Pfister *et al.* 2016). Pfister and colleagues (2016) estimate that microbial processing is responsible for 8-61% of total NO_3^- uptake attributed to microbes and phototrophs combined, and an average 32% of NH_4^+ flux in northeast Pacific tide pools containing NH_4^+-excreting mussels. It is likely that the interaction between microbes and phototrophs in this system generally is dependent on nitrogen availability, a limiting resource, but with NH_4^+ availability playing a singular role. This type of context-dependent competitive interaction in terms of nutrient resources has been shown repeatedly in terrestrial systems (Wilson and Tilman 1991, 1993; Chamberlain *et al.* 2014).

This study reports experiments isolating the interaction between marine phototrophs (algae) and benthic microbes in terms of NH_4^+, a shared nutrient resource, in outdoor laboratory mesocosms maintained under ambient climate conditions. Experiments tested the hypothesis that the interaction between benthic microbes and primary producers is bidirectional and dependent on NH_4^+ availability, specifically examining: A) the effects of phototrophs and seawater NH_4^+ addition on microbial biofilm structure and function; and B) the effect of microbial biofilm abundance and seawater NH_4^+ addition on a target phototroph (**Figure 2.1**). These experiments tested the net interaction between benthic microbes and phototrophs under abundant NH_4^+ conditions, such as those that occur in animal-inhabited intertidal zones (Bracken 2004; Pfister 2007; Pather *et al.* 2014), as well as the variability of microbial NH_4^+ use in response to competition from primary producers (**Figure 2.1**).

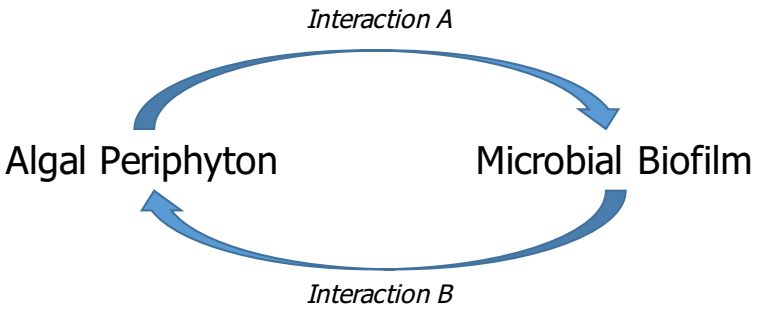

Hypothesized Interaction Process	Predicted Supporting Evidence
A1. Algae utilize ammonium resource	Seawater ammonium drawdown by elevated algae; Increased algal productivity under elevated ammonium
A2. Algae compete with microbes for ammonium resource	Decreased microbial nitrification under elevated algae
B1. Microbes utilize ammonium resource	Seawater ammonium drawdown by elevated microbes; Increased nitrification under elevated ammonium
B2. Microbes compete with algae for ammonium resource	Decreased algal productivity under elevated microbes

Figure 2.1. A model for the bidirectional algal-microbial interaction in terms of a shared nutrient resource, NH_4^+. Both sides of this model are explicitly addressed in this study, with focal hypotheses that phototrophs influence microbial NH_4^+ use (arrow A) and microbial biofilm influences algal NH_4^+ use (arrow B).

MATERIALS AND METHODS

Study system, and overview of experimental design

Two parallel mesocosm experiments were conducted to evaluate hypothesized competitive interactions between algal periphyton and benthic microbes in response to elevated NH_4^+, the N-form excreted by fauna: Interaction A, the influence of microbial presence on algal nitrogen use, and Interaction B, the influence of algal presence on microbial nitrogen use (**Figure 2.1**, **Table 2.1**). Use of two manipulative experiments permitted isolation of each interaction via

two levels of algal periphyton abundance and two levels of microbial biofilm abundance separately, with each experiment conducted with two levels of NH_4^+ addition. Mesocosms allowed us to use parallel experiments to test whether NH_4^+ was a driver of both microbial and phototropic community compositions. To robustly address the bidirectional interaction, each biotic component was manipulated in a two-way experiment, allowing reciprocal isolation of each biotic variable.

Both sets of experimental mesocosm manipulations were conducted in four identical seawater tables (shallow flow-through tanks) at Friday Harbor Laboratories (48°33'N, 123°00'W) with inflow lines from a shared seawater pipe. Except where shading was applied to reduce periphyton amount (Interaction A experiment), tables were subject to ambient light, air temperature, and precipitation conditions. Seawater table outflow occurred at vertical standpipes at opposite ends of each table from inflow line. Within each table, an array of 8 4.5L mesocosm tubs was established. Tall standpipes (4 cm above lip of mesocosm tubs) maintained connectivity among tubs for 22 h/day. Manual switching to short standpipes (2 cm below lip of tub) allowed for separation of mesocosms into eight distinct experimental units within the four seawater tables. Experiments varying algal periphyton and microbial biofilm were both conducted under varying levels of NH_4^+ addition. During the daily 2 h period of mesocosm separation, NH_4^+ (aqueous NH_4Cl) addition was conducted as a pulsed daily treatment (2 h/day) to mimic simplified tide pool dynamics. Repeated daily over each experimental period, this pulsed mesocosm isolation and NH_4^+ addition treatment served as a conditioning period for biotic components (microbial biofilm, algal periphyton) of each mesocosm.

All experiments utilized a 2x2 factorial design (**Table 2.1**), with two levels of NH_4^+ addition and two levels of a biotic variable (described below). As such, unless otherwise

described, response variables measured at the conclusion of each experimental conditioning period were analyzed with two-way ANOVA in R (R Core Team, 2015). Microbial sequence data were analyzed following multivariate techniques described in greater detail below.

Table 2.1. Two 2x2 factorial designs for mesocosm experiments testing bidirectional algal-microbial interaction in terms of NH_4^+ availability: Interaction components tested are 1) effect of microbial biofilm on algal periphyton, and 2) effect of algal periphyton on microbial biofilm, both under variable NH_4^+ conditions.

Interaction Tested	Treatment	Biotic Variable	Relative Ammonium Addition
A. Effect of algae on microbial biofilm	A.1	Ambient periphyton	Ambient NH_4^+
	A.2	Reduced periphyton	Ambient NH_4^+
	A.3	Ambient periphyton	Elevated NH_4^+
	A.4	Reduced periphyton	Elevated NH_4^+
B. Effect of microbial biofilm on algae	B.1	Elevated microbial biofilm	Ambient NH_4^+
	B.2	Ambient microbial biofilm	Ambient NH_4^+
	B.3	Elevated microbial biofilm	Elevated NH_4^+
	B.4	Ambient microbial biofilm	Elevated NH_4^+

Microbial biofilm and algal periphyton cultivation

For both experiments, microbial biofilm and benthic periphyton were collected on replicated units of inert artificial substrate.

Microbial biofilm was elevated and collected on high surface area 1” round, sinking plastic BioBalls (Coralife ®) housed within perforated 18” lengths of 1.5” interior diameter opaque flexible plastic drainage tubing sealed at ends with zip ties (30 BioBalls/length of drainage tubing). This provided a low light environment to limit phototrophic growth, but allowed free flow of seawater and microbial colonization. Prior to loading into perforated drainage tubing, BioBalls were placed in weighted 1.5cm plastic mesh bags and attached to the

Friday Harbor Laboratories' dock at 5' depth for 30 days to promote seeding by the community of microbes local to the laboratory seawater system.

Benthic periphyton was grown on standard glass microscope slides (75mm x 25mm) arranged in alternating slots in open plastic slide cases. Slide cases filled with 6 clean slides were submerged into mesocosms on Day 1 of each experiment, and each slide served as a replicate periphyton quantification unit within the mesocosm at each experiment's termination. The dominant fouling organism in the periphyton community was the chain diatom *Fragilaria*, characterized by rapid growth in slow flow, high light, low herbivory marine environments.

Preconditioning: Influence of microalgae on microbial nitrogen use and influence of microbial biofilm on microalgal growth when NH_4^+ differs

Microalgal periphyton density was varied by allowing ambient light (ambient periphyton) or blocking light with plywood (reduced periphyton). Plywood tank covers effectively blocked light from designated low-light treatments (99.7% light intensity reduction; average light intensity reduction in shade = 5361 lux), but due to the flow-through nature of seawater tables, temperature was not highly influenced by this application of shade treatment (2.4% temperature reduction; average temperature reduction in shade = 0.3°C). In ambient diatom treatments, algae were allowed to accumulate in mesocosms for 2 weeks prior to the start of experimentation. When shaded, accumulated mass of diatoms and other biofilm components was reduced by 96.7% (measured as dry mass). The mesocosm community was conditioned via daily isolation of all mesocosms from the flow-through seawater tables, and NH_4^+ additions in via syringe addition of 20mL of aqueous 1.5M NH_4Cl at the start of each 2hr treatment period, raising mesocosm

NH_4^+ concentration in NH_4^+ addition treatments to 60μM. This conditioning treatment array was maintained from 9 June to 2 July 2014 (24 days).

A second, parallel mesocosm experiment was conducted to test the influence of microbial biofilm on algal use of NH_4^+ (**Figure 2.1**). Microbial density was varied (elevated versus ambient) by increasing the amount of colonized substrate surface area using BioBalls. Elevated microbial density mesocosms contained locally seeded BioBalls that grew freely, while BioBalls in ambient microbial abundance mesocosms were replaced with clean, non-seeded BioBalls daily. As above, NH_4^+ was varied via daily 2h addition of concentrated synthetic aqueous NH_4Cl in 4.5L mesocosms. Here, NH_4^+ concentration in NH_4^+ addition treatments was elevated to 1000 μM to ensure resource surplus for microbial nitrifier activity. This conditioning treatment array was maintained from 4-10 August 2013 (7 days).

Abiotic and biotic response variables were measured at the end of the 2h incubation period on the final day of each conditioning period, including DIN, algal periphyton biomass, stable isotopes in algal periphyton tissue, algal periphyton chlorophyll *a* concentration, and microbial community structure.

Terminal experiments and response measurements

At the conclusion of the conditioning period associated with each mesocosm experiment, a terminal experimental NH_4^+ addition incubation was performed and paired with response variable sampling. This terminal treatment period took place on experimental day 24 in the experiment where periphyton density differed, and on experimental day 7 in the experiment varying microbial density.

To collect samples for seawater DIN analysis, water was syringe-filtered (Whatman glass-fiber filter GF/C) into separate acid-washed 60mL high-density polyethylene bottles, and frozen (-20°C) prior to analysis. Nutrient concentrations (ammonium (NH_4^+), nitrite (NO_2^-), nitrate (NO_3^-)) were measured at the University of Washington Marine Chemistry Laboratory (methods from UNESCO 1994).

Periphyton abundance and productivity was measured via dry biomass and chlorophyll *a* concentration. For each parameter, a fouled slide was selected at random and fully scraped with a 1" razor blade into a preweighed foil packet for dry biomass and into a 1mL plastic vial for chlorophyll *a* analysis. Samples for dry biomass were dried at 60°C for 48h and reweighed. Samples for chlorophyll *a* were kept in the dark following collection, and were frozen (-20°C) prior to extraction. Chlorophyll *a* in periphyton was measured following spectrophotometric methods modified from Sterman (1988) for use on benthic rather than water column samples; here, periphyton from a known surface area (two sides of a standard 75mm x 25mm microscope slide; 37.5cm^2) was scraped and extracted in 10 ml of acetone. Concentration of chlorophyll *a* (μg chl/mL extract) was calculated with equations from Jeffrey and Humphrey (1975).

Periphyton samples for elemental and isotopic analysis were collected from microscope slides within each mesocosm at the start and end of each conditioning period. Periphyton samples were collected by scraping both sides of a single slide with a razor blade into pre-weighed foil packets, dried at 60°C for 48h, and stored at room temperature. Dried samples were ground in 1mL rubber capped tubes containing a 3mm ball bearing using a GenoGrinder®. Elemental and isotopic analyses (%N, %C, $\delta^{15}N$, $\delta^{13}C$) were made at the University of Chicago Stable Isotope Facilities using a Costech 2010 Elemental Analyzer combustion system coupled to a Thermo DeltaV Plus IRMS via a Thermo Conflo IV interface.

The terminal 2-hour experimental NH_4^+ incubation period and response sampling described above was performed for both competition experiments. To further probe the mechanistic influence of elevated periphyton density on microbial processing of the NH_4^+ resource, ^{15}N-enriched NH_4^+ was also added to individual mesocosms in a stable isotope tracer enrichment experiment. In each mesocosm, benthic periphyton (primarily the diatom genus *Fragilaria*) was present at 'natural' abundance via ambient light or nearly eliminated via shaded light. Prior to the terminal experimental NH_4^+ incubation and ^{15}N-enriched tracer addition to mesocosms, 100mL of mesocosm water was syringe-filtered (Whatman glass-fiber filter GF/C) into separate HDPE bottles as a record of natural abundance $^{15}NH_4^+$ and for nutrient concentration determination. ^{15}N enriched ammonium chloride (^{15}N-NH_4Cl) was then added to separated mesocosms in a simultaneous manner with daily nutrient addition to approximate a 1000‰ enrichment assuming ambient NH_4^+ treatment mesocosms $[NH_4^+]$ = 1.24 μM and elevated NH_4^+ treatment mesocosms $[NH_4^+]$ = 60.00 μM. Tracer and nutrient additions were immediately stirred. Tracer additions had a negligible effect on overall NH_4^+ concentrations. Water samples were immediately collected for measuring initial ^{15}N enrichment, then at 2h to determine dynamics of isotopes of N and seawater nutrients.

The transfer of enriched ^{15}N to nitrite (NO_2^-) and nitrate (NO_3^-) pools was estimated by measuring $^{15}N_{NH4+}$, $^{15}N_{NO2-}$ and $^{15}N_{NO3}$. Isotopic composition was determined via a sodium azide – acetic acid reaction method (McIlvin and Altabet 2005). This method converts NO_2^- to N_2O before analysis on an isotope ratio mass spectrophotometer (IRMS). Reference materials were used to standardize results, as in (McIlvin and Altabet 2005).

To measure NH_4 isotopic composition, NH_4 was oxidized to hypobromite then reduced to N_2O using acetic acid-buffered sodium azide before IRMS analysis (Zhang *et al.* 2007). Samples

Plate 2.1. Presidential greetings are an important and persistent pattern in the development of intertidal community ecologists (e.g. Dayton 1970). Here, future President Hillary Rodham Clinton (right) visited the author's (center) hometown in 1996 to wish her well on her pathway towards a doctoral degree.

were diluted to <500‰ to avoid isotopic contamination of the natural-abundance level mass spectrophotometer. The Zhang et al. (Zhang *et al.* 2007) procedure was modified in two ways, following Pather et al. (Pather *et al.* 2014): Briefly, preexisting NO_2^- was removed prior to hypobromite addition by reaction with sulfamic acid, and 6mol L^{-1} HCl was added to reduce the pH of the sample below 7.0 prior to the addition of an azide-100% acetic acid reagent. Data were calibrated using a standard curve derived from co-analysis of international standards per Zhang *et al.* (Zhang *et al.* 2007).

All seawater isotope analyses were conducted at University of Massachusetts Dartmouth using a CV IsoPrime IRMS, a custom purge-trap sample preparation system, and a CTC PAL autosampler.

The rate of microbial NH_4^+ oxidation to NO_2^- (µmol L^{-1} hr^{-1}) in mesocosms was calculated using NH_4^+ and NO_2^- isotopic ratio values (‰) and concentration values (µM) at the initial and final time points of the 2h $^{15}NH_4$ tracer and NH_4Cl incubation period. This calculation utilized **Equation 2.1** (modified from Lipschultz (2008), where *R* is the atom% ratio of $^{15}NO_2^-$ or $^{15}NH_4^+$ x 100, $\overline{[NO_2]}$ is the mean NO_2^- concentration measured over the terminal 2-hour incubation experiment (µM), and *t* is 2h).

$$\mathrm{NH_4^+ Oxidation\ Rate} = \frac{(R_t NO_2 - R_0 NO_2)}{(R_t NH_4 - R_0 NO_2) \times \Delta t} \times \overline{[NO_2]} \qquad \text{Equation 2.1}$$

Although animals were omitted from the mesocosm community and their effects were instead mimicked via synthetic aqueous NH_4Cl additions, it is likely that small invertebrates entered mesocosms through laboratory seawater inflow lines and colonized both BioBalls and mesocosm periphyton blooms. The rate of NH_4^+ remineralization (µmol L^{-1} hr^{-1}) in each

mesocosm was quantified by estimating isotopic dilution, using the $^{15}N\text{-}NH_4^+$ signal in seawater at the initial and final time points of the terminal experimental 2h $^{15}NH_4$ tracer and NH_4Cl incubation period. The remineralization rate was calculated using **Equation 2.2** (reproduced from Pather and colleagues (2014), where $-b$ is the exponential decay constant determined from an exponential fit to the isotopic dilution data at times 0h and 2h ($y = ae^{-bx}$, where $y = \delta NH_4^+$ (‰), x = time (h), and a and b are fitted parameters) and $\overline{[NH_4]}$ is the mean NH_4^+ concentration (in μM) measured over the terminal 2-hour incubation experiment.

$$NH_4^+ \text{ Remineralization Rate} = |-b| \times \overline{[NH_4^+]} \qquad \text{Equation 2.2}$$

The assumption of constancy in b was supported by R^2 values > 0.9 for exponential fits of data from a similarly conducted tide pool tracer enrichment experiment (Pather et al 2014).

Microbial community analysis

To query whether microbial community structure differed in ambient and elevated NH_4^+ addition treatments, 3 BioBalls per experimental mesocosm were stored at -80°C at the end of the 24-day conditioning period and final nutrient addition and isotope tracer experiment. Biofilm DNA was extracted using a PowerSoil kit (MoBio™). For each sample, material was sampled off of three replicate BioBalls per mesocosm using sterile cotton swabs, which were then placed in PowerSoil PowerBead tubes. Subsequent extraction followed the PowerSoil protocol. The PCR amplification protocol followed Caporaso et al. (2010a) for multiplexing 16S rRNA samples. PCR products were cleaned with MoBio™ UltraClean htp PCR Clean-up kit. The V4 variable region of the 16S rRNA gene was amplified from community DNA using bar-coded

primers according to Earth Microbiome Project standard protocols (Caporaso *et al.* 2012a), yielding paired-end sequence data.

Sequence data were analyzed via QIIME (v. 1.9.1, Quantitative Insights into Microbial Ecology) to filter reads and identify OTUs as described in Caporaso et al. (2010b). Briefly, the script for open reference OTU picking (pick_open_reference_otus.py) was applied to raw data, which clustered sequence data with the Greengenes database (May 2013) at the 97% similarity level for OTU identification, then performed *de novo* clustering of taxa that did not align with the database. Chloroplast and singleton sequences were removed prior to downstream analyses. Representative sequences for each OTU were aligned using PyNast, with a minimum alignment overlap of 75 base pairs (Caporaso *et al.* 2010a). Diversity metrics between NH_4^+ treatments were computed using the QIIME core_diversity_analyses.py script in QIIME, which generates alpha diversity metrics and beta diversity distances between samples, and to build principal component (PCoA) plots, which accounted for both phylogenetic composition (Lozupone *et al.* 2011) and relative abundance of taxa among samples. All samples were analyzed at the lowest sequencing depth of included samples for these diversity analyses.

To test for significant sample groupings by NH_4^+ treatment based on these distance metrics, ANOSIM was conducted in QIIME using the compare_categories.py script. This test compares the mean of ranked dissimilarities between groups to the mean of ranked dissimilarities within groups in multivariate data, yielding a test statistic, R, and a p-value. The group_significance.py script was applied to test whether presence of specific OTUs differed significantly between NH_4^+ treatments using a G test. The G test of independence determines whether OTU presence/absence is associated with a category (e.g. NH_4^+ treatment) using a Bonferroni-corrected ANOVA analysis procedure.

To test whether microbial taxa in BioBalls incubated at varying levels of NH_4^+ were associated with particular nitrogen metabolism pathways, the software package PICRUSt (Phylogenetic Investigation of Communities by Reconstruction of Unobserved States) was used to query predicted functional capacity of the communities (Langille *et al.* 2013). PICRUSt estimates the gene families based on a predicted metagenome from bacteria or archaea identified via 16S rRNA sequencing. Prior to performing the PICRUSt procedure, the script for closed reference OTU picking (pick_closed_reference_otus.py) was applied to raw 16S rRNA sequence data, which clustered sequence data with the Greengenes database (May 2013) at the 97% similarity level for OTU identification, ignoring taxa that did not align with the database. Chloroplast and singleton sequences were removed prior to PICRUSt analyses. A list of genes associated with particular nitrogen metabolisms was created using the KEGG orthology database (Kyoto Encyclopedia of Genes and Genomes; (Kanehisa *et al.* 2016)) (**Table 2.A.1**), and R (R Core Team, 2015) was used to generate counts and percent abundance contributions of each metabolism associated with each sample and compare mesocosm treatment categories.

RESULTS

The influence of periphyton on microbial N-processing depends on NH_4^+ *addition*

Experimental manipulation of NH_4^+ and periphyton suggested that presence of periphyton reduces microbial nitrogen-processing function. Change in dissolved inorganic nitrogen (DIN; NH_4^+, NO_2^-, NO_3^-) conditions from ambient mesocosm levels prior to pulsed experimental conditioning to final measurement at the end of the NH_4^+ addition period on experimental day 24 showed an increase in NH_4^+ when it was experimentally added, and a drawdown when periphyton was present (**Figure 2.2A, Table 2.2**). NH_4^+ addition to high NH_4^+ mesocosms was

equal among replicates, but concentrations were reduced with high periphyton treatment, suggesting phototrophic uptake of this resource. NO_2^- concentration decreased in all treatments (**Figure 2.2B**), but was greatest in the high periphyton-ambient NH_4^+ treatment, and least when in low periphyton treatments (**Figure 2.2B, Table 2.2**), suggesting that any NO_2^- produced via nitrification is utilized within mesocosms, and that periphyton is responsible for much of this uptake. NO_3^-, the second product of nitrification, was generated in both low periphyton treatments, with a ~8 μM decrease in high periphyton treatments (**Figure 2.2C**). In low NH_4^+ treatments, NO_3^- drawdown from initial conditions was strongest in the presence of abundant ambient periphyton.

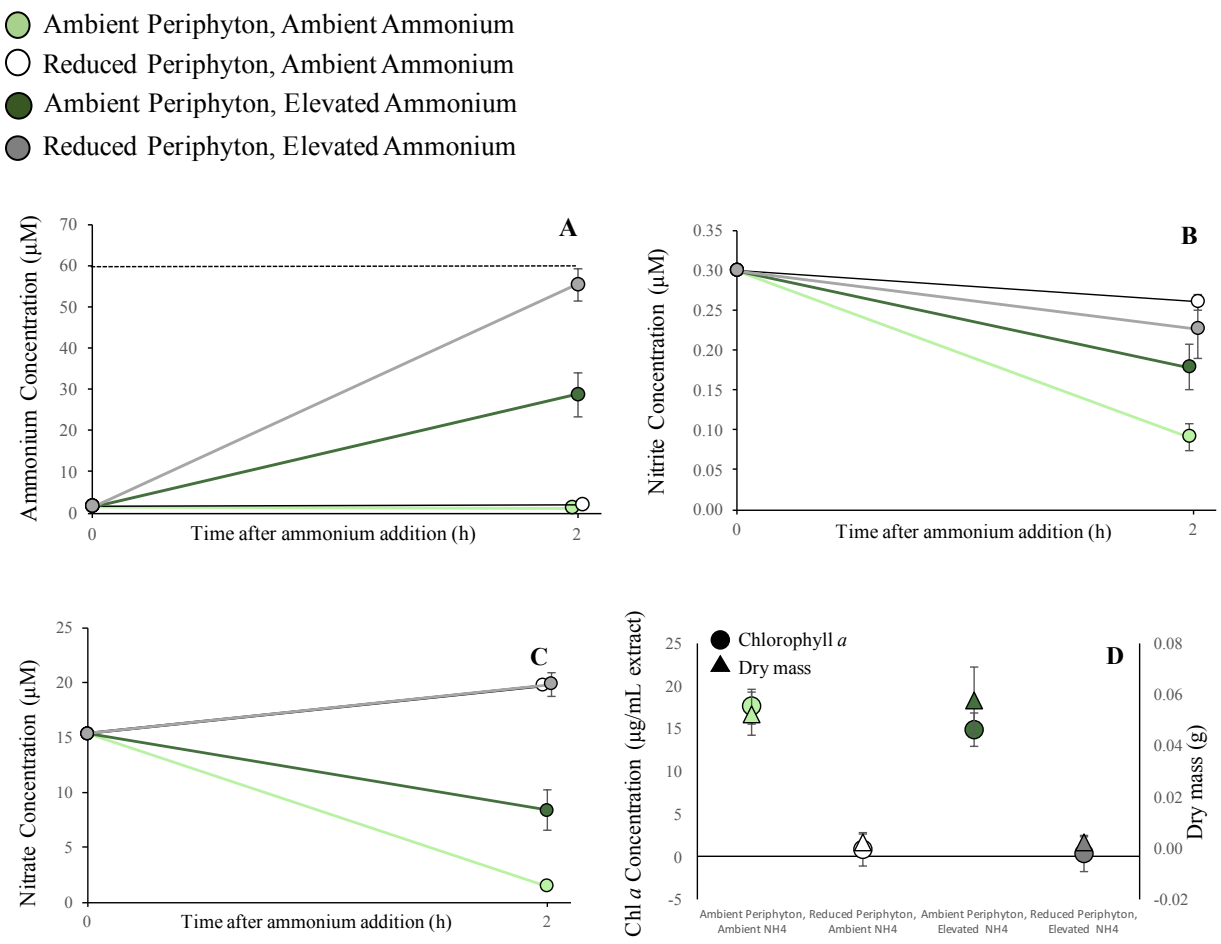

Figure 2.2. Responses to periphyton abundance and NH_4^+ addition in experimental mesocosms. **A**. [NH_4^+] (µM), **B**. [NO_2^-] (µM), **C**. [NO_3^-] (µM)), and **D.** periphyton chlorophyll *a* (µg/mL extract) and dry biomass (g/slide). DIN data are change from initial concentration prior to the treatment period on experimental day 1 to final concentration at the conclusion of 2h incubation treatment period on day 24. Horizontal dotted line on panel A indicates NH_4^+ addition level. Periphyton data are from samples scraped from both sides of a fouled microscope slide at the end of 2h incubation period on day 24. All data are treatment means $\pm$ SE. Statistical test results (two-way ANOVA) are reported in **Table 2.2.**

Table 2.2. Statistical test results for seawater nutrient and periphyton responses to manipulated periphyton density and NH_4^+ addition in experimental mesocosms. Tabled values are two-way ANOVA results. Means (+/- SE) for these findings are displayed in **Figure 2.2**.

Response Variable	Periphyton Density	NH_4^+ Addition	Periphyton Density * NH_4^+ Addition
Δ Seawater [NH_4]	$F_{1, 27} = 13.05$ **p = 0.001**	$F_{1, 27} = 148.40$ **p < 0.001**	$F_{1, 27} = 15.43$ **p < 0.001**
Δ Seawater [NO_2]	$F_{1, 27} = 20.89$ **p < 0.001**	$F_{1, 27} = 1.35$ p = 0.26	$F_{1, 27} = 6.38$ **p = 0.02**
Δ Seawater [NO_3]	$F_{1, 27} = 181.82$ **p < 0.001**	$F_{1, 27} = 10.90$ **p = 0.003**	$F_{1, 27} = 9.67$ **p = 0.004**
Periphyton Chl *a*	$F_{1, 28} = 101.79$ **p < 0.001**	$F_{1, 28} = 1.10$ p = 0.30	$F_{1, 28} = 0.49$ p = 0.49
Periphyton dry biomass	$F_{1, 28} = 42.88$ **p < 0.001**	$F_{1, 28} = 0.10$ p = 0.76	$F_{1, 28} = 0.10$ p = 0.76
Periphyton %N	$F_{1, 11} = 42.74$ **p < 0.001**	$F_{1, 11} = 0.14$ p = 0.72	$F_{1, 11} = 0.08$ p = 0.79
Periphyton %C	$F_{1, 11} = 120.42$ **p < 0.001**	$F_{1, 11} = 0.002$ p = 0.96	$F_{1, 11} = 0.08$ p = 0.78

Periphyton growth and productivity varies with light, not nutrient availability

Although seawater nutrient analysis indicated rapid uptake of supplemental NH_4^+ by periphyton in elevated NH_4^+ treatments, periphyton biomass, chlorophyll *a*, and periphyton elemental isotope analysis indicated that these phototrophs were not NH_4^+ limited in the mesocosm system. Periphyton biomass and chlorophyll *a* in ambient light (high periphyton) conditions were strongly elevated relative to shaded light (reduced periphyton) conditions (5 fold increase in biomass, 30 fold increase in chlorophyll *a*), with no effect of NH_4^+ (**Figure 2.2D**, **Table 2.2**). Similarly, analysis of elemental composition of periphyton under ambient light conditions revealed a 1.5% increase in percent nitrogen and 15% percent increase in carbon

relative to shaded (reduced periphyton) treatments, with no response to NH_4^+ availability (**Table 2.2**).

Microbial biofilm and periphyton nutrient use driven by NH_4^+ resource availability

Experimentally added NH_4^+ resource was utilized by both microbial biofilm and periphyton. Nitrification (microbial NH_4^+ oxidation to NO_2^-) rate, measured via analysis of $^{15}NH_4^+$ and $^{15}NO_2^-$ dynamics in seawater, was detected at low levels under elevated NH_4^+ addition treatments (**Table 2.3**). The strongest nitrification was measured in the reduced periphyton treatment, but this measurement was unreplicated due to compromise of samples during analysis. NH_4^+ oxidation to NO_2^- was undetectable in either ambient NH_4^+ treatment.

Algal periphyton actively removed NH_4^+ from the water column over the course of the terminal 2h experiment. Periphyton took up greater amounts of tracer-enriched $^{15}NH_4$ when NH_4^+ was elevated, but uptake was unrelated to periphyton density (**Figure 2.3A**). Carbon uptake rate (not shown here) was the same in light and in shade (preferential use of lighter isotope lead to depletion in ^{13}C signal), indicating that C uptake rate was proportional to %C initially available.

Though not explicitly anticipated through experimental design, NH_4^+ remineralization, detected through isotopic dilution of tracer-enriched $^{15}NH_4^+$ (**Figure 2.3B)**, was measured in all mesocosms. The NH_4^+ remineralization rate was greatest under elevated NH_4^+ addition treatments **(Table 2.3**), suggesting that micrograzers and other small invertebrates colonized algal periphyton and BioBalls in greater numbers when NH_4^+ was elevated.

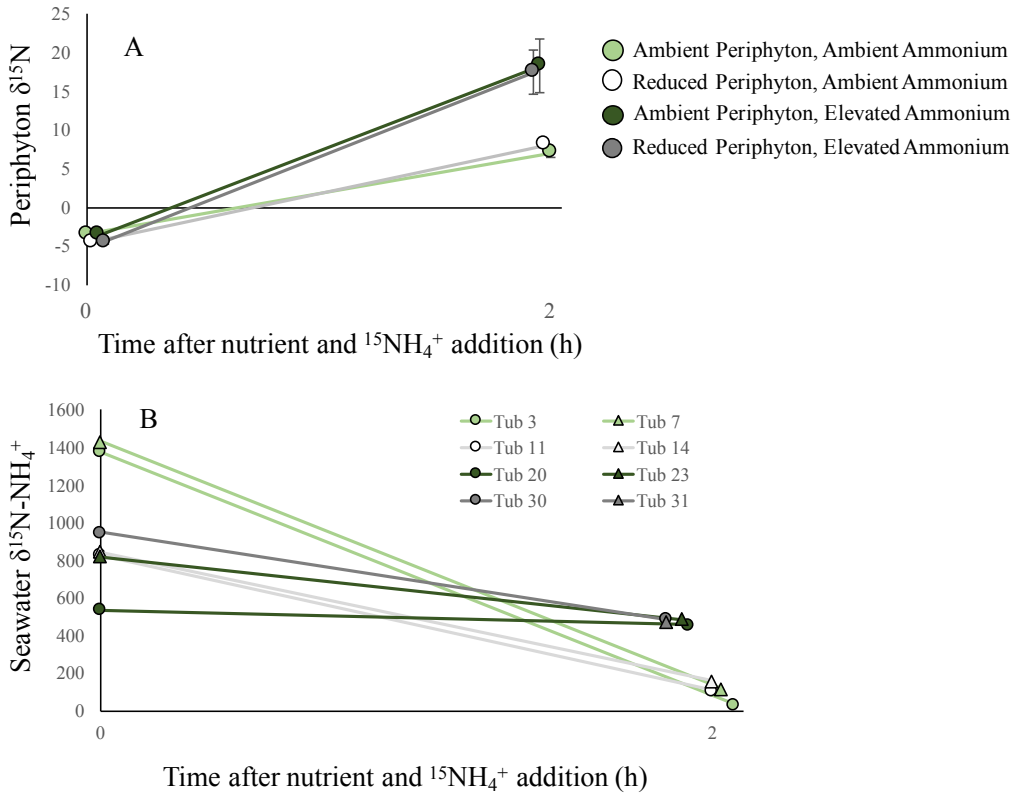

Figure 2.3. A. Periphyton nitrogen isotope ratio ($\delta^{15}N$) dynamics over the terminal 2-hr $^{15}NH_4^+$ tracer incubation period. Plotted data are treatment means ± SE. Symbols are jittered on the x-axis for clarity. **B**. Seawater $\delta^{15}N$-NH_4^+ dynamics over terminal 2-hr $^{15}NH_4^+$ tracer incubation period.

Table 2.3. NH_4^+ dynamics in mesocosms: source-sink nitrification (NH_4^+ oxidation to NO_2^-) (**Equation 2.1**) and NH_4^+ remineralization rates (**Equation 2.2**).

Treatment	Relative Periphyton Density	Relative Ammonium Addition	Sample	2h ammonium oxidation rate (µmol L^{-1} hr^{-1})	2h ammonium remineralization rate (µmol L^{-1} hr^{-1})
A.1	Ambient periphyton	Ambient NH_4^+	1	*Below detectable limits*	2.24
			2	*Below detectable limits*	1.58
A.2	Reduced periphyton	Ambient NH_4^+	1	*Below detectable limits*	1.72
			2	*Below detectable limits*	1.54
A.3	Ambient periphyton	Elevated NH_4^+	1	0.001	3.72
			2	*Below detectable limits*	12.23
A.4	Reduced periphyton	Elevated NH_4^+	1	0.005	21.95
			2	*No data*	*No data*

NH_4^+ concentration and periphyton presence drive microbial community structure and function

The BioBall-associated microbial community structure varied with NH_4^+ availability and periphyton density. In a PCoA analysis based on weighted UniFrac distances (**Figure 2.4**), samples cultured in the absence of neighboring periphyton (reduced light treatment) clustered separately from samples cultured in the presence of periphyton (ANOSIM (light) $R = 0.32$, $p = 0.001$). Samples cultured at ambient versus elevated NH_4^+ addition did not cluster significantly (ANOSIM (NH_4^+ addition) $R = 0.10$, $p = 0.06$), but the effect of NH_4^+ addition on microbial community structure appeared to act interactively with periphyton density; samples cultured in the presence of periphyton clustered distinctly with NH_4^+ addition, while samples cultured without periphyton showed no clustering regardless of NH_4^+ addition.

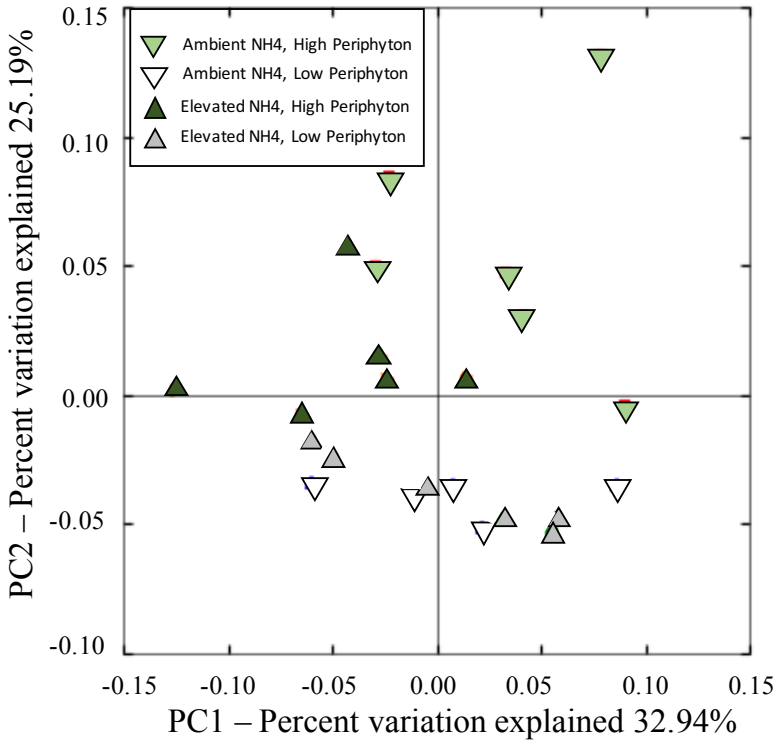

Figure 2.4. PCoA ordination of microbial community samples, showing OTU beta diversity of microbial communities cultured under four mesocosm treatments (high and low periphyton presence, ambient and elevated NH_4^+ addition). Prior to analysis, chloroplast sequences and singletons were removed from the data. Samples were rarified to even depth (105,000 sequences). The weighted UniFrac distance measure was used to incorporate relative abundance. PC 1 explained 32.94% of variance, and PC 2 explained 25.19%. Clustering by treatment was significant (ANOSIM R = 0.30, p = 0.002).

Eight microbial taxa were differentiated between the four treatments at the Bonferroni-corrected $p \leq 0.05$ significance level (G test of independence, **Table 2.B.1**). Of these taxa, seven occurred at 5- to 100-fold greater mean abundance under high periphyton (high light) conditions than under low periphyton (low light) conditions. The bacterial genera most differentiated among treatments were *Dinoroseobacter* and *Glaciecola*, with greatest relative abundance under high periphyton (high light) conditions.

Although microbial community structure varied with periphyton density and NH_4^+ addition, no differences were found in nitrogen metabolisms nitrification, denitrification,

nitrogen fixation, and NO_3^- reduction, as assessed by counts of functional gene sequences predicted using PICRUSt (**Table 2.A.1, Table 2.4**).

Table 2.4. Mean counts of OTUs containing gene sequences associated with five key nitrogen metabolisms, with results of associated two-way ANOVA statistical tests. Tabled means are untransformed, but ANOVA tests performed on log-transformed (log(x) + 0.01) data to meet assumptions of normality.

Treatment	Nitrification	Denitrification	Nitrogen fixation	Assimilatory Nitrate Reduction	Dissimilatory Nitrate Reduction
Ambient NH_4, High Periphyton	4855	210481	30900	123939	312281
Ambient NH_4, Low Periphyton	3635	133765	25317	76389	208860
Elevated NH_4, High Periphyton	5904	210416	31145	122719	309428
Elevated NH_4, Low Periphyton	5183	158139	29066	82086	227854
NH_4	$F_{1,19} = 2.66$, $p = 0.12$	$F_{1,19} = 1.09$, $p = 0.31$	$F_{1,19} = 1.06$, $p = 0.31$	$F_{1,19} = 0.79$, $p = 0.38$	$F_{1,19} = 0.96$, $p = 0.34$
Light	$F_{1,19} = 0.54$, $p = 0.47$	$F_{1,19} = 2.17$, $p = 0.16$	$F_{1,19} = 1.17$, $p = 0.29$	$F_{1,19} = 2.44$, $p = 0.13$	$F_{1,19} = 2.14$, $p = 0.16$
*NH_4 * Light*	$F_{1,19} = 0.00$, $p = 0.95$	$F_{1,19} = 1.00$, $p = 0.33$	$F_{1,19} = 0.96$, $p = 0.34$	$F_{1,19} = 1.06$, $p = 0.32$	$F_{1,19} = 0.93$, $p = 0.35$

Microbial biofilm utilizes NH_4^+ *and alters seawater nutrients*

DIN concentrations in mesocosms varied by both NH_4^+ addition and microbial density at the conclusion of this 7-day experiment (**Figure 2.5**, **Table 2.5**), providing evidence that the mesocosm community was capable of utilizing and transforming added NH_4^+, and that this use was influenced by microbial biofilm. Specifically, prior to the start of the experiment, DIN concentrations did not vary among tubs in four seawater tables (n = 16 tubs, average concentration values (μM) $\pm$ SE were: $[NH_4^+] = 2.14 \pm 0.04$, $[NO_2^-] = 0.25 \pm 0.01$, $[NO_3^-] = 19.25 \pm 0.35$); following one week of daily 2 h NH_4^+ addition incubations, all three forms of DIN

measured (NH_4^+, NO_2^-, NO_3^-) were elevated relative to no-addition treatments (**Figure 2.5A-C, Table 2.5**). When microbes were greater in density, NH_4^+ increases as a result of addition were decreased by a factor of 1.5 (**Figure 2.5A)**. NO_2^- was generated in elevated NH_4^+ mesocosms, while a net drawdown of NO_2^- was measured in tubs without supplemental ammonium (**Figure 2.5B**). No difference in NO_2^- concentration was measured between microbial treatments, for either level of NH_4^+ addition. This suggests that microbial nitrification occurred independent of the microbial treatment. NO_3^- drawdown was measured in all treatments, and was nearly 5 times greater in ambient NH_4^+ mesocosms, and was always greatest with an elevated microbial biofilm (**Figure 2.5C**). Taken together, these results indicate that 1) while mesocosm periphyton use of NO_3^- was ubiquitous, the microbial biofilm was also utilizing this resource and 2) elevated NH_4^+ may ameliorate the use of NO_3^-. Enhanced microbes and NH_4^+ contributed to the change in seawater [NH_4^+] interactively, with evidence for nitrification (i.e. elevated NO_2^- concentration) only in high NH_4^+ conditions.

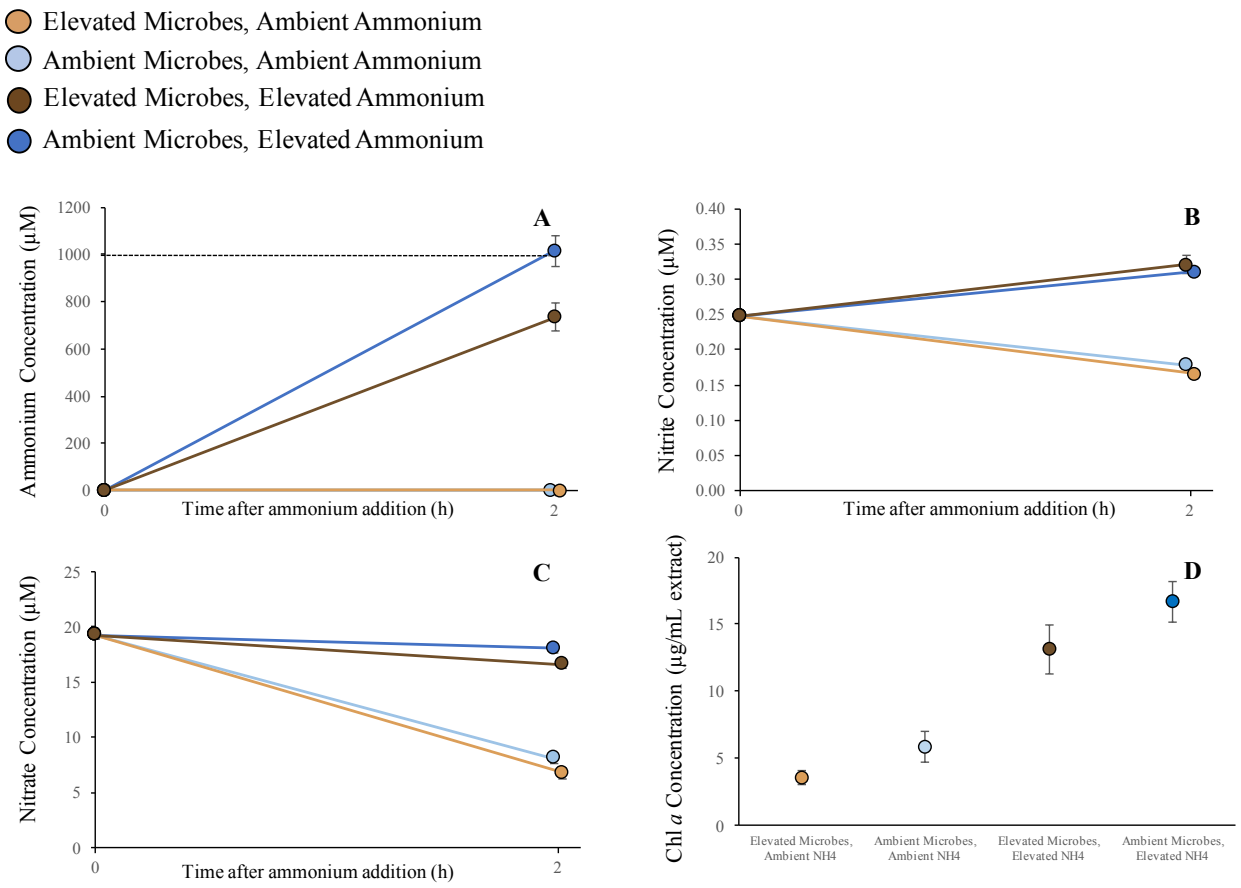

Figure 2.5. Seawater DIN (**A**. $[NH_4^+]$, **B**. $[NO_2^-]$, **C**. $[NO_3^-]$) and Periphyton (**D.** Chlorophyll *a*) responses to experimentally manipulated microbial abundance and NH_4^+ addition in mesocosms. Seawater DIN data are change from initial concentration (µM) prior to the treatment period on experimental day 1 to final concentration (µM) at the conclusion of 2h incubation treatment period on experimental day 7. Horizontal dotted line on panel A indicates NH_4^+ addition level. Periphyton data are from samples scraped from both sides of a single 7-day fouled microscope slide at the end of 2h incubation period on experimental day 7. Plotted data are treatment mean $\pm$ SE.

Table 2.5. Statistical test results for seawater DIN (N = 32) and periphyton (N = 31) responses to manipulated microbe density and NH_4^+ addition in experimental mesocosms. Tabled values are two-way ANOVA results. Means (+/- SE) for these findings are displayed in **Figure 2.5**.

Response	Microbe Density	NH_4^+ Addition	Microbe Density * NH_4^+ Addition
Δ Seawater [NH_4]	$F_{1, 28} = 9.28$ **p = 0.005**	$F_{1, 28} = 188.96$ **p < 0.001**	$F_{1, 28} = 9.29$ **p = 0.005**
Δ Seawater [NO_2]	$F_{1, 28} = 0.290$ p = 0.60	$F_{1, 28} = 298.15$ **p < 0.001**	$F_{1, 28} = 1.10$ p = 0.30
Δ Seawater [NO_3]	$F_{1, 28} = 8.02$ **p = 0.008**	$F_{1, 28} = 181.78$ **p < 0.001**	$F_{1, 28} = 0.81$ p = 0.38
Periphyton Chl a	$F_{1, 27} = 5.91$ **p = 0.022**	$F_{1, 27} = 56.99$ **p < 0.001**	$F_{1, 27} = 0.26$ p = 0.62

Periphyton utilizes NH_4^+*, and this response varies with microbial density*

The chlorophyll *a* content of periphyton was 3-fold higher when conditioned under elevated NH_4^+ as compared to periphyton that was conditioned under ambient NH_4^+ concentration. At each level of NH_4^+ addition, though, extracted chlorophyll *a* (a proxy for productivity) was 2-3 $\mu g\ mL^{-1}$ lower in the treatment with elevated microbial density (**Figure 2.5D, Table 2.5**).

Microbial communities in this experimental trial did not vary by NH_4^+ treatment and there was no evidence for differences in gene abundance predicted with PICRUSt (**Table 2.6**).

Table 2.6. Mean counts of OTUs containing gene sequences associated with five key nitrogen metabolisms, with results of associated one-way ANOVA statistical tests. Tabled means are untransformed, but ANOVA tests were performed on log-transformed (log(x) + 0.01) data to meet assumptions of normality.

Treatment	Nitrification	Denitrification	Nitrogen Fixation	Assimilatory Nitrate Reduction	Dissimilatory Nitrate Reduction
Ambient NH_4	1174	36290	5111	18981	61186
Elevated NH_4	2029	42326	6210	22568	68073
Ammonium Addition	$F_{1,8} = 0.28$, p = 0.61	$F_{1,8} = 0.55$, p = 0.48	$F_{1,8} = 1.46$, p = 0.26	$F_{1,8} = 1.08$, p = 0.32	$F_{1,8} = 0.41$, p = 0.54

DISCUSSION

The interaction between rocky intertidal algae and microbial biofilm in terms of a shared nutrient resource, animal-excreted NH_4^+, showed evidence of bi-directionality (**Figure 2.1**). First, periphyton blooms depressed microbial nitrogen use when NH_4^+differed. Second, microbial biofilm affected macroalgal growth when NH_4^+ differed. Both findings suggest that these competitive interactions are context-dependent of these interactions, suggesting that relative NH_4^+ levels will determine whether the interactions among microbes and algae are negative, positive, or neutral.

When light levels were used to manipulate periphyton, further evidence of periphyton effects on microbes was seen. The periphyton assimilated experimentally elevated NH_4^+, as indicated by drawdown of this resource in ambient light mesocosms (**Figure 2.2A**). NH_4^+ is thought to be a preferred nitrogen source for many marine algae, given the relatively low bioenergetic cost of using of this reduced form of DIN (Dortch 1990; Cohen and Fong 2004). Because nitrifying bacteria and archaea use NH_4^+ for nitrification, NO_2^- and NO_3^- production in elevated NH_4^+ mesocosms indicated nitrification (**Figure 2.2B, 2.2C**), when periphyton were limited. Seawater NO_2^- and NO_3^- concentrations also indicated an interaction between periphyton and BioBall-associated microbes. Despite likely preference for NH_4^+, periphyton utilized NO_3^- too, and at the greatest rates in elevated ammonium treatments where they were most abundant. The ability of these microalgae to utilize NO_2^- and NO_3^- illuminates a potential positive interaction between these ecological groups that compete for NH_4^+ (**Figure 2.2B, 2.2C**).

Although mesocosm periphyton productivity was not nitrogen limited, as shown through equivalent biomass and chlorophyll *a* between NH_4^+ addition treatments at each factor of light availability (**Figure 2.2D**), periphyton did differentially affect DIN. NO_2^- and NO_3^-

concentrations were reduced in high light mesocosms only, suggesting a competitive interaction for the NH_4^+ resource or, as outlined above, an ability of periphyton to be generalists in terms of nitrogen resource use (**Figure 2.2B, C**).

Periphyton biofilm in shade treatments was lower in chlorophyll *a* compared to periphyton growing in ambient light (**Figure 2.2D**). However, the biofilm community in shade versus ambient light utilized NH_4^+ at similar rates (**Figure 2.3**), suggesting that the shade community may be taxonomically distinct and include more chemolithotrophs. The $^{15}NH_4^+$ tracer addition results showed nitrification to be highest in low periphyton mesocosms where NH_4^+ availability was greater (**Table 2.3**), a scenario where NH_4^+ oxidizing microbes may have been released from competition with algae. In contrast, high light conditions likely promoted algal uptake of NH_4^+ and was associated with lowered microbial DIN-processing (**Table 2.3**).

The extent to which algae and NH_4^+ oxidizing microbes interact in coastal marine systems is relatively little understood in comparison to interactions among macrobiota. In contrast, competitive interactions between microbes and plant roots in soil systems have been demonstrated repeatedly (reviewed in Kuzyakov and Xu (2013), with microbes being short-term winners. Indeed, agricultural systems rely on microbicides that target nitrifiers to insure NH_4^+ delivery to crop plants (Wolt 2004). Previous research in marine sediments has similarities to our findings: algae reduce microbial nitrogen uptake and nitrification activity (Risgaard-Petersen *et al.* 2004). The strength of this interaction may be dependent on the concentration of DIN, echoing an extensive amount of terrestrial plant research that shows changing competitive interactions with productivity (Wilson and Tilman 1991, 1993). Our ability to manipulate microbial populations revealed that the interaction is likely competitively reciprocal with microbes applying competitive pressure when microbes are increased in density, though the

competitive versus collaborative potential of algae and bacteria are still a new area of research (Amin *et al.* 2012).

Microbial community structure was driven by NH_4^+ availability and periphyton presence interactively. Communities were strongly differentiated by presence or absence of neighboring periphyton; when periphyton was abundant, microbial communities were differentiated by NH_4^+ availability. Under low periphyton conditions, though, this differentiation by nutrient availability did not occur. Together, these findings support a conclusion that benthic microbes responded competitively to periphyton presence in this system (**Figure 2.4**). *Dinoroseobacter*, the genus most strongly statistically differentiated among treatments (greater abundance under high periphyton (high light) conditions), is a phototrophic, aerobic taxon (Tomasch *et al.* 2011). These data suggest that the high light conditions that benefitted phototrophic eukaryotes also drove the microbial response, an additional line of evidence for phototrophic microbes outcompeting chemolithotrophic bacterial genera for the NH_4^+ resource.

Among OTUs sequenced from the BioBall-associated microbial community, a differential abundance of the nitrifying archaeal genus *Nitrosopumilus* was found between ambient and elevated mesocosms in both mesocosm experiments. In the first mesocosm experiment (Interaction A, varied NH_4^+ and periphyton density), *Nitrosopumilus* sp. mean relative abundance was 0.0007 and 0.0018 under ambient and elevated NH_4^+, respectively. In the second mesocosm experiment (Interaction B, varied NH_4^+ and microbial density), *Nitrosopumilus* sp. mean relative abundance was 0.0005 and 0.0006 under ambient and elevated NH_4^+, respectively. This genus, which includes the recently described *Nitrosopumilus maritimus* ('tiny ammonia oxidizer of the sea'), is likely capable of outcompeting phytoplankton for ammonia in seawater (Martens-Habbena *et al.* 2009). Other nitrifying genera identified from these experiments (*Nitrospina*,

Nitrospira, *Paracoccus*) did not occur at differential abundance between NH_4^+ addition treatments.

A search of microbial sequences from these experiments for genes with known function in nitrogen metabolism revealed no differences that reflect the measured microbial activity differences (**Table 2.4**). This finding is consistent with a recent meta-analysis by Rocca and colleagues (2015), which found that gene counts may not be a dependable proxy for microbial activity, as relationships between protein-encoding gene abundance and corresponding function process are frequently assumed despite being observed relatively rarely. Previous work in coastal marine systems also did not find strong correlations between gene abundance and microbial function (Pfister *et al.* 2014b), though this could also indicate microbial community stability that resists perturbation by nutrient enrichment (Bowen *et al.* 2011, 2012).

Macroalgae, periphyton, and microbes co-occurring in mesocosms utilized experimentally elevated NH_4^+, based on drawdown of elevated NH_4^+ from mesocosm seawater (**Figure 2.5A**). Periphyton chlorophyll *a*, a proxy for productivity, was higher in elevated NH_4^+ treatments (**Figure 2.5D**). Seawater DIN concentration data provided evidence of microbial use of NH_4^+ in experimentally elevated NH_4^+ treatments. NO_2^- increased in mesocosms that had NH_4^+ added relative to controls (**Figure 2.5B**). Since this form of nitrogen is only derived from microbial processes, this finding suggests microbial nitrification.

This experiment yielded multiple lines of evidence demonstrating a competitive interaction between mesocosm microbial biofilm and algae. A comparison of seawater NH_4^+ changes with and without experimentally elevated microbial biofilm presence revealed greater drawdown in the presence of elevated microbes (**Figure 2.5A**), and thus evidence of direct competition for the

NH_4^+ resource when it was abundant. Further, the positive productivity response of periphyton (chl *a*) to NH_4^+ addition was greater in the relative absence of microbes (**Figure 2.5D**).

CONCLUSIONS

A bidirectional algal-microbial competition for seawater NH_4^+ was demonstrated when NH_4^+ addition, periphyton, and microbial density were manipulated. Microbial metabolisms are an increasingly appreciated contributor to coastal biogeochemical processing (Pather *et al.* 2014; Pfister *et al.* 2014a; Moulton *et al.* 2016) where the interaction between microbes and phototrophs is highly context-dependent, varying depending on the type of DIN available (Risgaard-Petersen *et al.* 2004). Although nitrogen is often a limiting nutrient in coastal marine systems, human activities have increased the availability of this nutrient over the past century (Fowler *et al.* 2013).

This study presents evidence that periphyton depressed microbial nitrification and that microbes, in turn, limited the access of periphyton and algae to nitrogen. The importance and strength of these competitive interactions was dependent upon NH_4^+ concentration. Although competitive microbial-algal interactions may play an important role in community interactions and nitrogen and carbon cycling, little is known about their broader role in coastal marine ecosystems. This paper provides a baseline for interactions between algae and microbial biofilm that could be expected in natural systems, and suggests that animal-produced NH_4^+ may provide a template for a range of interactions between phototrophs and chemolithotrophs.

ACKNOWLEDGEMENTS

The research described in this paper has been funded in part by the United States Environmental Protection Agency (EPA) under the Science to Achieve Results (STAR) Graduate Fellowship (OMM). This work was supported by NSF OCE-0928232 (CAP), NSF OCE-0928152 (MAA), the Earth Microbiome Project (JAG), The University of Chicago Committee on Evolutionary Biology Hinds Fund (OMM), Friday Harbor Laboratories Graduate Fellowships (OMM). We thank Friday Harbor Laboratories for access to outdoor mesocosm space, G. Siegmund, A. Thomson, K. Biederbeck, and A. Henry for experimental assistance, J. Hampton-Marcell and S. Owens for sequencing assistance, G. Olack for algal stable isotope laboratory analysis assistance, J. Larkum for seawater isotope laboratory assistance, and G. Dwyer, J. Gilbert, M. Coleman, and J.T. Wootton for helpful comments on research design, analysis, and the manuscript.

APPENDIX 2A: KEGG Orthologs associated with nitrogen metabolism.

Table 2A.1. Gene orthologs identified as having functional roles in specific nitrogen metabolism categories. Orthologs were retrieved from the KEGG database nitrogen metabolism pathway map.

Nitrogen Metabolism	Corresponding KEGG Orthologs
Nitrification	K10944, K10945, K10946, K10535
Denitrification	K00370, K00371, K00374, K00373, K02567, K02568, K00368, K15864, K04561, K02305, K15877, K00376
Nitrogen Fixation	K02588, K02586, K02591, K00531
Assimilatory Nitrate Reduction	K00367, K10534, K00372, K00360, K00366, K17877
Dissimilatory Nitrate Reduction	K00370, K00371, K00374, K00373, K02567, K02568, K00362, K00363, K03385, K15876

APPENDIX 2B: Microbial OTUs driving community structuring by treatment.

Table 2B.1 OTUs found to be strongly explanatory of with the PCoA ordination of microbial communities from two levels of ammonium addition and two levels of periphyton abundance (**Figure 2.4**) (Bonferroni-corrected $p \leq 0.05$) using a G-test of Independence. Taxa are identified to lowest possible taxonomic level.

OTU I.D. (Greengenes)	Taxon	Mean Count High Periphyton, Ambient NH4	Mean Count Low Periphyton, Ambient NH4	Mean Count High Periphyton, Elevated NH4	Mean Count Low Periphyton, Ambient NH4	G-value	Bonf. Corr. p-value
New.0.CleanUp.ReferenceOTU135005	*Dinoroseobacter* sp. (Family: Rhodobacteraceae)	39.33	0.33	25.33	0.50	26.31	0.01
New.1.CleanUp.ReferenceOTU199860	*Dinoroseobacter* sp. (Family: Rhodobacteraceae)	41.00	0.33	27.00	0.50	23.84	0.02
New.0.CleanUp.ReferenceOTU32172	Oceanospirillaceae	0.00	0.00	3.83	0.00	23.41	0.02
New.0.CleanUp.ReferenceOTU409731	*Unassigned*	30.50	2.83	59.67	2.67	22.84	0.02
80086	*Glaciecola* sp. (Family: Alteromonadaceae)	41.17	4.17	56.67	1.17	21.86	0.03
New.0.ReferenceOTU1347	*Glaciecola* sp. (Family: Alteromonadaceae)	401.83	12.50	892.33	7.67	20.69	0.05
New.0.CleanUp.ReferenceOTU394064	Rhodobacteraceae	394.83	56.83	301.67	57.33	20.52	0.05
New.1.CleanUp.ReferenceOTU244849	Rhodobacteraceae	392.50	56.00	301.67	56.17	20.44	0.05

CHAPTER III

DRIVERS OF VARIABILITY AMONG NORTHEAST PACIFIC ROCKY INTERTIDAL MICROBIAL COMMUNITIES

ABSTRACT

In rocky shore environments, microbes can be influenced by both local abiotic and biotic factors, as well as larger-scale physical drivers. Using spatially and temporally broad field surveys, we characterized microbial community composition and structure from a rocky intertidal benthic biofilm across four sites and two years to address three questions: 1) Within a site (<100m), do the benthic surfaces of tide pools and emergent rock host distinct microbial communities? 2) Do intertidal microbial communities vary on a regional scale (>25km), between sites? And 3) Are microbial communities temporally stable? Culturing and 16S rRNA amplicon sequencing was used to examine microbial communities *in situ* on replicated artificial surfaces deployed May-August in 2013 and 2014 at four southwest-facing sites in the San Juan Islands, WA, USA on both emergent rock and in permanent tide pools. Simultaneous with microbial community analysis, we quantified neighboring macrobiota and local environmental variables. Strong local control of microbial community composition was observed. Microbial communities were highly differentiated between habitat types (tide pools, emergent rock) using both abundance-weighted and unweighted phylogenetic distance metrics. Several phototrophic cyanobacteria were tightly associated with emergent substrate. Supervised learning techniques could predict source habitat based on microbial community structure, though site could not be correctly classified. Sites, despite variation in macroscopic community composition, maintained only weakly different microbial communities. We observed community turnover on a coarse annual scale (August

2013 to August 2014), with maintenance of source habitat identity. Although distribution of microbial taxa was broadly regional, microbial community structure in this NE Pacific rocky intertidal system was differentiated by surface type.

INTRODUCTION

Biological variability exists in a multi-dimensional hypervolume (Hutchinson 1965) whereby individual organisms are influenced by myriad environmental variables, both biological and physical, which range over time and space. A continuous challenge for ecologists is to condense these multiple axes of variability to provide some tangible examination of the factors that lead to differences in microbial community structure. The temperate rocky intertidal zone is one of the best-described systems in community ecology; many interaction links are well known, but in much of this research microbial participants have been omitted (but see Ogilvie *et al.* 1997; Risgaard-Petersen *et al.* 2004). Little is known about the spatial and temporal variability of marine microbial communities (Pfister *et al.* 2014; Tan *et al.* 2015), but evidence of the ecological importance of these communities is accumulating (Thompson *et al.* 2004; Pfister *et al.* 2010; Golléty and Crowe 2013; Moulton *et al.* 2016). For example, microbial utilization of nutrient resources is increasingly known as an important contributor to coastal nutrient cycling (Pfister *et al.* 2016; Moulton *et al.* 2016). Microbial transformations of nitrogen can equal or exceed contributions of phototrophs (algae and seagrasses) to nitrogen dynamics in coastal marine systems (Pfister *et al.* 2016).

Biofilms, which cover most hard surfaces immersed in shallow water, are an important functional component of the benthos in marine ecosystems (Castenholz 1961; Underwood and Jernakoff 1984; Hill and Hawkins 1991; Thompson *et al.* 1998). The photosynthetic component

of biofilms, composed of mixed culture of microalgae and bacteria (mostly Cyanobacteria), follow some general patterns across the temperate rocky intertidal zone, including strong seasonality (Jenkins *et al.* 2001), greater abundance in the lower intertidal than upper (Underwood 1984), limitation by physical stressors like high light and desiccation (Lamontagne *et al.* 1989), and maintenance at an early successional stage by grazers (Lubchenco and Gaines 1981). However, how these factors interact to structure benthic biofilm communities remains complex and hard to interpret (Williams 1994; Harley 2002; Thompson *et al.* 2004). Further, the biofilm distribution of chemolithotrophic microbes, which could play a major role in nutrient cycling, are relatively undescribed.

A defining feature of the intertidal zone is periodic exposure to air and its associated stressors (e.g. desiccation (Bell 1995), extreme temperature range (Somero 2002), freshwater shock during precipitation events (Torres *et al.* 2004), and predation by terrestrial and avian organisms (Marsh 1986)). Tide pools, depressions in rocky substrate that hold isolated volumes of seawater when the tide has retreated, are refugia from the stress of isolation from the oceanic water column and thus provide a distinct habitat type for marine flora and fauna within the rocky intertidal habitat. Within centimeters of space, the physical conditions for intertidal inhabitants can be vastly different depending on habitat type.

Nutrient limitation, which occurs during periodic separation from the oceanic water column during low tides, is a considerable stressor on intertidal primary producers. Coastal marine systems in temperate regions are typically nitrogen limited, and nitrate, delivered to the northeast Pacific Ocean coastline via upwelling, quantitatively dominates the nitrogen pool available to phototrophs. The rocky intertidal zone frequently experiences periodic nitrogen limitation during low tide, when organisms are isolated from the water column nitrate pool (Bracken 2004).

However, nearshore and intertidal animals deliver regenerated nitrogen, ammonium, which ameliorates this nitrogen limitation (Bracken 2004; Pfister 2007). In a classic example of bottom-up mechanics, ammonium availability elevates primary productivity across a diverse suite of photosynthesizers (Taylor and Rees 1998; Bracken 2004; Pfister 2007) which in turn yields elevated consumer diversity and abundance. Intertidal animal regenerated ammonium is available to both primary producers (macroalgae, microalgae) and benthic microbes capable of ammonium metabolism, setting the stage for competition in habitats like tide pools where ammonium is relatively abundant (Chapter II).

In this study, we used field surveys to characterize microbial community composition and structure present in rocky intertidal benthic biofilm. Given the importance of tide pools in ameliorating nitrogen limitation that can occur at low tides when intertidal macrophytes are cut off from the oceanic nutrient pool, tide pool-associated microbial communities were contrasted with adjacent emergent rock-associated microbes. We contrast four rocky intertidal sites in the San Juan Islands, WA with different relative abundances of macrophytes (seaweeds and seagrass) versus macroinvertebrates to test whether these sites with distinct macrobiota also entrain distinct microbial communities. Finally, we tested the temporal stability of these intra- and inter-site factors by repeating sampling over two consecutive summer seasons. Our *a priori* expectation was that environmental drivers of microbial community variability would vary at one or more levels of sampling (habitat, site, year), and that this nested approach to biogeographic sampling would reveal the correlative roles of habitat (emergent rock versus tide pool), macroscopic community composition, and physical environmental parameters with microbial community structure and stability (spatial and temporal). We hypothesized that microbial diversity is intimately tied to the surrounding community members and to physical conditions

varying on intra- and inter-site scales. Improved understanding of multiple axes of variability in microbial community structure, along with biotic and abiotic drivers, provides important baseline data for benthic microbes, an understudied component of the well-studied temperate rocky intertidal zone.

MATERIALS AND METHODS

Study Sites

To test the relative importance of local habitat versus broad geographical factors as drivers of rocky intertidal benthic microbial communities, we sampled tide pool and emergent rock at four rocky sites in the San Juan Islands archipelago (WA, USA) (**Figure 3.1**). All sites were located within relatively high wave exposure regions of the south/southwest sides of San Juan and Lopez Islands on Haro Strait (Dayton 1971; Menge 1972; Menge and Menge 1974; Harrison *et al.* 1994), and site selection maximized variability in macroscopic community composition between physically similar sites. Westside Preserve, the northernmost site, is relatively animal-depauperate, while sites on the southern tips of San Juan and Lopez Islands (Cattle Point and Iceberg Point respectively) host abundant and diverse invertebrates. This variability in macroscopic community composition was confirmed through explicit surveys (**Figure 3.8**, **Table 3.C.1**).

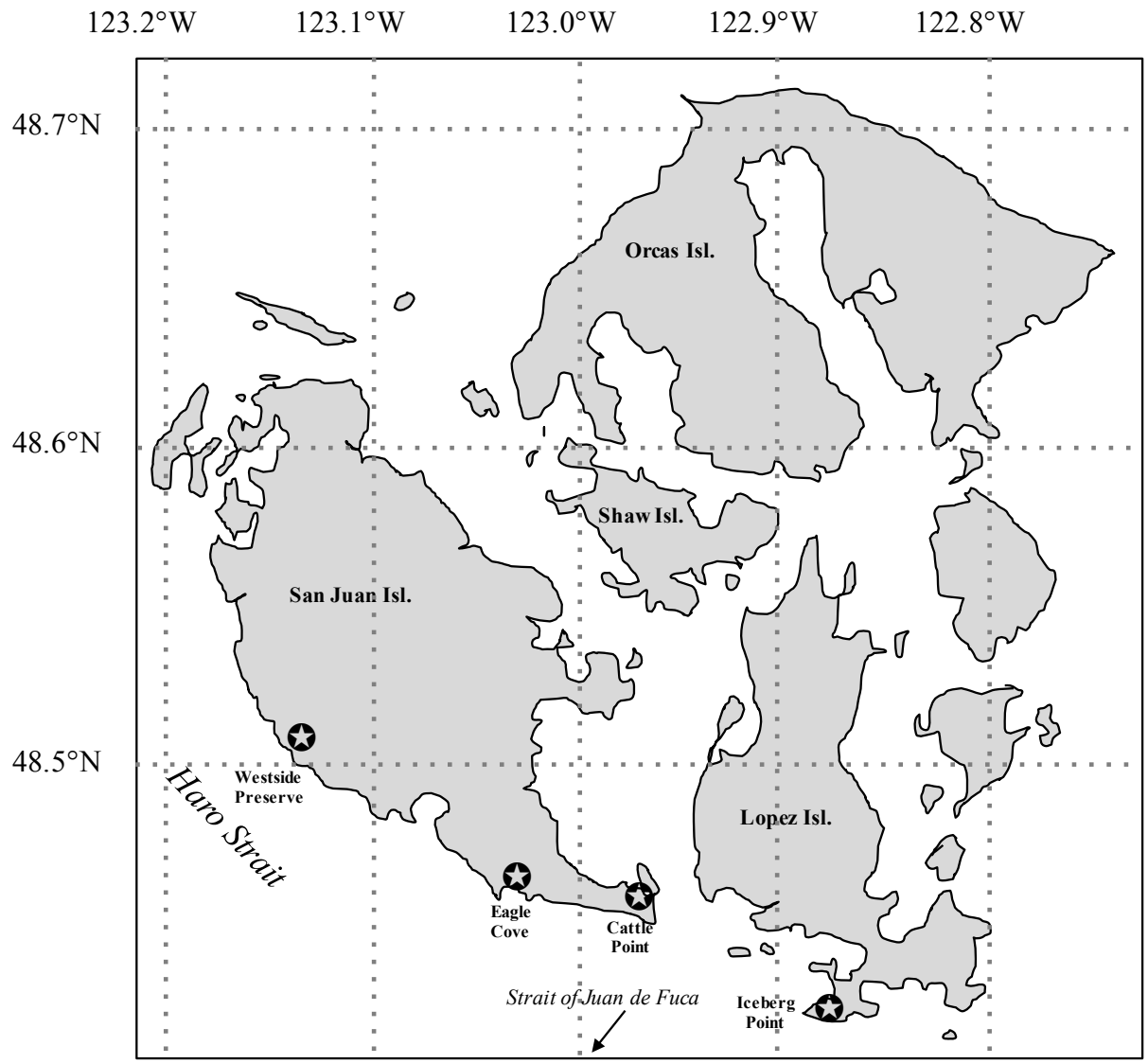

Figure 3.1. Map of study sites in the San Juan Islands archipelago, Washington, USA.

Nested Microbial Community Sampling Design

To probe for differences in microbial community structure and distribution between tide pools and emergent rock habitat, among sites, and between years, we assayed the microbial communities that established on uniform artificial substrate across all sites. We deployed pouches containing 12 BioBalls each in five replicate tide pool/exposed rock pairs at approximately equal tidal height (0m MLLW, mean lower low water) at the four San Juan Islands sites. BioBalls (Coralife ®) are 2.5cm diameter pegged spherical plastic units that

provide high surface area for settlement of microbial biofilm. Pouches were constructed of black plastic 1.5cm mesh, and were attached to rocky substrate using stainless steel screws, washers, and plastic wall anchors. BioBall pouches were deployed for 3 months over two consecutive summer intervals: May-August 2013 and May-August 2014. In August of each year, BioBalls were placed on ice upon removal from the field, and stored at -80°C within 24h of collection.

Community DNA was sampled from BioBalls and sequenced via amplification of the 16S rRNA gene using barcoded primers according to Earth Microbiome Project (Gilbert *et al.* 2014) standard protocols as in Chapter II (see Caporaso *et al.* 2010a, 2012), yielding paired-end sequence data.

Microbial Sequence Analysis

Preliminary microbial sequence data analysis was performed in QIIME (v. 1.9.1, Quantitative Insights into Microbial Ecology; www.qiime.org) using protocols identical to those outlined in Chapter II. Diversity metrics between factors (site, pool versus exposed substrate, and year) were computed using the QIIME core_diversity_analyses.py script in QIIME, which generates alpha diversity metrics and beta diversity distances between samples (weighted and unweighted UniFrac), and to build principal component (PCoA) plots, which accounted for both phylogenetic composition (Lozupone *et al.* 2011) and relative abundance of taxa among samples. All samples were analyzed at the lowest sequencing depth of included samples for these diversity analyses.

To test for significant sample groupings by sampling category (pool versus emergent substrate, site identity, sample year) based on these distance metrics, ANOSIM was conducted in QIIME using the compare_categories.py script. This test compares the mean of ranked

dissimilarities between groups to the mean of ranked dissimilarities within groups in multivariate data, yielding a test statistic (R), and a p-value. The ANOSIM R-value test statistic compares between-group mean of ranked sample dissimilarities with within-group mean of ranked sample dissimilarities. An ANOSIM R-value close to 1 suggests dissimilarity between groups while an R value close to 0 suggests even dissimilarity within and between groups. We tested the robustness of the categorical distinction using the Random Forest Supervised Learning procedure script (supervised_learning.py). This procedure uses a subset of OTU data to determine the relationship between a categorical variable and OTUs, then attempts to classify reserved data to a selected set of categories based upon that training. The resulting baseline error to observed error ratio allows us to infer classification robustness, with a value > 2 considered significant. Finally, the group_significance.py script was applied to test whether the abundance of any specific OTUs differed significantly between categories using Bonferroni-corrected ANOVA one-way analysis of variance. This test compares the within-group variance to the between-group variance in order to assess whether or not the sample groups (pool versus emergent rock, site identity, year) have even frequencies of a given OTU.

Analysis of macrobiota as drivers of microbial community structure

Microbial associations with macrobiota are ubiquitous, and can have strong implications for ecological function in coastal marine systems (Moulton et al 2016). We quantified the abundance of rocky intertidal macrobiota, i.e. macrofauna and macrophytes (seaweeds and surfgrass), at the four study sites as a hypothesized correlate with microbial community composition. To address our nested biogeographic questions, we surveyed macrobiota broadly across each site as well as immediately adjacent to the BioBall samplers.

To contrast macroscopic community structure between sites, we surveyed entire-site communities in point-contact vertical transects spanning space from 0m MLLW to the upper edge of the intertidal habitat. 8-16 transects were completed at each site, with the identity of the organism attached to the rock directly beneath the transect tape recorded every 25 cm. Organisms were identified to lowest practical taxonomic level. We confirmed variability of macroscopic community by habitat and site using non-metric multidimensional scaling (hereafter NMDS) ordination (Kruskal 1964). Here, we ordinated communities of macrobiota based on level of membership of algal, seagrass, invertebrate, and intertidal fish taxa in survey samples. Because tide pools and emergent rock were surveyed differently (total pool survey versus specific quadrat size on emergent rock), we used the Jaccard distance measure, which is based on presence/absence of taxa. NMDS on the Jaccard distance measure is also robust to non-normal data that contain high numbers of zeroes, typical characteristics of ecological community abundance data.

To consider the effect of macroscopic community structure immediately adjacent to the sampled microbial community at 0m MLLW, we surveyed the exposed substrate in the ~1 m surrounding BioBalls (n = 5 per site) and entire contents of BioBall-containing tide pools (n = 5 per site) ranging in perimeter from 60 – 1200 cm (mean perimeter = 500cm). Community structure of macroscopic organisms surrounding exposed rock microbial BioBall pouches was surveyed via percent cover estimates in ½ m^2 quadrats placed to South, East, North, and West of each pouch. Tide pool inhabitants were surveyed through complete counts of discrete macrofaunal individuals and percent cover estimates of sessile colonial animals and phototrophs within each pool. Using these 0m MLLW macrobiota survey results, a broad ‘faunal contribution’ metric associated with each microbial sampling unit (BioBalls) was calculated as

the sum of faunal counts (motile animals) and percent cover (sessile animals) as a fraction of the total macroscopic community (fauna and flora).

Analysis of abiotic factors as drivers of microbial structure

An alternative to biotic control of microbial structure is the determination by physical factors. We tested the role of multiple physical parameters measured in tandem with microbial and macroscopic community surveys as potential environmental correlates with biotic community distribution. Environmental variables measured were seawater nutrients, site-level temperature and light intensity at 0m MLLW, and dissolved oxygen in seawater.

Seawater nutrients can be indicative of large-scale environmental processes (e.g. upwelling) and local-scale nutrient cycling (e.g. regeneration) on temporal and spatial scales. We collected samples twice for seawater nutrient analyses at all four study sites, first in mid May and second in mid August 2014, to capture any seasonal differences through the summer. At each time point, samples were collected from both tide pool and exposed seawater to capture intra-site nutrient variability across a 25km region. Water samples collected for seawater nutrient analysis were syringe-filtered (Whatman glass-fiber filter GF/C) into separate acid-washed 60mL high-density polyethylene bottles, and frozen (-20°C) prior to analysis. Nutrient concentrations (NH_4^+, NO_3^-, NO_2^-, PO_4^{3-}, and SiO_4^{4-}) were measured at the University of Washington Marine Chemistry Laboratory (methods from UNESCO 1994).

Temperature and light intensity are commonly used correlates with productivity in intertidal systems. Periods of oceanic upwelling are marked by lower than average seawater temperatures, and are often followed by seawater chlorophyll blooms. Intertidal (0m MLLW) temperature (°C) and light intensity (lux) were measured over the entire the 3-month duration of

microbial BioBall incubation at the 4 field sites, each with one automated data logger (HOBO Pendant® Temperature/Light 64K Data Logger, Onset, Wareham, MA) installed at 0m MLLW. Measurements were logged every 10 minutes 24h/day to capture both seawater data (when tidal height was above 0m MLLW) and air data (when tidal height fell below 0m MLLW). Pendant data loggers were also installed in the pools with largest and smallest volume at each site to capture the range of temperature and fluctuation experienced by the set of 5 study pools per site.

Capacity of seawater to contain dissolved oxygen is tightly linked to temperature, but levels are simultaneously driven by biotic oxygen production and use. We collected paired exposed seawater and tide pool dissolved oxygen and temperature data on multiple dates throughout the 3 month microbial BioBall incubation period to quantify differences between sites, and between ocean and tide pools. More specifically, we measured inter-site variability, ocean/tide pool difference at single time points, and distinct trajectories of seawater DO and temperature within a low tide period in the coastal ocean compared to relatively very small volume tide pools with known biotic components.

Similarity of microbial communities based on level of membership of OTUs in samples was visualized and quantified using NMDS ordination. Groups clustered by categorical factor 'habitat' (emergent rock versus tide pool) were compared in relation to measured environmental gradients. As in the NMDS ordination of macrobiota, this analysis used the Jaccard distance measure, which is based on presence/absence of OTUs. Sample units (BioBall pouches) were ordinated on two axes, using a joint plot to demonstrate the relationship between environmental variables and ordination scores. The proportion of variance represented by each axis was determined by the coefficient of determination (r^2) between distances in ordination space and

distances in original space. Finally, correlations with each ordination axis were used to measure strength and direction of individual taxa and environmental parameters.

To test whether microbial taxa in biofilm BioBalls incubated at two levels of the categorical factor 'habitat' and four levels of the factor 'site' were associated with particular nitrogen metabolism pathways, the software package PICRUSt (Phylogenetic Investigation of Communities by Reconstruction of Unobserved States) (Langille *et al.* 2013) was used to query predicted functional capacity of the communities as in Chapter II. PICRUSt estimates the gene families contributed to a predicted metagenome by microbes identified using 16S rRNA sequencing. A list of genes associated with nitrogen metabolisms was created using the KEGG (Kyoto Encyclopedia of Genes and Genomes) (Kanehisa *et al.* 2016) orthology database (**Table 3D.1**), and R (R Core Team 2015) was used to generate counts and percent abundance contributions of each metabolism associated with each sample and compare nested geographic categories.

RESULTS

Microbial community structure differentiates by habitat type

When considering data from all four sites in each year separately via PCoA analyses, we found that microbial community structure was determined by substrate (tide pool versus emergent rock) in both 2013 (**Figure 3.2a**) and 2014 (**Figure 3.2b**) (ANOSIM on weighted UniFrac; $R = 0.623$ and 0.330, respectively; $p < 0.001$). The relative influence of substrate on microbial community structure was demonstrated by visual comparison of weighted (**Figure 3.2a, b**) and unweighted (**Figure 3.2c, d**) UniFrac distance between samples, and through a Procrustes Analysis (Gower 1975), which compares the shape of two PCoA plots by

optimally rotating and scaling one plot to best fit the other. In both weighted and unweighted ordinations, the first principle coordinate clearly demarcates benthic substrate (**Figure 3A.1**). With few exceptions, tide pool and emergent substrate samples cluster in distinct groups in both 2013 and 2014.

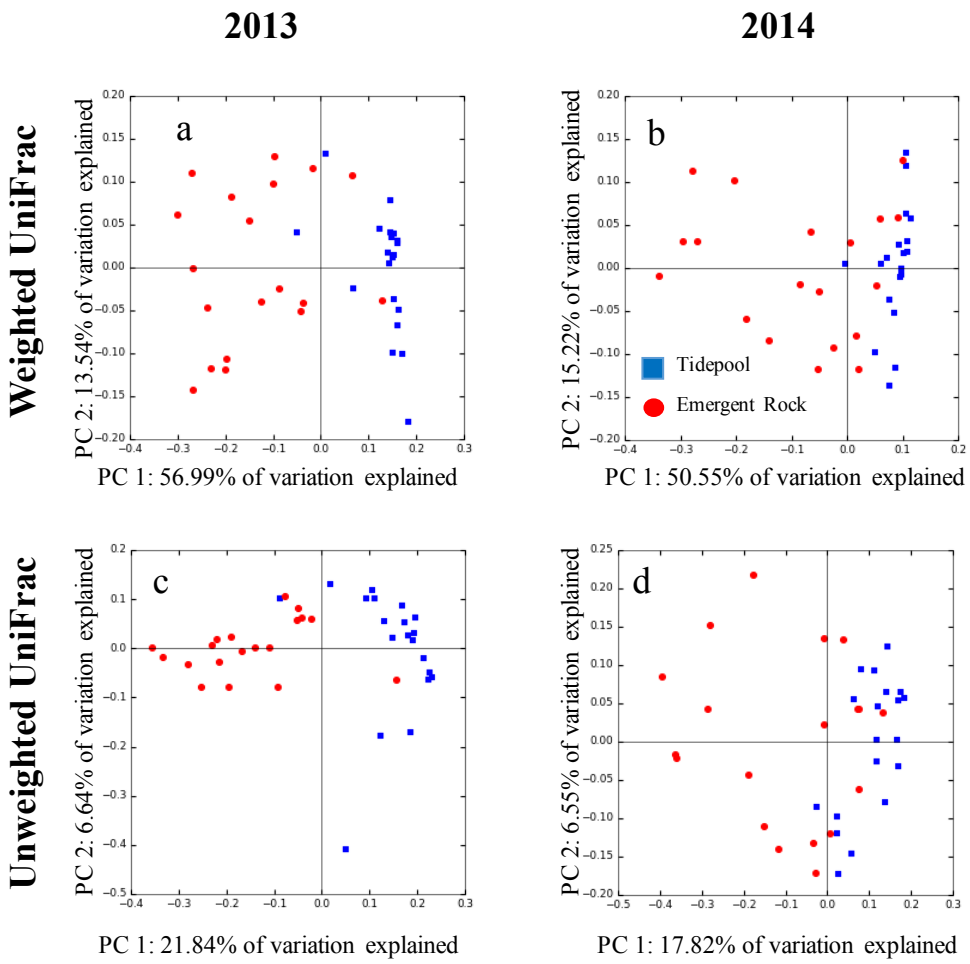

Figure 3.2. Ordination of samples based on weighted and unweighted phylogenetic dissimilarity in community composition (UniFrac). Panels **a** and **b** are principal coordinate (PCoA) plots for all samples in the study based on pairwise weighted UniFrac distance between samples, with sample points colored by habitat (tide pool, emergent rock) in 2013 and 2014, respectively. Panels **c** and **d** are PCoA plots, also colored by substrate, based on unweighted UniFrac distance.

In both sample years, the distinct microbial communities associated with two habitats (tide pools versus emergent rock) were predicted by random forest supervised learning. Samples were classified more than 6 times as effectively as one would expect by chance in 2013, though

only twice as effectively in 2014 (**Table 3.1**). This result further demonstrates differentiation in the microbial communities associated with these two different habitats.

Table 3.1. Summary of predictive accuracy of random forest supervised learning models in classifying microbial samples to habitat type in each study year. Tenfold cross validation models were constructed with 1,000 trees using OTUs from evenly rarified samples as predictors of origin habitat among samples cultured *in situ* in 2013 and 2014 separately.

Sample Subset	Predicted Category	N	Estimated error ± s.d.	Baseline error	Ratio
2013	Habitat	37	0.075 +/- 0.121	0.487	6.50
2014	Habitat	38	0.200 +/- 0.197	0.500	2.50

Many microbial operational taxonomic units (OTUs) were found to be differentially abundant between the benthic habitat types 'pool' and 'emergent rock' (180 taxa in 2013, 77 taxa in 2014; Bonferroni-corrected ANOVA $p \leq 0.05$). Of the 20 most abundant of those OTUs, 45% (9 OTUs) are abundant in both years (**Table 3.2a** (2013) and **Table 3.2b** (2014); Bonferroni-corrected G-test of independence $p \leq 0.05$). Of these 9 OTUs that were highly abundant in both sample years, seven were higher in association with emergent rock habitat and two were higher in association with tide pool habitat. Three cyanobacteria, including the two most abundant OTUs, where differentially abundant by habitat in each year, including two OTUs from the Pseudanabaenaceae (OTU 179845), and 1 from the Xenococcaceae (OTU 194304). The abundance of all three was markedly higher on emergent rock than on pool benthos. Of the 20 must abundant OTUs with differential abundance between habitats in both years, only 2 OTUs associated with Rhodobacteraceae (OTU 914108) and Gammaproteobacteria (OTU 556389) were more abundant in tide pools.

Table 3.2. Twenty most abundant OTUs (counts in OTU table) found to be differentially significant (Bonferroni-corrected $p \leq 0.05$) between substrata (tide pool, emergent rock) in **a**) 2013 and **b**) 2014 using G-test of Independence (years performed separately). Taxa are mostly identified to family, and genus where possible. Taxa present at significantly different abundance between habitats and occurring at high abundance in both years (**Tables 3.2a** and **3.2b)** are shaded in gray. Mean count is listed in bold text in the habitat column where a taxon is more abundant.

a.

OTU ID	Test Statistic	Mean Pool Count	Mean Emergent Count	Taxon ID
179845	913.8	123.3	**1115.3**	Pseudanabaenaceae
194304	516.6	264.6	**1065.6**	Xenococcaceae
New.0.ReferenceOTU145	727.0	118.05	**940.7**	*Unassigned*
104454	297.7	59.35	**413.3**	*Lewinella* sp. (Family Saprospiraceae)
589027	181.4	78.15	**344.9**	Pseudanabaenaceae
1779317	105.6	82.75	**271.2**	Rhodobacteraceae
829814	36.8	**373.75**	225.9	*Loktanella* sp. (Family Rhodobacteraceae)
914108	134.0	**528.7**	217.3	Rhodobacteraceae
4476096	136.8	26.05	**187.1**	*Lewinella* sp. (Family Saprospiraceae)
789831	110.6	447.3	**186.4**	Rhodobacteraceae
New.0.ReferenceOTU56	203.0	6.65	**181.7**	*Saprospira* (Family Saprospiraceae)
4476095	178.9	11.65	**181.2**	*Lewinella* sp. (Family Saprospiraceae)
556389	89.5	**390.65**	169.6	Unassigned Gammaproteobacteria
New.0.ReferenceOTU354	117.7	24.75	**166.7**	Saprospiraceae
New.0.ReferenceOTU238	64.6	43.9	**153.8**	Rhodobacteraceae
185015	46.8	55.2	**151.8**	Hyphomonadaceae
New.0.ReferenceOTU123	50.6	**289**	142.6	Rhodobacteraceae
New.0.ReferenceOTU305	89.8	17.9	**124.8**	*Rubricoccus* sp. (Family Rhodothermaceae)
New.0.ReferenceOTU411	58.4	30.5	**121.8**	*Lewinella* sp. (Family Saprospiraceae)
New.0.ReferenceOTU447	83.2	15.25	**112.4**	Flammeovirgaceae

Table 3.2. *Continued.*
b.

OTU ID	Test Statistic	Mean Pool Count	Mean Emergent Count	Taxon ID
179845	880.6	181.6	**1236.8**	Pseudanabaenaceae
194304	332.5	137.7	**620.6**	Xenococcaceae
914108	20.2	**483.1**	353.3	Rhodobacteraceae
556389	119.3	**491.1**	206.7	Unassigned Gammaproteobacteria
New.0.ReferenceOTU145	46.7	80.9	**192.3**	*Unassigned*
New.1.ReferenceOTU96	115.4	32.3	**182.2**	Rhodobacteraceae
757344	23.7	**272.4**	170.4	Unassigned Bacteria SC3-41
795328	32.7	73.8	**160.5**	Flavobacteriaceae
104454	76.2	35.5	**150.3**	*Lewinella* sp. (Family Saprospiraceae)
New.0.ReferenceOTU305	166.6	2.8	**137.8**	*Rubricoccus* sp. (Family Rhodothermaceae)
New.0.ReferenceOTU433	38.7	52.7	**136.9**	Pseudanabaenaceae
589027	101.1	15.3	**128.2**	Pseudanabaenaceae
New.1.ReferenceOTU105	75.1	19.3	**114.7**	Pseudanabaenaceae
894928	121.3	2.9	**104.4**	*Psychrobacter* sp. (Family Moraxellaceae)
1779317	26.1	38.8	**97.6**	Rhodobacteraceae
574890	62.0	13.0	**87.9**	*Phormidium* sp. (Family Phormidiaceae)
New.0.CleanUp.ReferenceOTU141904	41.0	20.7	**84.2**	Pseudanabaenaceae
750031	26.5	**161.0**	81.5	*Pseudoruegeria* sp. (Famliy Rhodobacteraceae)
105211	37.7	**178.9**	81.1	*Saprospira* sp. (Family Saprospiraceae)
New.0.ReferenceOTU56	93.5	0.4	**70.9**	*Saprospira* sp. (Family Saprospiraceae)

Weak microbial community differentiation across sites

At a site-level scale, microbial communities were only weakly differentiated. Only when habitat-specific microbial communities from 2013 and 2014 were considered individually did weighted UniFrac ordination suggest statistically significant site-specific clustering (ANOSIM on weighted UniFrac; **Figure 3.3b** R = 0.244, p = 0.022; **Figure 3.3c** R = 0.412, p = 0.001; **Figure 3.3d** R = 0.188, p = 0.049). Communities collected from pool habitats in 2013, however, did not cluster by site (**Figure 3.3a**; ANOSIM on weighted UniFrac; R = 0.076, p = 0.11).

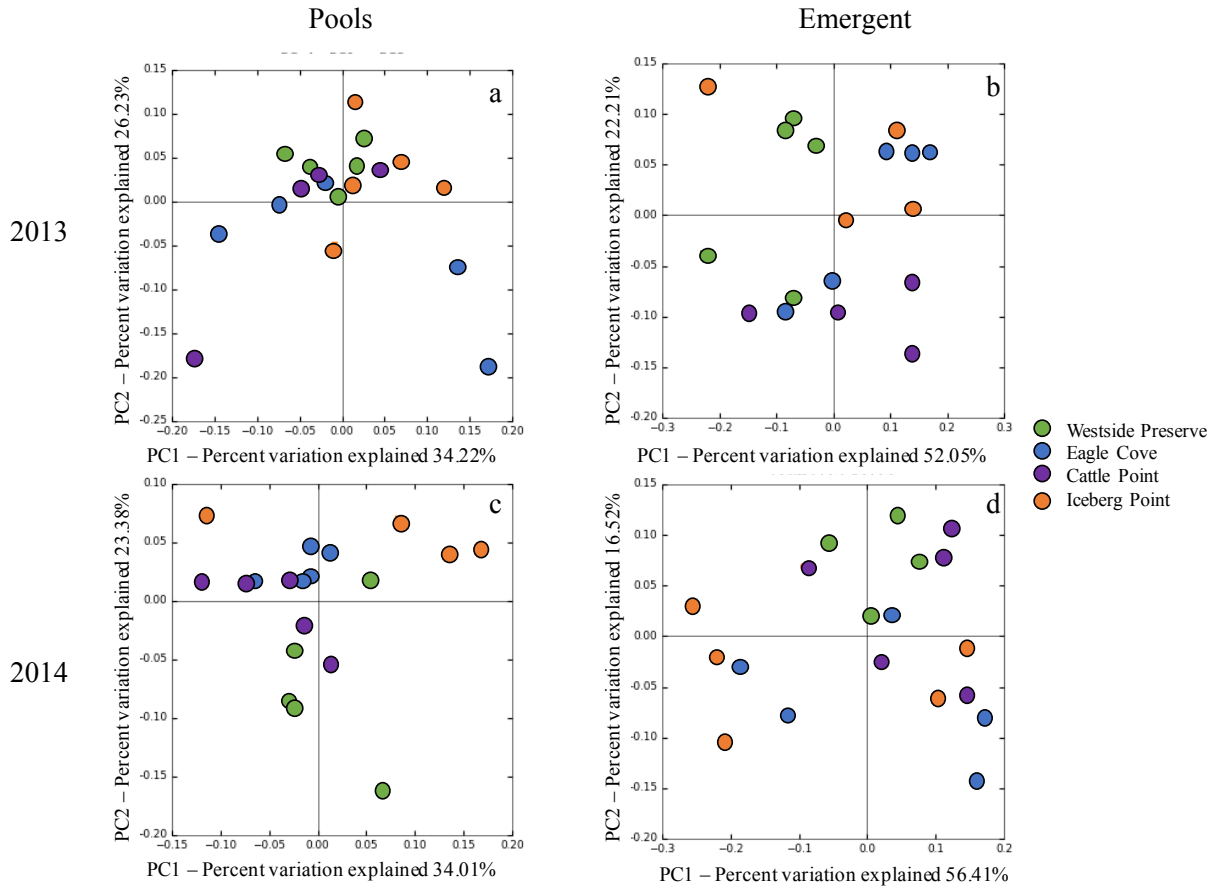

Figure 3.3. Ordination of samples based on weighted phylogenetic dissimilarity in community composition (UniFrac). Panels **a** and **b** are principal coordinate (PCoA) plots for all samples collected in 2013, and panels **c** and **d** are 2014 samples. In both years, pool and emergent benthic habitat are separated. Ordinations are based on pairwise weighted UniFrac distance between samples, and sample points are colored by site.

Random forest supervised learning models failed to determine which site a sample was taken from in either year for both pool and emergent rock samples (**Table 3.3**).

Table 3.3. Summary of predictive accuracy of random forest supervised learning models in classifying microbial samples to site in each habitat and study year. Tenfold cross validation models were constructed with 1,000 trees using OTUs from evenly rarified samples as predictors of origin site among samples cultured *in situ* in 2013 (pools, emergent rock) and 2014 (pools, emergent rock) separately. An error ratio of 1 indicates that the model is able to predict the category equally well as a random prediction, and a ratio greater than 2 is generally considered 'significant.'

Sample Subset	Predicted Category	N	Estimated error ± s.d.	Baseline error	Ratio
2013 Pools	Site	19	0.42 +/- 0.21	0.74	1.77
2013 Emergent	Site	18	0.55 +/- 0.11	0.72	1.31
2014 Pools	Site	19	0.62 +/- 0.26	0.74	1.19
2014 Emergent	Site	19	0.38 +/- 0.26	0.74	1.92

Temporal stability of microbial communities

Microbial communities sampled from tide pool and emergent rock habitats were significantly different between 2013 and 2014 using weighted UniFrac distance measures (**Figure 3.4a**, pools, ANOSIM R = 0.193, p = 0.001; **Figure 3.4b**, emergent rock, ANOSIM R = 0.318, p = 0.001), despite within-year maintenance of intra- and inter-site patterning described above (**Figure 3.2**, **Figure 3.3**). We tested whether this differentiation was a case of complete community turnover on a year-to-year temporal scale, a human-induced methodological artifact, or simply variability in membership of a community of rapidly reproducing organisms.

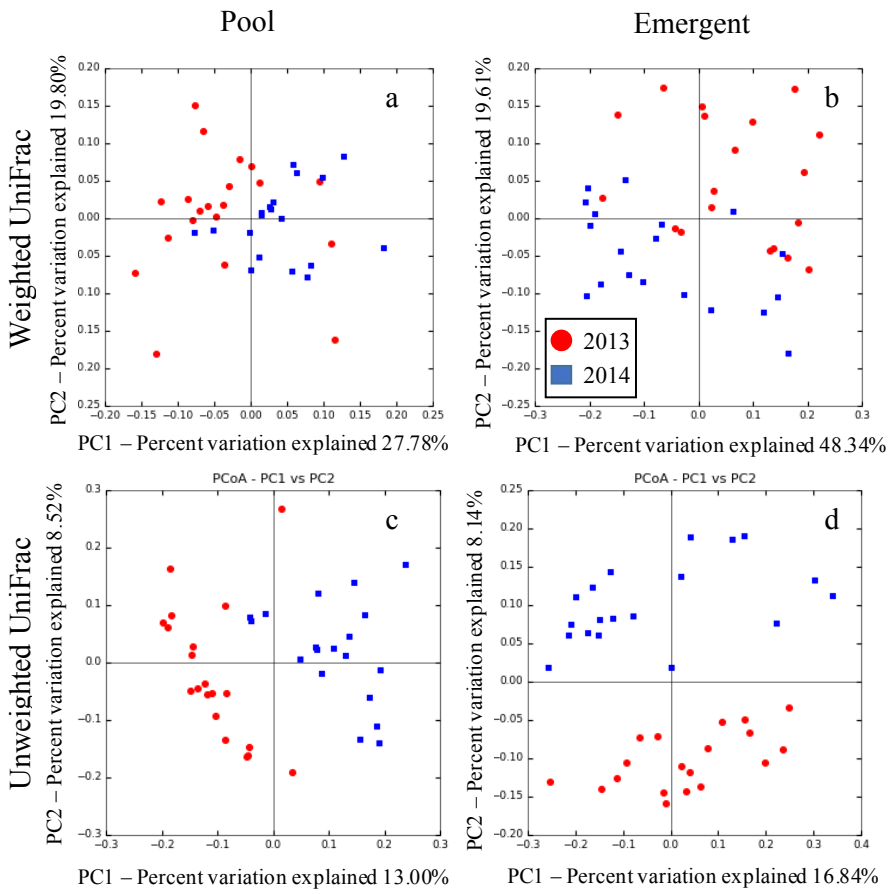

Figure 3.4. Ordination of microbial samples based on phylogenetic dissimilarity in community composition (UniFrac). Ordinations are based on pairwise UniFrac distances between samples, and sample points are colored by sampling year: Red = 2013, Blue = 2014. Panels **a** and **b** are principal coordinate (PCoA) plots for pool and emergent rock samples using Weighted UniFrac distance measure, and panels **c** and **d** are these same samples ordinated using Unweigted UniFrac distance.

Data ordinated using Unweighted UniFrac distance measure (**Figure 3.4c, d**) were more tightly clustered by year than when ordinated on Weighted UniFrac measure (pools ANOSIM R = 0.427, p = 0.001; emergent rock ANOSIM R = 0.349, p = 0.001). Since the Unweighted UniFrac distance measure credits rare taxa equally to abundant taxa, this result indicated that rare taxa could be driving the differentiation by year. Indeed, when taxa occurring in at least 5, 15, 25, and 35 of the 39 total samples were considered sequentially (**Figure 3.5**), the differentiation by year clustering was weakened (**Table 3.4**), demonstrating that spatially rare taxa are driving

inter-year differentiation in both pool and emergent rock habitats. To consider temporally rare OTUs as drivers of inter-year differentiation, we queried taxa occurring at least 500, 1000, 5000, and 10000 times in the dataset associated with each habitat type (**Figure 3.6**). Here, increasing the abundance threshold to 10000 yields loss of statistically significant differentiation by year in pools, while communities collected from emergent rock remain distinct between years at all abundance levels (**Table 3.5**).

PCoA ordination of microbial communities using a phylogenetic agnostic distance measure (Bray-Curtis) revealed a strengthened differentiation between years (**Figure 3.7**; pools ANOSIM $R = 0.66$, $p = 0.00$; emergent rock ANOSIM $R = 0.67$, $p = 0.001$) compared to ordinations on UniFrac distance measures (**Figure 3.4**).

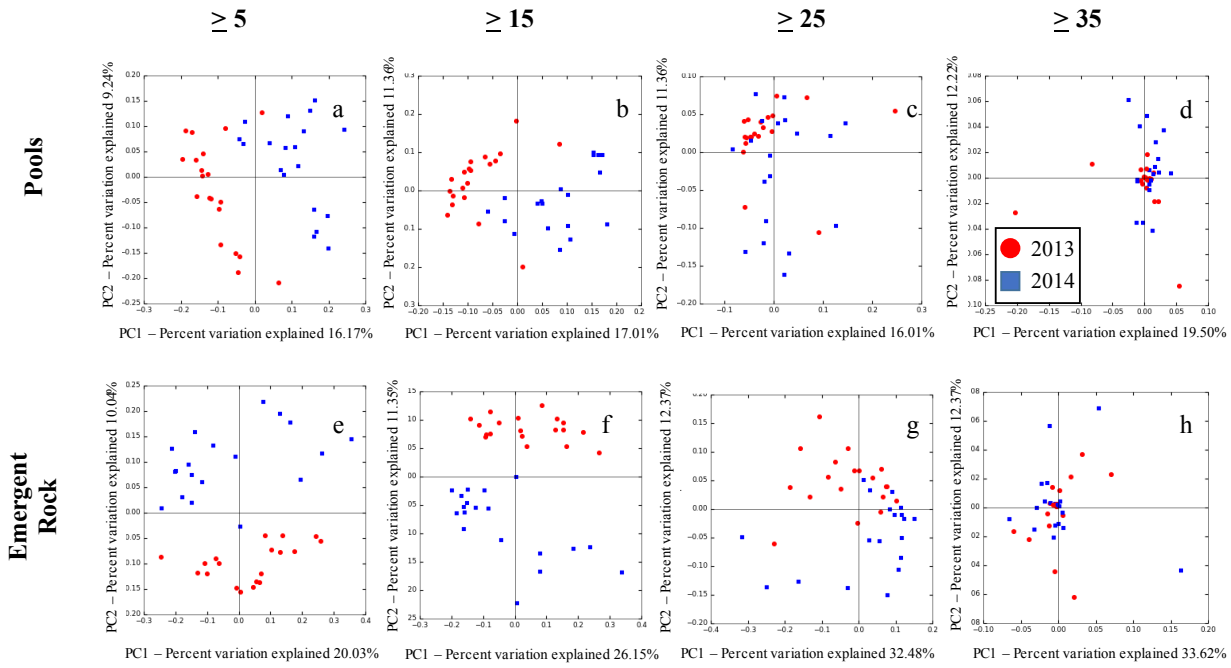

Figure 3.5. PCoA ordinations of microbial communities in OTU space, demonstrating importance of spatial rarity in community clustering. Ordinations are based on pairwise UniFrac distances between samples, and sample points are colored by sampling year: Red = 2013, Blue = 2014. Each column shows data filtered to include only those OTUs occurring in an increasingly stringent proportion of the full sample set (39 pool samples, 38 emergent rock samples). Ordinations are based on phylogenetic dissimilarity in community composition, taking abundance into account (weighted UniFrac). Panels **a - d** are principal coordinate (PCoA) plots for pool samples, and panels **e – h** are corresponding emergent rock samples.

Table 3.4. ANOSIM results (ANOSIM R and p-value) associated with PCoA clustering of microbial community samples by habitat at four levels of minimum OTU sample occurrence (**Figure 3.5**).

	≥ 5 Samples	**≥ 15 Samples**	**≥ 25 Samples**	**≥ 35 Samples**
Pools	R = 0.493 p < 0.001	R = 0.366 p < 0.001	R = 0.119 p < 0.001	R = 0.035 p = 0.030
Emergent Rock	R = 0.353 p < 0.001	R = 0.267 p < 0.001	R = 0.151 p = 0.002	R = 0.022 p = 0.093

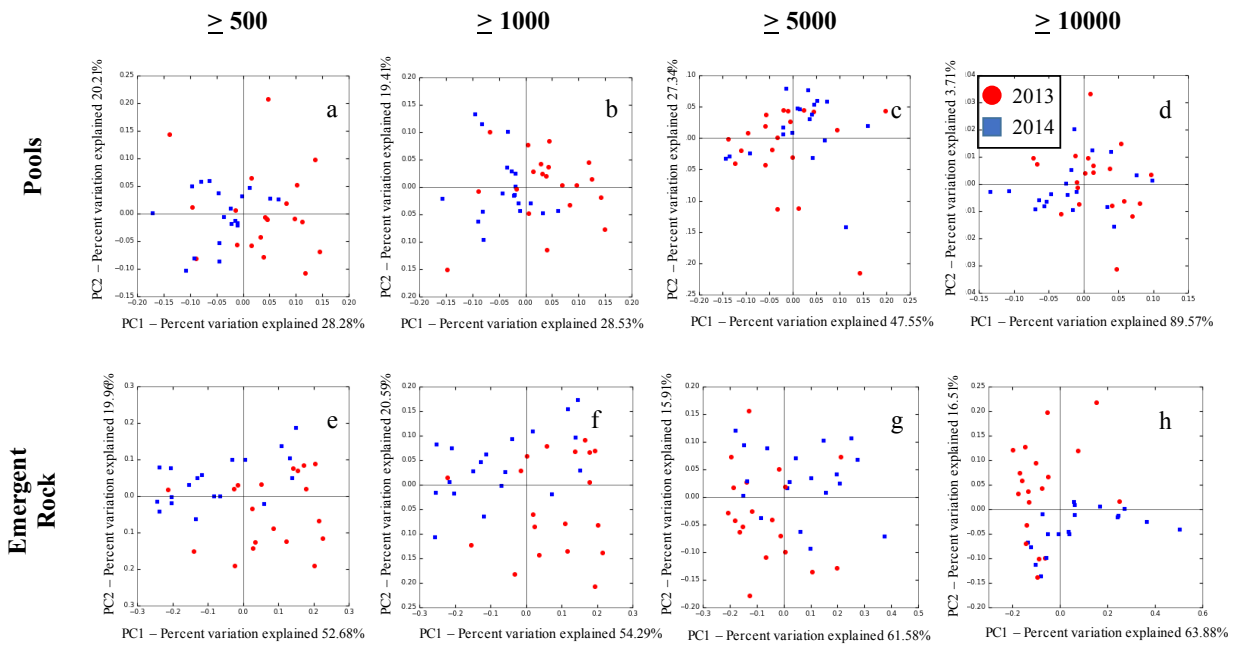

Figure 3.6. PCoA ordinations of microbial communities in OTU space, demonstrating importance of temporal rarity in community clustering. Ordinations are based on pairwise UniFrac distances between samples, and sample points are colored by sampling year: Red = 2013, Blue = 2014. Each column shows data filtered to include only those OTUs occurring at increasingly high abundance. Ordinations are based on phylogenetic dissimilarity in community composition, taking abundance into account (weighted UniFrac). Panels **a - d** are principal coordinate (PCoA) plots for pool samples, and panels **e – h** are corresponding emergent rock samples.

Table 3.5. ANOSIM results (ANOSIM R and p-value) associated with PCoA clustering of microbial community samples by habitat at four levels of minimum OTU abundance (**Figure 3.6**).

	≥ 500	**≥ 1,000**	**≥ 5.000**	**≥ 10,000**
Pools	R = 0.190 p < 0.001	R = 0.153 p < 0.001	R = 0.109 p = 0.008	R = 0.059 p = 0.078
Emergent Rock	R = 0.304 p < 0.001	R = 0.283 p < 0.001	R = 0.179 p = 0.010	R = 0.231 p < 0.001

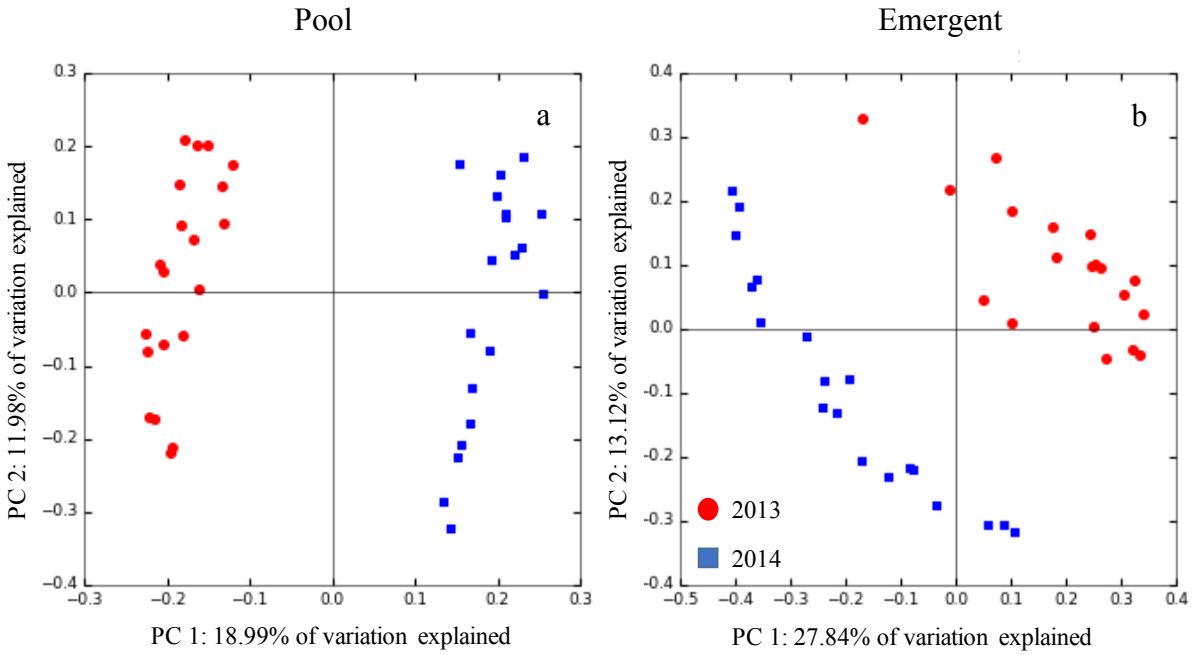

Figure 3.7. PCoA ordination of **a)** pool and **b)** emergent rock microbial community samples based on Bray-Curtis distance, a non phylogenetic measure of dissimilarity in community composition. Sample points are colored by sampling year: Red = 2013, Blue = 2014.

Random forest supervised learning on OTU tables collapsed to the Genus could robustly predict year. In pool and emergent rock samples separately, random forest models were successful at determining in which year a sample was collected, correctly classifying samples at least twice as effectively as one would expect (**Table 3.6**), indicating consistent weak differentiation in the substrate microbial communities collected in each sample year.

Table 3.6. Summary of predictive accuracy of random forest supervised learning models in classifying microbial samples to Sample Year in each habitat type. Tenfold cross validation models were constructed with 1,000 trees using OTUs from evenly rarified samples as predictors of Sample Year among samples cultured *in situ* in pools and on emergent rock separately. This analysis was run on collapsed absolute abundance OUT data at the Genus level.

Sample Subset	Predicted Category	N	Estimated error ± s.d.	Baseline error	Ratio
Pools	Sample Year	39	0.23 +/- 0.19	0.49	2.09
Emergent Rock	Sample Year	38	0.25 +/- 0.20	0.50	2.00

Biotic and abiotic factors correlate with differentiation of microbial community composition by habitat

Macrobiota surveyed immediately adjacent to microbial community sampling devices (BioBalls) differed by habitat (pool versus emergent rock), with weaker differentiation by site (**Figure 3.8**). Clustering by site was significantly different (ANOSIM $R = 0.241$, $p < 0.001$), with Westside Preserve and Iceberg Point being more similar, and clustering apart from Eagle Cove and Cattle Point in both emergent rock and tide pool data. In a visually striking contrast, habitat macrobiota were strongly clustered across NMDS axis 1 (ANOSIM $R = 0.634$, $p < 0.001$). Macrobiota with strongly negative scores (< -0.20) on NMDS axis 1, correlated more closely with emergent rock, are almost exclusively algal taxa (**Table 3C.1**). The three genera most strongly negatively associated with NMDS axis 1 are the brown algal species *Costaria costata* ($r^2 = -0.49$), *Ralfsia verrucosa* ($r^2 = -0.49$), and *Cymanthere triplicata* ($r^2 = -0.46$). In direct contrast, taxa with strongly positive scores (> 0.20) on NMDS axis 1, correlated more closely with the tide pool environment, are nearly all invertebrate taxa (**Table 3C1**). The three genera most strongly positively associated with NMDS axis 1 are the whelk *Nucella ostrina* ($r^2 = 0.39$), the nudibranch *Anisodoris nobilis* ('sea lemon') ($r^2 = 0.34$), and the crab genus *Hemigrapsus* ($r^2 = 0.33$) (**Table 3C.1**).

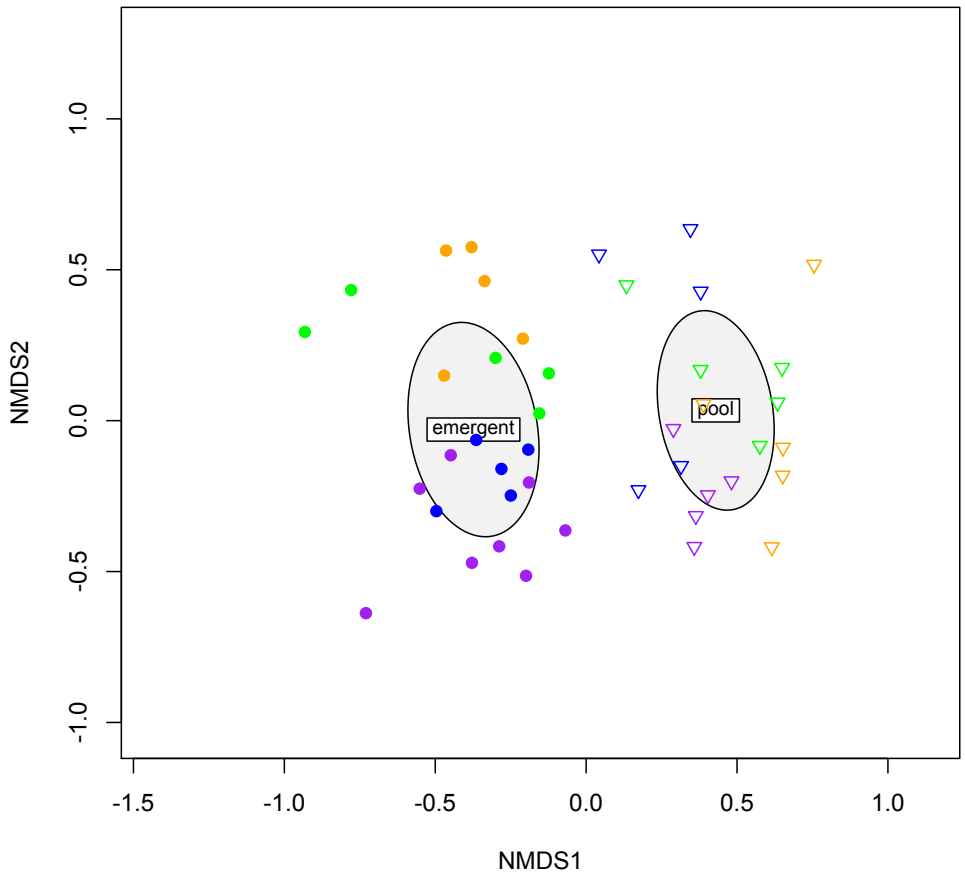

Figure 3.8. NMDS ordination of 2014 macrobiota community quadrat samples in species space (Jaccard distance). Plotted data are community surveys (quadrats on emergent hard substrate, total biota surveys in tide pools). Use of Jaccard distance standardizes these different survey types by collapsing survey data to presence/absence. Points are colored by site type (green = Westside Preserve, blue = Eagle Cove, purple = Cattle Point, orange = Iceberg Point), and shape-coded by habitat type (closed circle = Emergent Rock and open triangle = Pool).

Unconstrained ordination of microbial community samples with potential environmental drivers overlaid highlighted variables that were able to explain habitat (pool versus emergent rock) differentiation. In our NMDS ordination of 2014 microbial community samples in OTU space, a two-dimensional solution with low stress (11.46%) was reached (**Figure 3.9**). The identification of habitat type (pools versus emergent rock) formed a strong gradient on Axis 1.

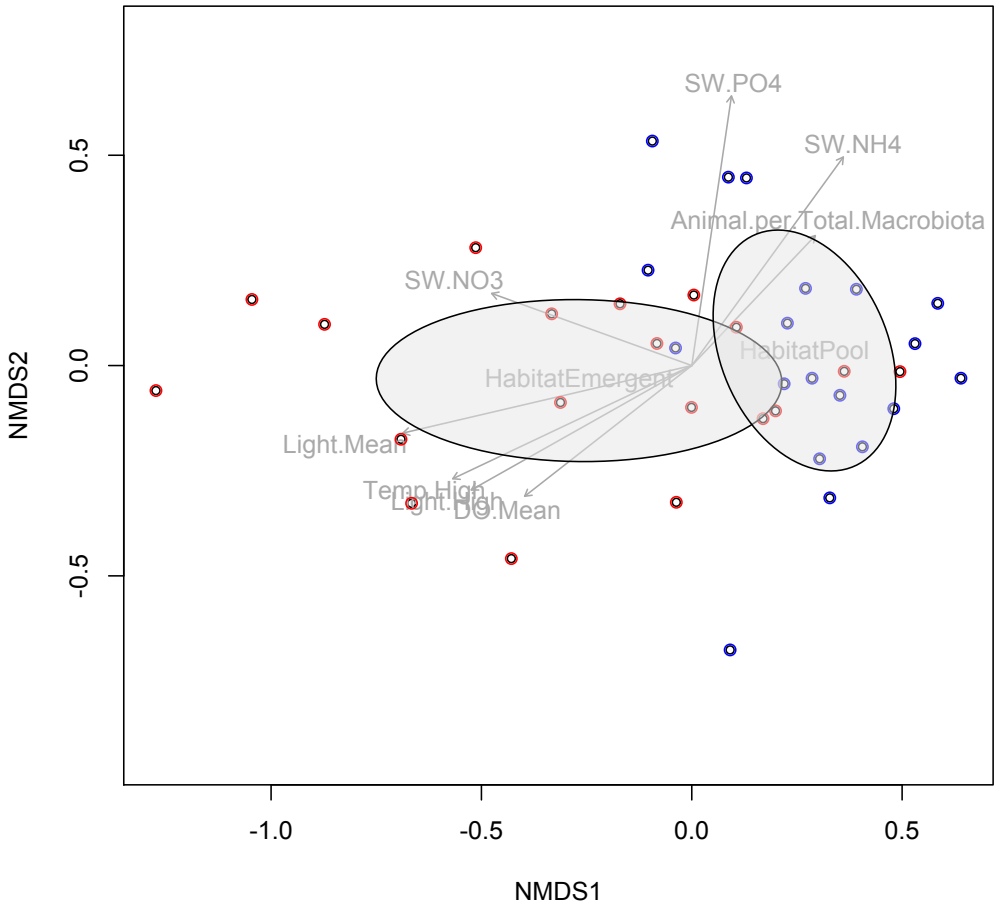

Figure 3.9. NMDS ordination of 2014 microbial community samples in OTU space (Jaccard distance). Points are colored by habitat type; Red = Emergent Rock and Blue = Pool. Environmental metadata measured in 2014 are overlaid, with bi-plot arrows shown for vectors correlated with axes at r^2 $p \leq 0.05$. Data used to create categorical data centroids and continuous data vectors are displayed in **Table 3.C.1**, and correlation strengths are displayed in **Table 3.7** and **Table 3.8**.

Environmental variables in the bi-plot overlay (r^2 cutoff of $p \leq 0.05$) also showed spread aligned with separate axes; arrows originating at the data centroid appear in two groups that are approximately perpendicular to one another. Parameters consistent with emergent rock habitat are aligned with Axis 1, while parameters consistent with pool habitat are aligned with Axis 2 (**Figure 3.9**).

Analysis of categorical factors associated with microbial community samples revealed that habitat is a strongly differentiating variable, while site is not significant (**Table 3.7**). Multiple continuous metadata parameters (vectors) emerge as significant explanatory variables in this ordination (**Table 3.8**). Vectors strongly negatively correlated with Axis 1 included seawater nitrate (NO_3^-) concentration, mean light intensity, maximum light intensity reached, and mean dissolved oxygen (DO), which were all higher at emergent rock habitat (**Table 3C.2**). Vectors strongly positively correlated with 2 are those observed to be indicative of tide pool conditions: seawater ammonium (NH_4^+) concentration, seawater phosphate (PO_4) concentration, and relative abundance 'animal' in surveys of macrobiota (**Table 3.8**).

Table 3.7. **a)** Correlation of the data centroids of all levels of two environmental metadata categorical factors (Site, Habitat) with NMDS Axes 1 and 2 (**Figure 3.8**). The reported correlation of the two levels of the factor 'Habitat' with each axis are redundant, as these are reciprocals of each other. **b)** Results of statistical test of goodness of fit associated with each categorical factor with the NMDS ordination of microbial community data.

a) Centroids

	NMDS 1	**NMDS 2**
Site: Cattle Point	0.110	-0.098
Site: Eagle Cove	0.108	-0.032
Site: Iceberg Point	-0.258	0.206
Site: Westside Preserve	0.016	-0.061
Habitat: Emergent rock	-0.268	-0.036
Habitat: Pool	0.268	0.036

b) Goodness of fit

	r^2	**Pr(>r)**
Site	0.136	0.138
Habitat	0.279	**0.001**

Table 3.8. Correlation of environmental metadata continuous vectors with NMDS Axes 1 and 2 (**Figure 3.8**), with results of statistical tests of probability of correlation strength associated with each vector.

	NMDS 1	NMDS 2	r^2	Pr (>r)
Seawater [NH_4^+] (μM)	0.589	0.809	0.340	**0.002**
Seawater [NO_2^-] (μM)	0.762	0.648	0.085	0.201
Seawater [NO_3^-] (μM)	-0.941	0.339	0.231	**0.012**
Seawater [PO_4] (μM)	0.146	0.989	0.379	**0.001**
Seawater [$Si(OH)_4$] (μM)	-0.558	0.830	0.027	0.626
Mean Light (lux)	-0.974	-0.228	0.450	**0.001**
Maximum Light (lux)	-0.871	-0.491	0.328	**0.002**
Mean Temperature (°C)	-0.867	0.499	0.153	0.055
Maximum Temperature (°C)	-0.904	-0.428	0.357	**0.001**
Mean Dissolved Oxygen (mg/L)	-0.788	-0.616	0.230	**0.010**
Relative abundance 'animal'	0.689	0.725	0.164	**0.042**

A search for gene sequences associated with nitrogen metabolisms among benthic field-cultured microbial samples allowed us to ask whether levels of the categorical factors 'habitat' and 'site' varied in the abundance of OTUs associated with each metabolism (**Figure 3.10**). Statistical variation by treatment was measured on log-transformed count data (two-way ANOVA; **Table 3.9**). Measures of two pathways were elevated on emergent rock relative to pools: nitrogen fixation (10-fold difference) and assimilatory nitrate reduction (2-fold difference). Site and habitat acted interactively to drive patterns of sequences associated with denitrification and dissimilatory nitrate reduction.

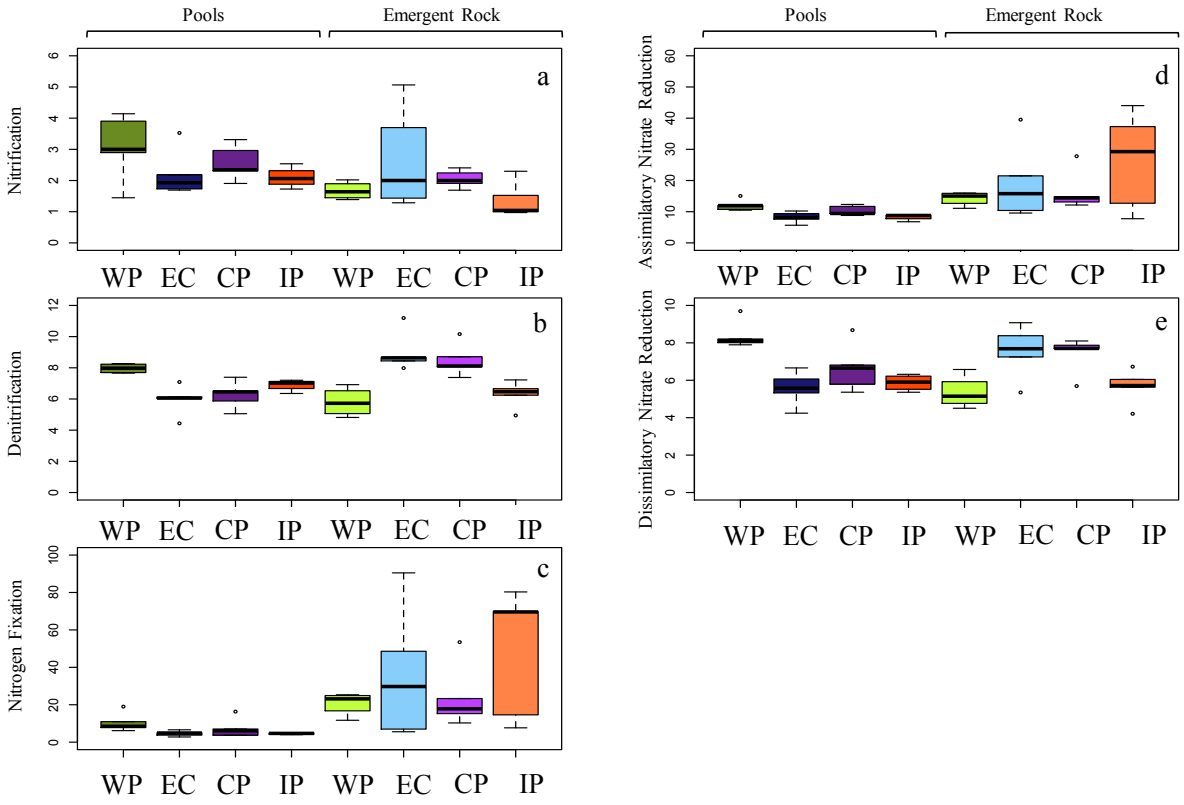

Figure 3.10. Mean counts of OTUs containing gene sequences associated with 5 key nitrogen metabolisms (a) Nitrification, b) Denitrification, c) Nitrogen Fixation, d) Assimilatory Nitrate Reduction, and e) Dissimilatory Nitrate Reduction) within samples from two habitats (pools, emergent rock) at four sites (Westside Preserve (WP), Eagle Cove (EC), Cattle Point (CP), and Iceberg Point (IP). Mean counts were generated by querying the corresponding OTU table for presence of KEGG orthologs (**Table 3.D.1**). Plotted data are untransformed counts.

Table 3.9. Results of two-way ANOVA statistical tests associated with counts of OTUs containing gene sequences associated with five key nitrogen metabolisms within samples from two habitats at four sites. Plotted means (**Figure 3.10**) are untransformed, but ANOVA tests performed on log-transformed (log(x) + 0.01) data to meet assumptions of normality.

	Nitrification	**Denitrification**	**Nitrogen fixation**	**Assimilatory Nitrate Reduction**	**Dissimilatory Nitrate Reduction**
Habitat	$F_{1,30} = 7.06$, $p = 0.13$	$F_{1,30} = 4.49$, **$p = 0.04$**	$F_{1,30} = 35.11$, **$p < 0.001$**	$F_{1,30} = 20.82$, **$p < 0.001$**	$F_{1,30} = 0.13$, $p = 0.72$
Site	$F_{3,30} = 2.09$, $p = 0.13$	$F_{3,30} = 1.49$, $p = 0.24$	$F_{3,30} = 0.50$, $p = 0.68$	$F_{3,30} = 0.32$, $p = 0.81$	$F_{3,30} = 2.90$, **$p = 0.05$**
*Habitat * Site*	$F_{3,30} = 1.78$, $p = 0.17$	$F_{3,30} = 17.11$, **$p = < 0.001$**	$F_{3,30} = 1.33$, $p = 0.28$	$F_{3,30} = 1.81$, $p = 0.17$	$F_{3,30} = 9.74$, **$p = < 0.001$**

DISCUSSION

Habitat control of microbial community composition

Microbial communities were highly differentiated between habitat types (tide pools, emergent rock) that were separated by small distances (less than 25 cm in most tide pool-emergent rock pairs). In PCoA ordinations (**Figure 3.2**), benthic samples clustered into distinct groups reflecting these two habitat types using both weighted and unweighted distance metrics, suggesting both similar abundance of shared taxa among samples cultured within a habitat type, as well as similar presence/absence of unique taxa within each habitat type.

Several phototrophic cyanobacteria were tightly associated with emergent substrate (**Table 3.2a, b**) (consistent across sample years). The most abundant taxon in all emergent rock samples was a cyanobacteria from the family Pseudanabaenaceae, an understudied but cosmopolitan filamentous group (Díez *et al.* 2007). In rocky intertidal biofilms, cyanobacteria form a critical component of the benthic food web via their contribution to intertidal productivity (Nagarkar 1996). The appearance of elevated cyanobacteria on emergent rock habitat signals presence of photosynthetic biomass, but also indicates that there is a surplus of primary productivity not controlled by grazers in this habitat (Thompson *et al.* 2004). An alternate explanation for this pattern is that abundant photosynthetic components of biofilm are actually not preferred by grazers, or, in the case of this study, inaccessible to grazers because of the complex pegged BioBall structure. Chlorophyll *a* concentration in BioBall communities cultured in tide pools versus on emergent rock was not measured here, but we would expect elevated levels on emergent rock where grazer abundance is lower (**Figure 3.8**) and light is elevated (**Table 3.C.2**). Previous studies in this system measured increased cyanobacterial concentrations on shells of mussels growing on emergent rock versus mussels in tide pools (Pfister *et al.*

2014b), providing evidence that this component of the biofilm is actually somewhat insensitive to grazing.

Cosmopolitan microbial community composition across sites

Though our supervised learning protocol was highly effective at distinguishing tide pool from emergent habitat for these samples, this method could not correctly classify samples by site. Sites, despite variation in macroscopic community composition (**Figure 8**, **Table 3C.1**), hosted only weakly differentially structured microbial communities (**Figure 3.3**). Any site-level difference was exceeded by prevailing distinction between pool and emergent rock habitat that was consistent across all sites in the region (**Figure 3B.1**). Although distribution of microbial taxa was broadly regional, microbial community structure in this NE Pacific rocky intertidal system was strongly environmentally selected. Inability of site identity to explain microbial community patterning (**Figure 3.9**, **Table 3.7**) allows us to conclude that regional factors that do explain microbial community structure, such as cyclical tidal disturbance parameters (temperature and light fluctuations, seawater nutrients (**Figure 9, Table 7, Table 3C.1**)), along with unquantified seawater currents and mixing, swamp any site-level microbial community signal.

Microbial communities show annual variability

We observed significant microbial community turnover on a coarse annual scale (August 2013 to August 2014) (**Figure 3.4**), despite maintenance of clustering by source habitat (**Figure 3.2**). While common taxa were similar in relative abundance between years, it was the apparent turnover of spatially relatively rare taxa that drove this temporal variability (**Figure 3.5**).

Although microbial communities sampled from diverse ecosystems are frequently dominated by the same taxa, it often is rare taxa that differentiate aquatic microbial communities (e.g. Sogin *et al.* 2006; Lennon and Jones 2011; Pfister *et al.* 2014).

Rare taxa in marine systems likely function as a microbial 'seed bank' that is variable across time and space (Lennon and Jones 2011; Caporaso *et al.* 2012b; Gibbons *et al.* 2013).. Microbial metabolism of marine nutrients can actually outpace eukaryotic primary producers, particularly when a resource (e.g. nitrogen) is limiting (Könneke *et al.* 2014; Pfister *et al.* 2016). If relatively rare microbial taxa capable of high nutrient metabolism are present and capable of a rapid numerical and functional response to changes in nutrient availability, it is possible that microbial communities serve an important buffering role in the face of rapid changes in nutrient availability in coastal systems (Fowler *et al.* 2013). Therefore, though rarity does not preclude functional importance, as shown through quantified metabolic activity of uncommon taxa (e.g. (Hamasaki *et al.* 2007; Pfister *et al.* 2016), the functional roles of the rare taxa we detected here are yet unknown.

Robust seasonal dynamics are a key feature of microbial communities in multiple environments (Bardgett *et al.* 1999; Caporaso *et al.* 2012b). Microbial community data from seawater at the English Channel L4 marine observatory reveal close alignment between taxa present within a sample randomly selected for deep sequencing and taxa present in many shallow-sequenced samples from multiple time points, suggesting that seasonal variability is simply numerical modulation of a persistent microbial community (Caporaso *et al.* 2012b). This pattern contrasts with an alternative hypothesis of seasonal changes in taxa present in the system. Our results follow a similar pattern on an annual timescale. The most common taxa driving major differentiation between tide pool and emergent rock show high similarity between years

(**Table 3.2**). Further, when we performed PCoA ordination and clustering statistics using a phylogenetic-agnostic distance measure (Bray-Curtis), years became more tightly clustered than when ordinated on phylogenetic distance (**Figure 3.7**). This increase in differentiation when all taxa are weighted equally in terms of uniqueness suggests that the taxa driving this distinction are likely closely related and perhaps that closely-related taxa are performing similar functional roles in this system. Seasonal variations in emersion stress are important regulators of intertidal microbial assemblages (Thompson *et al.* 2004), particularly photosynthetic components tied to insolation and grazer abundance (Nicotri 1977; Underwood 1984; Jenkins *et al.* 2001).

Overall, we conclude that dominant taxa are common between years, but that rarer groups, which may have high functional importance, show high turnover.

Physical and biotic correlates with microbial community composition explained by habitat type

Tide pools and emergent rock are associated with both dissimilar faunal abundances and distinctive seawater nutrient concentrations (Bracken 2004; Bracken and Nielsen 2004b; Pfister 2007; Pather *et al.* 2014) (**Table 3C.1**). Here, surveys of macrobiota revealed that tide pools are characterized by higher faunal composition than emergent rock at all study sites, with correspondingly elevated ammonium (NH_4^+) and phosphate (PO_4) concentrations (both associated with animal excretion). In tide pools, this animal excretion of nitrogen can ameliorate isolation from the nutrient-rich oceanic water column that occurs at low tide (Bracken 2004). Nitrate (NO_3^-) concentration is elevated in the oceanic water column relative to tide pools, where the limited quantity of this nutrient delivered with tidal exchange is a heavily contested resource that is accessed by both intertidal algae (Bracken 2004) and microbes (Pfister *et al.* 2010, 2016).

Analysis of gene orthologs identified as having functional roles in specific nitrogen metabolism pathways revealed a strong tide pool/emergent rock distributional pattern in genes associated with nitrogen fixation and assimilatory nitrate reduction. The mean abundances of OTUs associated with those pathways were 10-fold and 2-fold (respectively) elevated on emergent rock above mean abundance in pools (**Figure 3.9**, **Table 3.9**). Functionally, this suggests a capacity of cyanobacteria, which were strongly elevated on emergent rock (**Table 3.2**), to ameliorate isolation from seawater nutrient pool at low tide, a known stressor for intertidal biota (Bracken 2004).

This cyanobacterial distribution pattern has previously been recognized in mussel shell-associated microbial communities in tide pools versus on emergent rock benches (Pfister *et al.* 2010). Although most cyanobacteria are capable of fixing atmospheric nitrogen (N_2), Pfister et al. (2010) found strong tide pool-emergent rock differentiation occurring among photoautotrophic cyanobacteria, those that do not fix atmospheric nitrogen. The microbial samples in that study came directly from shells of live mussels, a continuous source of readily biologically accessible nitrogen in the form of ammonium, so nitrogen fixation was likely less important. In the current study, the finding of increased nitrogen fixation gene orthologs paired with increased cyanobacteria on inert emergent rock suggests that these taxa are indeed capable of fixing atmospheric nitrogen. This could be a scenario of continuous primary productivity on emergent rock where light is abundant despite periodic nutrient limitation stress caused by tidal cycles.

CONCLUSIONS

This multi-scale study reveals strong spatial structuring of microbial community composition by local habitat despite strong regional variation in community structure of macrobiota. Temporal turnover of microbial communities was high among rare taxa, despite maintenance of a common core set of microbial organisms.

Taken together, results from this study indicate strong inter-site (>25 km) homogeneity of intertidal microbial communities present in biofilm, with overwhelming intra-site (all samples collected within <100m horizontal transect) heterogeneity. This work contributes important and novel information about the importance of local-scale factors as drivers of distribution and function of intertidal microbial communities. Rocky intertidal ecosystems have long provided a useful field laboratory for investigation of relative importance of species interactions and interactions between species and physical factors in driving community organization. Nearshore oceanographic processes influence intertidal productivity (Menge *et al.* 1997), and predation further impacts community dynamics (Paine 1966). Nutrient ratios within organisms and the water column provide a unique perspective from which to view these issues (Sterner and Elser 2002). Here, seawater nutrients were important correlates with microbial community structure differentiation between intra-site intertidal habitats (**Figure 3.8**), underscoring the pertinence of including nutrient concentrations among drivers of whole ecosystem function. While productivity is an important factor governing intertidal communities, the role of nutrients in this process is not fully understood, and may contribute to the top-down impacts of predation in addition to the bottom-up impacts of nutrient loading or productivity (Menge *et al.* 1997).

Coastal systems host a diversity of macrobiota (multicellular flora and fauna) that contribute to nitrogen cycling through nitrogen production, retention, and removal (e.g. Nelson *et*

al. 2013) and have influential associations with microbiota that further influence nitrogen processing in coastal systems (Moulton *et al.* 2016). High nutrient fluxes (NH_4^+, NO_3^-, NO_2^-, PO_4^{3-}) in association with rocky intertidal biofilms (Magalhães *et al.* 2003) suggest that these inert substrata are also hotspots for elevated microbial activity. Here, seawater DIN concentrations were key correlates with microbial community structure (**Figure 3.8**). The coastal marine nitrogen cycle is undergoing rapid fluctuation, both via loss of faunal excretors (Roman and McCarthy 2010; Doughty *et al.* 2015) and increased anthropogenic inputs (Carpenter *et al.* 1998; Howarth 2008). By documenting natural patterns of variability in intertidal biota abundance and ways in which this distribution is associated with nitrogen availability, studies like this offer clues about possible functional roles of the biota in the nitrogen cycle. Our study suggests that the rocky intertidal-associated microbial community is robust to regional factors, but sensitive at very local scales. Improved understanding of nutrient uptake and use primary producers together with microbes will enable better protection of the temperate coastlines, where nitrogen-excreting fauna are being harvested at the highest rates (Pauly *et al.* 1998).

ACKNOWLEDGEMENTS

The research described in this paper has been funded in part by the United States Environmental Protection Agency (EPA) under the Science to Achieve Results (STAR) Graduate Fellowship (OMM). This work was also supported by NSF OCE-0928232 (CAP), the Earth Microbiome Project (JAG), The University of Chicago Committee on Evolutionary Biology Hinds Fund (OMM), and Friday Harbor Laboratories Graduate Fellowships (OMM). We thank San Juan County Land Bank and WA Bureau of Land Management for access to field sites, G. Siegmund, A. Thomson, K. Biederbeck, N. Rivlin, N. Colvard, M. Eisenlord, H. Hayford, and A. Henry for

field assistance, J. Hampton-Marcell and S. Owens for sequencing assistance, G. Olack for stable isotope analysis assistance, and G. Dwyer, J.T. Wootton, and M. Coleman for helpful comments on research design, analysis, and the manuscript.

APPENDIX 3A: Procrustes analysis comparing Unifrac distance measures.

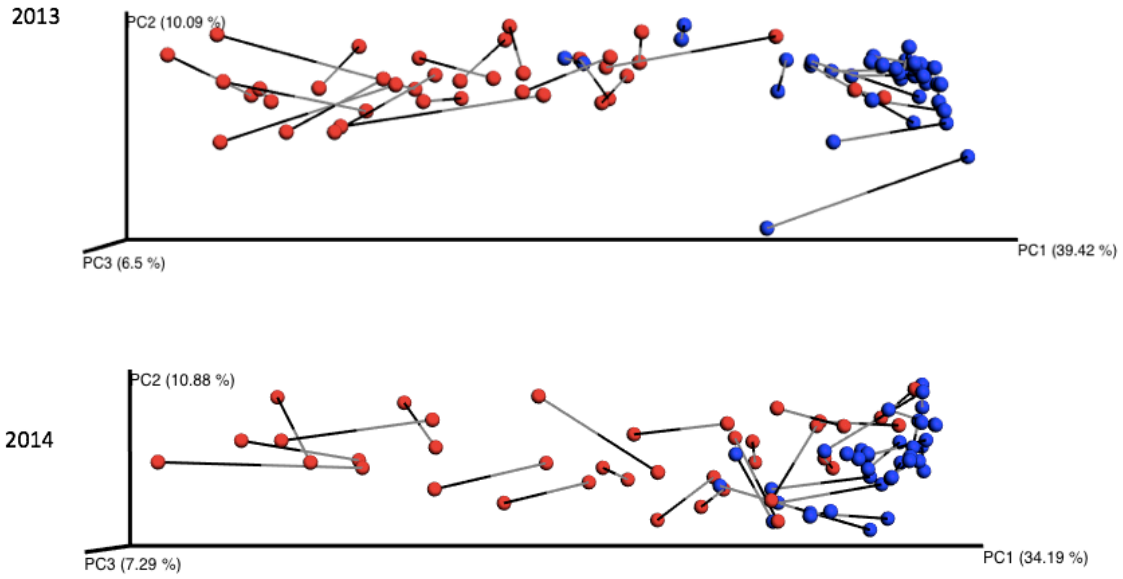

Figure 3.A.1. Procrustes analysis comparing microbial communities ordinated on weighted and unweighted Unifrac distance measures. Procrustes analysis compares the shape of two PCoA plots by optimally rotating and scaling one plot to best fit the other, with the goodness of fit measured by the M^2 statistic. P-values are generated using a Monte Carlo simulation in which sample identifiers are shuffled and resampled (here 1,000 times) and the M^2 statistic is compared to the distribution drawn from these permutations, generating a Monte Carlo resampling p-value. Points here are colored by habitat (blue = pool, red = emergent rock). The strong clustering pattern is consistent between methods in both sample years (2013 $M^2 = 0.286$, $p < 0.001$; 2014 $M^2 = 0.313$, $p < 0.001$), indicating that we can derive the same beta diversity conclusions from these data regardless of which distance metric is used. Further, in both years, weighted and unweighted Unifrac distance measures are more tightly coupled in pool data than emergent rock, indicating that within a year, abundance is less variable among OTUs found in pools.

Appendix 3B: Barplots of unique microbial taxa.

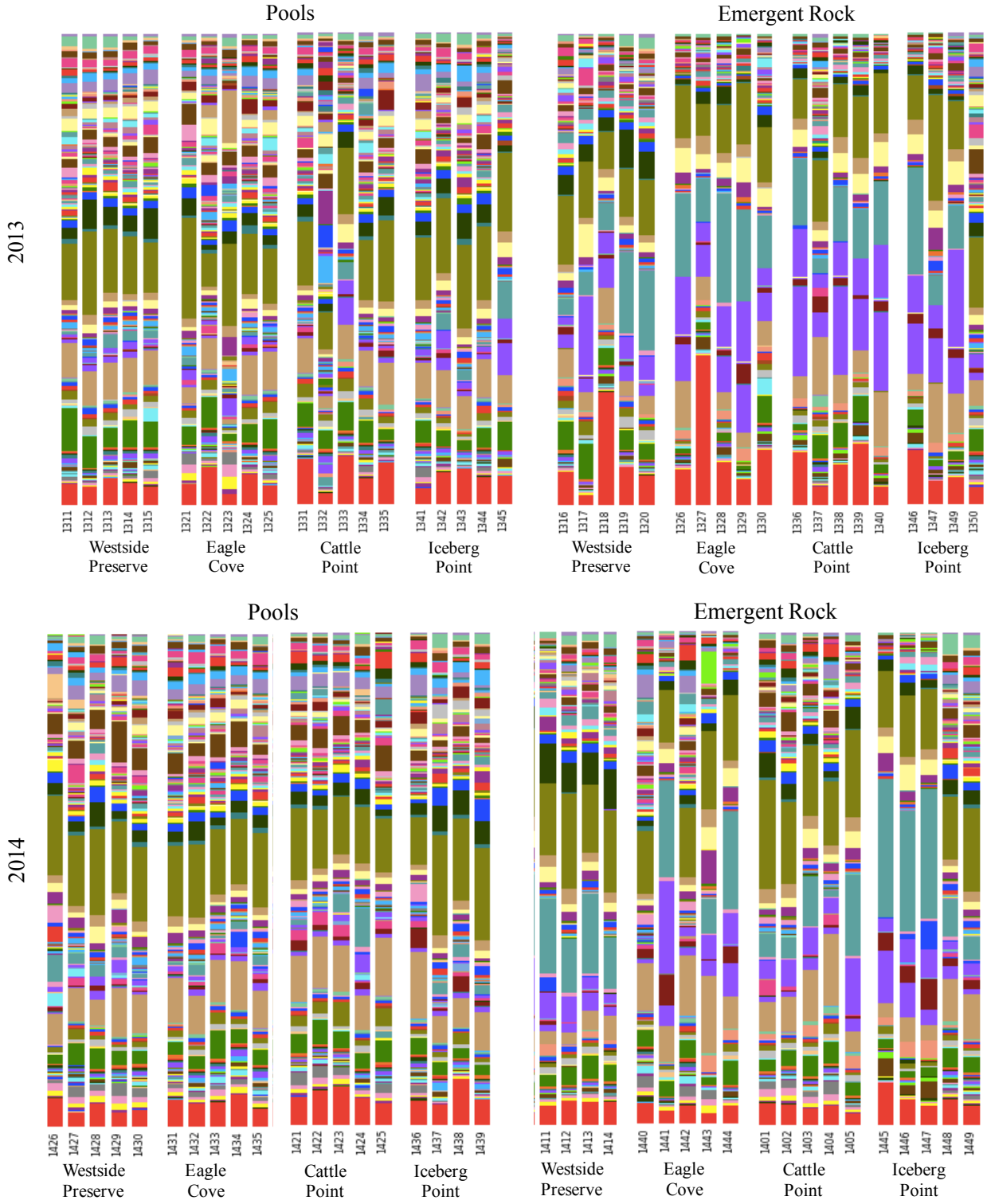

Figure 3.B.1. Barplots showing relative abundance of unique taxa at the genus level (L6) in all samples collected from two habitats (pool, emergent rock) at each site (Westside Preserve, Eagle Cove, Cattle Point, Iceberg Point) in both study years (2013, 2014).

Appendix 3C: Macrobiota species and associated environmental data.

Table 3.C.1. Correlations (r^2) of surveyed macrobiota (2014) with NMDS axes 1 and 2 (**Figure 3.8**). The analysis yielding these data was performed using the Jaccard distance metric, meaning that correlation of taxa with axes is based on presence/absence, not abundance within the sample unit.

Taxa	MDS1	MDS2
Costaria costata	-0.49	0.15
Ralfsia verrucosa	-0.49	0.15
Cymathere triplicata	-0.46	0.18
Alaria sp.	-0.31	0.02
Fucus gardneri	-0.24	0.14
Nemertean worm	-0.24	-0.14
Porphyra sp.	-0.24	0.26
Barnacle recruits	-0.22	0.27
Palmaria palmata	-0.21	-0.10
Mazzaella splendens	-0.20	-0.14
Leathesia difformis	-0.20	0.30
Cryptosiphonia woodii	-0.20	0.28
Halosaccion glandiforme	-0.20	0.20
Mastocarpus crust	-0.19	0.03
Desmarestia ligulata	-0.19	-0.23
Phyllospadix serrulatus	-0.18	0.25
Microcladia borealis	-0.18	0.07
Odonthalia floccosa	-0.18	-0.14
Endocladia muricata	-0.17	0.15
Egregia menziesii	-0.17	-0.16
Aplidium sp.	-0.17	-0.24
Mastocarpus papillatus upright	-0.17	-0.08
Bryozoans	-0.17	-0.13
Saccharina sessile	-0.16	-0.03
Osmundea sp.	-0.15	-0.22
Cryptopleura ruprechtiana	-0.14	-0.16
Ulva sp.	-0.13	0.04
Orange sponge	-0.12	-0.09
Saccharina latissima	-0.11	-0.21
Green sponge	-0.11	-0.06
Semibalanus cariosus	-0.09	-0.12
Urticina crassicornis	-0.08	-0.01
Leptosynapta sp.	-0.08	0.14
Juvenile *Cancer* sp.	-0.07	-0.04
Katharina tunicata	-0.07	0.05
Henricia leviuscula	-0.06	-0.21
Corallina sp.	-0.06	-0.02
Acmea mitra	-0.04	-0.19
Eudistylia vancouveri	-0.03	-0.13
Desmarestia viridis	-0.03	-0.23
Leptasterias sp.	-0.01	0.08
Balanus glandula	-0.01	-0.16

Taxa	MDS1	MDS2
Acrosiphonia coalita	0.01	0.26
Idotea sp.	0.02	0.07
Cryptochiton stelleri	0.03	0.19
Tectura scutum	0.03	-0.06
Gammaridean amphipods	0.04	0.17
Tonicella lineata	0.05	-0.09
Mytilus californianus	0.06	-0.12
Lottia pelta	0.07	0.07
Mopalia muscosa	0.07	-0.05
Diadora aspera	0.07	0.11
Pugettia gracilis	0.08	0.01
Phyllospadix scouleri	0.09	-0.03
Dodecaceria fewkesi	0.09	0.00
Crustose coralline algae	0.11	-0.01
Nucella lamellosa	0.11	-0.12
Prionitis sternbergii	0.12	0.24
Pholidae	0.16	-0.05
Strongylocentrotus droebachiensis	0.18	0.01
Neorhodomela oregona	0.18	0.17
Hermit crabs	0.19	-0.09
Cryptolithodes sitchensis	0.19	-0.22
Red crust algae	0.19	-0.02
Calliostoma sp.	0.21	-0.07
Chthalamus dalli	0.21	-0.13
Nucella canaliculata	0.21	-0.15
Amphissa columbiana	0.23	0.09
Strongylocentrotus purpuratus	0.25	0.09
Searlesia dira	0.25	0.01
Sculpin	0.26	-0.07
Red sponge	0.28	-0.06
Littorina scutulata	0.30	-0.14
Rostanga pulchra	0.30	-0.04
Anemone	0.30	-0.11
Pisaster ochreaceus	0.31	-0.01
Polysiphonia sp.	0.32	0.17
Littorina sitkana	0.32	-0.21
Lottia digitalis	0.33	-0.19
Purple sponge	0.33	0.03
Hemigrapsus sp.	0.33	-0.10
Anisodoris nobilis	0.34	-0.10
Nucella ostrina	0.39	0.24

Table 3.C.2. Measures of key biotic and abiotic variables coincident with microbial rRNA analyses within tidepools and on emergent rock in 2013 and 2014 at 4 locales in the San Juan Islands, WA.

Sample	Site	Habitat	[NH4] (μM)	[NO2] (μM)	[NO3] (μM)	[PO4] (μM)	[Si(OH)4] (μM)	Light Mean (Lux)	Light Max. (Lux)	Temp. Mean (°C)	Temp. Max (°C)	DO Mean (mg/L)	Rel. Abun. Animal
1401	CP	Emergent	1.33	0.45	13.24	1.63	25.20	10644.28	330668.90	12.42	34.59	11.97	0.17
1402	CP	Emergent	1.33	0.45	13.24	1.63	25.20	10644.28	330668.90	12.42	34.59	11.97	0.17
1403	CP	Emergent	1.33	0.45	13.24	1.63	25.20	10644.28	330668.90	12.42	34.59	11.97	0.17
1404	CP	Emergent	1.33	0.45	13.24	1.63	25.20	10644.28	330668.90	12.42	34.59	11.97	0.17
1405	CP	Emergent	1.33	0.45	13.24	1.63	25.20	10644.28	330668.90	12.42	34.59	11.97	0.17
1421	CP	Pool	8.13	0.88	13.18	2.67	36.95	88.64	2069.07	12.53	26.00	9.56	0.81
1422	CP	Pool	9.15	0.92	4.24	2.67	17.44	88.64	2069.07	12.53	26.00	9.55	0.47
1423	CP	Pool	10.69	1.20	11.91	3.16	27.47	88.64	2069.07	12.53	26.00	2.30	0.52
1424	CP	Pool	6.75	0.88	4.10	2.13	13.11	88.64	2069.07	12.53	26.00	2.75	0.42
1425	CP	Pool	10.64	0.81	4.27	3.38	31.03	88.64	2069.07	12.53	26.00	5.41	0.59
1440	EC	Emergent	1.12	0.35	17.41	2.06	36.21	16045.95	308624.30	12.32	35.97	11.64	0.28
1441	EC	Emergent	1.12	0.35	17.41	2.06	36.21	16045.95	308624.30	12.32	35.97	11.64	0.28
1442	EC	Emergent	1.12	0.35	17.41	2.06	36.21	16045.95	308624.30	12.32	35.97	11.64	0.28
1443	EC	Emergent	1.12	0.35	17.41	2.06	36.21	16045.95	308624.30	12.32	35.97	11.64	0.28
1444	EC	Emergent	1.12	0.35	17.41	2.06	36.21	16045.95	308624.30	12.32	35.97	11.64	0.28
1431	EC	Pool	7.27	0.33	0.58	5.43	50.20	74.81	1759.90	11.91	25.22	6.22	0.43
1432	EC	Pool	16.51	0.60	1.78	5.79	60.44	74.81	1759.90	11.91	25.22	2.85	0.48
1433	EC	Pool	20.33	0.88	4.02	4.05	43.44	74.81	1759.90	11.91	25.22	3.24	0.39
1434	EC	Pool	11.96	0.98	5.62	3.59	30.45	74.81	1759.90	11.91	25.22	3.75	0.67
1435	EC	Pool	12.85	0.42	0.99	4.98	45.46	74.81	1759.90	11.91	25.22	3.53	0.23
1445	IP	Emergent	1.41	0.44	15.64	2.20	39.64	25134.18	264535.10	13.66	35.65	14.88	0.28
1446	IP	Emergent	1.41	0.44	15.64	2.20	39.64	25134.18	264535.10	13.66	35.65	14.88	0.28
1447	IP	Emergent	1.41	0.44	15.64	2.20	39.64	25134.18	264535.10	13.66	35.65	14.88	0.28
1448	IP	Emergent	1.41	0.44	15.64	2.20	39.64	25134.18	264535.10	13.66	35.65	14.88	0.28

Table 3.C.2. *Continued*.

Sample	Site	Habitat	[NH4] (µM)	[NO2] (µM)	[NO3] (µM)	[PO4] (µM)	[Si(OH)4] (µM)	Light Mean (Lux)	Light Max. (Lux)	Temp. Mean (°C)	Temp. Max (°C)	DO Mean (mg/L)	Rel. Abun. Animal
1449	IP	Emergent	1.41	0.44	15.64	2.20	39.64	25134.18	264535.10	13.66	35.65	14.88	0.28
1436	IP	Pool	13.49	0.47	10.03	2.67	24.92	44.71	1617.20	12.27	26.90	7.90	0.61
1437	IP	Pool	18.93	0.70	12.40	10.87	24.91	44.71	1617.20	12.27	26.90	6.13	0.92
1438	IP	Pool	12.58	1.34	29.99	15.57	29.54	44.71	1617.20	12.27	26.90	6.22	0.49
1439	IP	Pool	17.23	1.11	17.89	10.54	28.23	44.71	1617.20	12.27	26.90	2.54	0.43
1411	WP	Emergent	0.99	0.34	18.84	2.00	43.00	9324.03	330668.90	11.12	30.56	10.11	0.23
1412	WP	Emergent	0.99	0.34	18.84	2.00	43.00	9324.03	330668.90	11.12	30.56	10.11	0.23
1413	WP	Emergent	0.99	0.34	18.84	2.00	43.00	9324.03	330668.90	11.12	30.56	10.11	0.23
1414	WP	Emergent	0.99	0.34	18.84	2.00	43.00	9324.03	330668.90	11.12	30.56	10.11	0.23
1426	WP	Pool	9.65	1.14	15.00	3.00	38.03	36.22	1129.66	11.12	24.16	2.15	0.49
1427	WP	Pool	4.34	0.58	13.73	1.95	34.25	36.22	1129.66	11.12	24.16	6.88	0.17
1428	WP	Pool	12.82	1.09	6.94	3.96	49.94	36.22	1129.66	11.12	24.16	2.60	0.47
1429	WP	Pool	7.08	0.88	5.70	2.78	37.38	36.22	1129.66	11.12	24.16	11.19	0.32
1430	WP	Pool	4.27	0.36	1.29	1.34	20.95	36.22	1129.66	11.12	24.16	13.96	0.65

Appendix 3D: KEGG Orthologs associated with nitrogen metabolism.

Table 3.D.1. Gene orthologs identified as having functional roles in specific nitrogen metabolism categories. Orthologs were retrieved from the KEGG database nitrogen metabolism pathway map.

Nitrogen Metabolism	Corresponding KEGG Orthologs
Nitrification	K10944, K10945, K10946, K10535
Denitrification	K00370, K00371, K00374, K00373, K02567, K02568, K00368, K15864, K04561, K02305, K15877, K00376
Nitrogen Fixation	K02588, K02586, K02591, K00531
Assimilatory Nitrate Reduction	K00367, K10534, K00372, K00360, K00366, K17877
Dessimilatory Nitrate Reduction	K00370, K00371, K00374, K00373, K02567, K02568, K00362, K00363, K03385, K15876

CHAPTER IV

ALGAL-MICROBIAL RESPONSE TO ROCKY INTERTIDAL AMMONIUM AVAILABILTY

ABSTRACT

In the nearshore and intertidal environment, nitrogen limitation can be ameliorated by animal regenerated ammonium, but algae and ammonia oxidizing benthic microbes compete for this shared resource. We used field dispensers to elevate ammonium several times above ambient levels at sites with measured differences in animal composition, testing test the hypothesis that ammonium availability drives algal and microbial function in a temperate rocky intertidal system. We queried whether elevated ammonium gets immediately incorporated into local microbes and phototrophs, and whether a site with elevated animal abundance (and animal-excreted ammonium) leads to a microbial community that utilizes this ammonium based on microbial identities and associated genes. Our simulated animal regenerated ammonium drove microbial community structure to resemble that in naturally high ammonium tide pools, but only at our low-animal site. Macroalgae did not utilize our experimentally elevated ammonium, but the photosynthetic biofilm did show an ammonium treatment response that was strongest at the low-animal site. This study contributes to better prediction of the consequences of human induced changes in nutrient cycles in the temperate rocky intertidal habitat.

INTRODUCTION

Nitrogen availability is vital to multiple ecological processes, including primary production and decomposition. About 78% of the Earth's atmosphere is composed of nitrogen, but natural atmospheric nitrogen (N_2) exists in a form unavailable for biological use. This leads

to a scarcity of useable nitrogen in many of Earth's ecosystems, including temperate coastal marine systems. In the northeast Pacific Ocean, nitrate (NO_3^-), delivered to the coast via upwelling, quantitatively dominates the nitrogen pool available to nearshore and intertidal phototrophs. However, nearshore and intertidal animals deliver regenerated nitrogen in the form of ammonium, which may be a preferred source for local primary productivity (Bracken and Stachowicz 2006; Aquilino *et al.* 2009) and microbial autotrophs (Pather *et al.* 2014). In a classic example of bottom-up mechanics, there is evidence that increased ammonium availability facilitates rates of primary productivity in diverse organisms, which in turn yields elevated consumer diversity and abundance. In the nearshore and intertidal environment, nitrogen limitation can be ameliorated by animal regenerated ammonium (Williamson and Rees 1994; Bracken 2004; Pfister 2007).

In an evolved complementarity, plants are limited by a nutrient that resident animals constantly excrete. Animal excretions can ameliorate nitrogen limitation (McNaughton 1979; Bracken 2004; Croll *et al.* 2005; Pfister 2007), and yet, in almost every ecosystem, animal biota is in decline (Ricciardi and Rasmussen 1999; Sodhi *et al.* 2004; Worm *et al.* 2006). Human activities have caused declines in large consumer abundance and biomass (Jackson *et al.* 2001; Worm *et al.* 2006), but we know little about how the loss of consumers has affected nitrogen availability via lost excretion products and recycling and even less about the role of microbes in mediating that interaction. Positive interactions between nitrogen-excreting organisms and the primary producers that utilize nitrogen can strongly influence community structuring (Bracken 2004; Pfister 2007). Animal regeneration of nitrogen may benefit both phototrophs and nitrifying microbes, while microbes may serve a valuable ecosystem function via nitrogen-retention. These interactions, mediated via the resource of nitrogen, thus enhance the variety and types of species

interactions we should expect in the nearshore, yet microbial composition and function has been largely ignored in both rocky shore community structuring and in rationale for marine protected area site selection.

Rocky intertidal communities have long provided a useful system for investigation of relative importance of top-down and bottom-up forces, and nutrient ratios within organisms and the water column provide a unique perspective from which to view these issues. Nearshore oceanographic processes influence intertidal productivity (Menge *et al.* 1997), and predation further impacts community dynamics (Paine 1966). While productivity is an important factor governing intertidal communities, the role of nutrients in this process, while clearly important, is not fully understood, and may contribute to the top-down impacts of predation in addition to the bottom-up impacts of nutrient loading or productivity (Menge *et al.* 1997). Nutrient loading via anthropogenic impacts has the potential to severely alter bottom-up impacts, which are increasingly severe. Human activity creates reactive nitrogen via three mechanisms: encouragement of biological nitrogen fixation associated with agriculture, production of synthetic nitrogen fertilizer, and inadvertent creation of reactive nitrogen through reaction with oxygen as biomass and fossil fuels are burned (Galloway *et al.* 2004, 2008); at this time, agricultural sources are the largest source of nitrogen pollution to many of the planet's coastal marine ecosystems (Carpenter *et al.* 1998; Howarth 2008).

Rapid uptake and assimilation of animal-regenerated ammonium by microbes that oxidize ammonia for growth (Ward 2013; Pather *et al.* 2014) and phototrophs that prefer ammonium for energetic reasons (Magalhães *et al.* 2003; Bracken and Stachowicz 2006; Zehr and Kudela 2011) sets a stage for competition. Our understanding of animal contributions to intertidal nitrogen budgets suggests variability in microbial assemblages across the landscape,

and we have confirmed this through our own observational dataset (Chapter III). The Pacific Northwest intertidal zone biota occurs in a high-diversity mosaic (Menge *et al.* 1993), so we predict that the distribution of microbes intimately linked to animal presence (e.g. nitrifiers) is correlated with available resources for physiological processes (Herbert 1999; Pfister *et al.* 2010). To probe biogeochemical cycling, functional capacity of fauna, and microbial function on intertidal shores, we selected two sites in the San Juan Islands, WA, USA with community structures that differed in the ratios of sessile animals to marine flora (algae, seagrass)).

In an earlier observational field study, we measured strong differences in microbial community structure between tide pool versus emergent rock habitats at multiple field sites in the San Juan Islands (Chapter III). One key factor that differentiates tide pools and emergent rock habitat is continuous submergence in a high DIN environment (Bracken 2004; Bracken and Nielsen 2004a; Pfister 2007). We thus test whether the microbial communities are responsive to experimentally added ammonium in the lower rocky intertidal zone.

Nitrogen, a limiting resource in many temperate coastal systems, is typically elevated in tide pools compared to adjacent coastal ocean in the form of animal excreted ammonium; tide pools are characterized by a greater faunal taxonomic richness and abundance than adjacent emergent rock (Chapter III). Specifically, can experimental artificial ammonium addition on emergent rock yield microbial communities more closely resembling those in 'pool' habitat? Further, is the interaction between benthic microbial communities and the nutrient resource ammonium context-dependent based on local macroscopic community composition and oceanic water motion?

We hypothesized that local enhancement of ammonium *in situ* in the lower rocky intertidal zone would yield a range of resulting phototrophic and microbial responses depending on

environmental conditions, as we have previously demonstrated context-dependent algal-microbial competition for this resource in a laboratory mesocosm setting (Chapter II). We tested this hypothesis by elevating ammonium several times above ambient levels at sites with measured differences in animal composition. We queried whether elevated ammonium gets immediately incorporated into local microbes and phototrophs, and whether a site with elevated animal abundance (and animal-excreted ammonium) leads to a microbial community that utilizes this ammonium based on microbial identities and associated genes.

MATERIALS AND METHODS

Study system and experimental nutrient manipulation

We tested to what degree intertidal animal abundance is associated with elevated ammonium, algal productivity, and microbial nitrifiers by selecting two rocky intertidal sites on San Juan Island (WA, USA), Westside Preserve and Cattle Point (**Figure 4.1**). Given the expected importance of animal-excreted ammonium in driving microbial community structure, sites were selected to maximize variability in macroscopic community composition between physically similar sites that share a regional body of tidal seawater, Haro Strait. The south and west sides of San Juan Island are exposed to strong waves, particularly in the winter, and are among the most exposed coastlines in the San Juan Islands archipelago (Dayton 1971; Menge 1972, 1974). Westside Preserve, the northernmost site, is relatively animal-depauperate, while Cattle Point, on the southern tip of San Juan Isl., hosts abundant and diverse invertebrates. Cattle Point is exposed to westerly swells from the Strait of Juan de Fuca, making it one of the most exposed sites in the San Juan Islands archipelago and more subject to upwelling periods associated with the outer coast California Current Large Marine Ecosystem (Harrison *et al.* 1994). Most seawater

nutrients delivered to the intertidal in this region are supplied as a result of coastal upwelling of deep, nutrient-rich, high-salinity oceanic water that moves from the outer coast shoreward via the Strait of Juan de Fuca (Harrison *et al.* 1994).

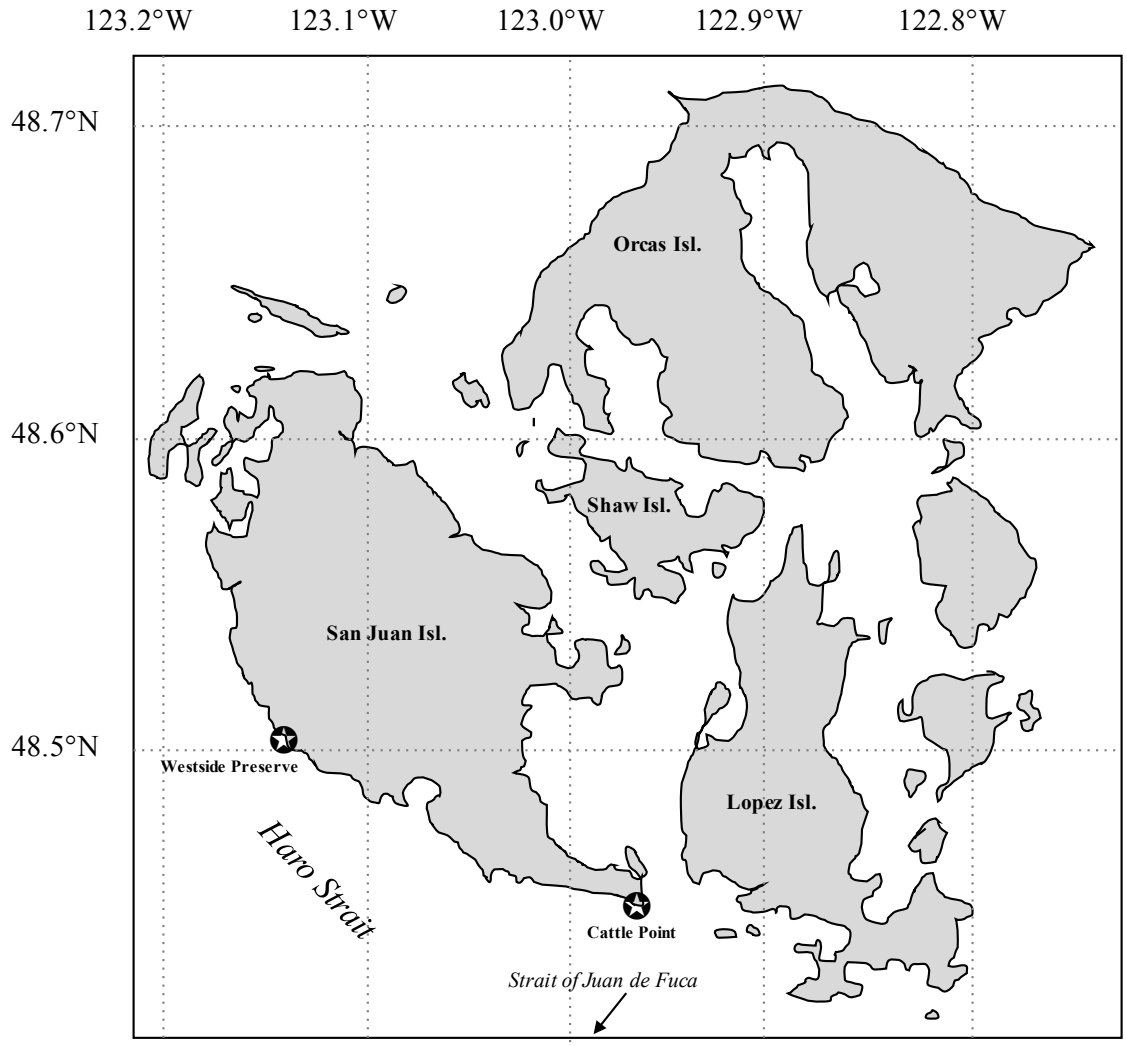

Figure 4.1. Map of study sites on San Juan Island, Washington, USA.

We manipulated local ammonium availability in the lower intertidal zone (0m MLLW (mean lower low water)) using nutrient dispensers that released ammonium (NH_4^+) from agar, which were prepared in the lab. Threaded 2" Schedule 80 PVC plugs, perforated eight times in the sidewall, were wrapped in Parafilm, placed on ice, and filled with ammonium chloride dissolved

in melted agar (1.5M NH_4Cl). Agar was allowed to cool and solidify, and these filled plugs were stored in the refrigerator (4°C) prior to deployment in the field. A 100m horizontal transect across rocky substrate at 0m MLLW was permanently marked at each site with stainless steel bolts placed at 0, 25, 50, 75, and 100m. Points on the transect were randomly assigned to one of two ammonium elevation treatments: 'NH_4^+' (N = 8) or 'Control' (N = 8). If a dispenser or control point was placed within 3m of another during the random assignment process, its location on the transect was redrawn until all dispensers and control points were assigned to spaces at least 3m apart in order to avoid flow-over nutrient effects. At each 'NH_4^+' point, a threaded 2" Schedule 80 PVC cap was installed into the rocky substrate using a hex head stainless steel lag bold, plastic trilobe wall anchor, stainless steel washer, and neoprene washer. Freshly prepared NH_4^+ agar plugs were screwed into pre-installed PVC caps at each field site every 12-14 days between 14 May and 9 August 2014 (**Plate 4.1**, **Plate 4.2**). Corresponding randomly-assigned control points were permanently marked on the 100m horizontal transect using stainless steel screws.

Verifying effectiveness of experimental nutrient enhancement

An explicit goal of this study was to query the strength of ammonium concentration alone as a driver of tide pool-emergent rock microbial community structure difference observed at multiple rocky intertidal sites in the San Juan Islands (Chapter III). We confirmed experimental elevation of ammonium on emergent rock to relevant tide pool concentrations by collecting three concurrent water samples for nutrient analysis on 14-15 May 2014, at the start of the experimental period: 1) immediately above dispensers as the rising tide first washed over them (N = 8 per site), 2) at control points on the experimental 100m horizontal transect as the rising

tide reached 0m MLLW (N = 3 per site), and 3) from tide pools between 0 and 1m MLLW that had been isolated from the coastal water column for between 2 and 3 hours (N = 5 per site). Samples analyzed for seawater nutrient analysis (NH_4^+, NO_2^-, NO_3^-) were collected and analyzed as described above.

Ammonium output from freshly deployed and spent nutrient agar plugs was measured in both controlled laboratory and natural *in situ* settings. In the field, seawater was sampled for ammonium concentration just above dispensers as the low tide re-covered 0m MLLW on the day of fresh plug deployment and again just before the low tide dropped below 0m MLLW on the day of plug exchange 12-14 days later. A volume- and diffusion time-standardized maximum expected ammonium output from fresh agar plugs was measured in standing seawater in a lab setting. Replicated fresh nutrient agar caps were placed in 4.5L tanks for 3h, at which time the seawater was sampled for standing ammonium concentration. Spent plugs (following 12-14-day deployment) from each site were sampled for maximum possible ammonium output in the same controlled method (water sampled after 3h in 4.5L seawater tanks). As above, all water samples collected for seawater nutrient analysis were syringe-filtered into separate acid-washed 60mL high-density polyethylene bottles, and frozen (-20°C) prior to analysis, and ammonium concentration was measured at the University of Washington Marine Chemistry Laboratory (methods from UNESCO 1994).

Plate 4.1. Field ammonium dispenser, contained within PVC cap and plug, installed into rocky substrate with a stainless steel bolt.

Plate 4.2. Field ammonium dispenser (**A**) installed at 0m MLLW and associated response variable measurement devices: Cylindrical plaster dissolution block for measuring water motion (**B**), Vexar pouch containing 12 BioBalls for culturing benthos-associated microbial community (**C**), bare rock adjacent to ammonium dispenser device to be scraped for benthos-associated biofilm (**D**), marked *Saccharina* individual for elemental analysis of macroalgal tissue (**E**), and glass microscope slide epoxied to rocky substrate for measurement of benthic chlorophyll (**F**).

Site metadata and experimental treatment effectiveness

Quantification of site-wide macrobiota community composition

Whole-site macroscopic community composition was measured along transect tapes placed on rocky substrate, following all contours, from each field ammonium dispenser and control point at 0m MLLW (n = 8 NH_4^+, n = 8 Control) to the top of high intertidal zone. Vertical transects were positioned perpendicular to the 100m horizontal experimental transect at 0m MLLW. We recorded the identity of the organism attached to the rocky substrate beneath the 'vertical' transect lines every 25m from 0m MLLW to the top of the inhabitable high intertidal zone considered habitable to intertidal organisms. A total of 16 vertical transects were performed at each site, with a species identification to lowest practical taxonomic level recorded for every 25 cm of transect length. In areas where the vertical transect tapes traversed bare rock or dead barnacle, 'inert substrate' was the recorded value for those sample points. Due to topographical variation, transect lengths were variable both within and between sites; this sampling regimen yielded 868 data points at Westside Preserve and 1,226 data points at Cattle Point.

We analyzed the measured macroscopic community structure associated with each site using non-metric multidimensional scaling (hereafter NMDS) ordination (Kruskal 1964). Here, we ordinated communities of macrobiota based on level of membership of algal, seagrass, invertebrate, and intertidal fish taxa in vertical transects. Non-metric multidimensional scaling iteratively searches for the best positions of sample units on multiple dimensions (axes) that minimize the stress of the multi-dimensional configuration (McCune *et al.* 2002). In this procedure, the best solution with a random starting configuration and number of dimensions is selected from the run with the lowest final stress and is reapplied to determine a final ordination. Because relative abundance of taxa associated with each site provided meaningful information

about the overall community structure, we used the Bray-Curtis distance measure, which incorporates abundance data in ordination. NMDS on the Bray-Curtis distance measure is also robust to non-normal data that contain high numbers of zeroes, typical characteristics of ecological community abundance data. This multivariate approach allows one to identify environmental correlates with community structure. In the ordination of communities of macrobiota, the sample unit was a single vertical transect (equivalent to a quadrat in similar community analysis studies), for a total of 16 sample units per site.

Capability of microbial community to utilize ambient seawater nitrogen

To assess the ability of microbial biofilm community to utilize nutrients present in ambient seawater, we transferred BioBall-associated microbial communities directly from Control points along horizontal experimental transects at Westside Preserve and Cattle Point to separate 4.5L seawater mesocosms (N = 4) at Friday Harbor Laboratories. BioBalls are 1" diameter pegged spherical plastic units. Due to the high surface area provided by pegs, BioBalls are commercially marketed to aquarists as microbial settlement devices for microbes that control nitrogen waste (nitrifiers) (Englert 1992). BioBalls and associated microbial communities, which had been allowed to develop under ambient field conditions for 3 months (14 May - 9 August 2014), were transported on ice in a darkened cooler, and were placed in seawater mesocosms within 4 hours of removal from the field. Water samples for seawater nutrient analysis were collected immediately upon addition of BioBalls to mesocosms (0 h), and again after a 4 h incubation period. All water samples collected for seawater nutrient analysis were syringe-filtered (Whatman glass-fiber GF/C filters) into separate acid-washed 60mL high-density polyethylene bottles, and frozen (-20°C) prior to analysis. Seawater nutrient sample collection

and analysis for NH_4^+, NO_3^-, NO_2^-, PO_4^{3-}, and SiO_4^{4-} concentrations was measured at the University of Washington Marine Chemistry Laboratory (methods from UNESCO 1994).

Predictions for local advection of experimentally elevated nutrients

Water motion has key importance in mixing of locally generated and utilized nutrients across the rocky intertidal zone. Angle of shoreline relative to larger ocean currents, wind direction, and tidal flow can lead to sites with vastly different nutrient supply because the residence time of seawater in the shallow intertidal zone becomes variable. Further, small-scale variations in topography can drive within-site variability in water flow. We used replicated dissolution blocks to compare water flow between and within our two field sites. Dissolution blocks were produced from gypsum dental plaster (calcium sulfate) in cylindrical plastic film canisters (5.1cm x 3.2cm) with stainless steel wood screws inserted into the plaster before it hardened. The plastic film canisters were then peeled away from the hardened cylindrical plaster. Pre-weighed dry plaster dissolution blocks were deployed for four 24h periods at each NH_4^+ dispenser point along the experimental 100m 0m MLLW horizontal transect (29-30 May, 15-16 June, 27-28 June, and 14-15 July 2014). For each deployment, dissolution blocks were screwed into the same plastic wall anchors installed *in situ* (N = 8 per site) (**Plate 4.2**), ensuring that wave action of the same precise location was being measured repeatedly. Upon removal from the field following 24h deployment (~2 full tidal cycles), plaster blocks were dried at 60°C to constant mass (~48h) and reweighed. Plaster mass lost was used as a proxy for water motion at each field ammonium dispenser and control point along the experimental transect at each site.

Biotic responses to experimental ammonium availability

Reflection of ammonium availability in microbial community structure and function

To investigate the effect of ammonium availability on benthic microbial communities, and to query whether this effect varied between sites, we assayed the microbial community that developed on a uniform artificial substrate deployed along the experimental 100m horizontal transect at both Westside Preserve and Cattle Point. We deployed pouches containing 12 BioBalls each immediately adjacent to PVC nutrient dispensers (N = 8 pouches) and marked control points (N = 8 pouches) using stainless steel bolts (**Plate 4.2**). To capture strong microbial community differentiation that can occur between emergent and pool intertidal habitats within centimeters of distance (Chapter III), an additional five pouches were installed in tide pools ranging in volume from approx. 5-100L between 0 and +1m MLLW as possible at each site. Pouches were constructed of 1cm plastic mesh, and were attached to rocky substrate using stainless steel screws, washers, and plastic wall anchors. BioBall pouches were deployed for the duration of the experimental nutrient elevation period (14 May – 9 August 2014). At the conclusion of the experiment, BioBalls were removed from pouches and placed on ice upon removal from the field, and stored at -80°C within 24h of collection.

Biofilm DNA was extracted using a PowerSoil kit (MoBio™). Material was sampled off of BioBalls using sterile plastic spatulas and cotton swabs then placed in PowerSoil PowerBead tubes, and subsequent extraction followed the PowerSoil protocol. The PCR amplification protocol followed Caporaso et al. (Caporaso *et al.* 2010a) for multiplexing 16S rRNA samples. PCR products were cleaned with MoBio™ UltraClean htp PCR Clean-up kit. We amplified the V4 variable region of the 16S rRNA gene from community DNA using bar-coded primers

according to Earth Microbiome Project standard protocols (Gilbert *et al.* 2014), yielding paired-end sequence data.

Preliminary microbial sequence data analysis was performed in QIIME (v. 1.9.1, Quantitative Insights into Microbial Ecology; www.qiime.org) using protocols identical to those outlined in Chapter II. Diversity metrics between factors (site, source location (treatment)) were computed using the QIIME core_diversity_analyses.py script in QIIME, which generates alpha diversity metrics and beta diversity distances between samples (weighted and unweighted UniFrac), and to build principal component (PCoA) plots, which accounted for both phylogenetic composition (Lozupone *et al.* 2011) and relative abundance of taxa among samples. This script generates a table containing all OTUs and their relative abundance by site treatment, which was used to compare relative abundance of 13 known nitrifying taxa between ambient and field ammonium dispenser treatments at each site (**Table 4.A.1**). All samples were analyzed at the lowest sequencing depth of included samples for these diversity analyses.

To test for significant sample groupings by sampling category (three levels of within-site source location (emergent rock NH_4^+ treatment, emergent rock control, tide pool); two levels of site identity (Westside Preserve, Cattle Point) based on these distance metrics, ANOSIM was conducted in QIIME using the compare_categories.py script. This test compares the mean of ranked dissimilarities between groups to the mean of ranked dissimilarities within groups in multivariate data, yielding a test statistic (R), and a p-value. The ANOSIM R-value test statistic compares between-group mean of ranked sample dissimilarities with within-group mean of ranked sample dissimilarities. An ANOSIM R-value close to 1 suggests dissimilarity between groups while an R value close to 0 suggests even dissimilarity within and between groups.

We tested the robustness of source location as an explanatory category for microbial community within a site using a Random Forest Supervised Learning procedure script (supervised_learning.py). This procedure uses a subset of evenly rarified OTU data to determine the relationship between a categorical variable and OTUs, then attempts to classify reserved data to a selected set of categories based upon that training. A high ratio of baseline error to observed error indicates statistically robust classification (significance inferred for ratio values > 2). Prior to performing the Random Forest Supervised Learning procedure, all samples were rarified to an even depth (200 sequences). To emphasize cosmopolitan microbial taxa that might be differentially abundant based on source location (pool, ambient emergent rock, ammonium addition on emergent rock), a stringent membership requirement was passed, that is, OTUs must have occurred in at least 14 of the 15 samples at a site to be included in the analysis.

To test whether microbial taxa in biofilm on BioBalls incubated at two categorical levels of experimental ammonium addition treatment (NH_4^+ and control) and two levels of the factor 'site' (Westside Preserve, Cattle Point) were associated with particular nitrogen metabolism pathways, we used the software package PICRUSt (Phylogenetic Investigation of Communities by Reconstruction of Unobserved States) (Langille *et al.* 2013) to query predicted functional capacity of the communities. PICRUSt estimates gene presence contribution to a predicted metagenome by bacteria or archaea identified using 16S rRNA sequencing. A list of genes associated with particular nitrogen metabolisms was created using the KEGG (Kyoto Encyclopedia of Genes and Genomes; (Kanehisa *et al.* 2016)) orthology database (**Table 4.A.2**), and R (R Core Team 2015) was used to generate counts and percent abundance contributions of each metabolism associated with each sample and compare nested categories of factors.

Experimentally elevated ammonium uptake and assimilation by phototrophs

We examined intertidal algae adjacent to field ammonium dispensers and control points to determine the phototrophic response to local nutrient conditions. To assess ammonium uptake and assimilation by this ecological guild, we measured algal elemental isotope composition and benthic chlorophyll *a* concentration. To capture a range of turnover rate and thallus size, which we predicted to play an important role in the rate and magnitude at which phototrophs could respond to experimentally elevated ammonium, we measured algal elemental isotopic composition in biofilm and in a common lower intertidal kelp.

At the beginning of the experimental period, we scraped $2cm^2$ patches adjacent to all ammonium dispensers and at control points down to bare rock with a razor blade. Biofilm microalgae that developed during the experimental period were then collected from these $2cm^2$ clearings clean razor blades. Biofilm samples were collected into 1.5mL centrifuge tubes and immediately stored on ice; samples were then emptied into aluminum foil packets and dried at 60°C for 48h for isotopic analysis.

We sampled *Saccharina sessile* (hereafter *Saccharina*) from all field ammonium dispenser and control points at both sites as a macroalgal representative. *Saccharina* is a long-lived, lower intertidal kelp ubiquitous to rocky intertidal sites in the Pacific Northwest. At the experimental period's initiation (May 2014) and conclusion (August 2014), we collected small amounts (<0.2g wet mass) of *Saccharina* from freshly grown tissue of each marked observational thallus. Macroalgal samples were dried at 60°C for 48h and stored at room temperature in aluminum foil packets.

All dried biofilm and macroalgal samples were ground in 1mL rubber capped tubes containing a 3mm ball bearing using a GenoGrinder®, and elemental and isotopic analyses (%N,

%C, $\delta^{15}N$, $\delta^{13}C$) were made at the University of Chicago Stable Isotope Facilities using a Costech 2010 Elemental Analyzer combustion system coupled to a Thermo DeltaV Plus IRMS via a Thermo Conflo IV interface.

Rocky intertidal biofilm productivity was measured via benthic chlorophyll *a* concentration. Standard size glass microscope slides (75mm x 25mm) were secured to rocky substrate immediately adjacent to installed PVC nutrient dispensers and marked control points using marine epoxy (A-788 Splash Zone Compound: Z-Spar) (**Plate 4.2**). Slides were sampled periodically throughout the microbial BioBall incubation period by wiping the exposed surface completely with a clean cotton swab. Cotton swabs were placed in 1.5mL centrifuge tubes, kept in the dark immediately following collection, and stored at -20°C within 3 hours of collection. Chlorophyll *a* was extracted with acetone following methods from Sterman (1988), and pigment absorbance was measured spectrophotometrically at 630, 647, and 664nm using a HACH® DR5000™ UV-Vis spectrophotometer. Concentration was calculated following **Equation 4.1**, which incorporates readings at all three wavelengths to determine chlorophyll *a* concentration (μg chl/mL extract) in mixed microalgae samples using 90% acetone solvent for extraction (Jeffrey & Humphrey 1975). Coefficients in **Equation 4.1** were calculated from extinction coefficients of chlorophyll in 90% and 100% acetone at red maxima, and the use of three separate coefficients reflects expected presence of chlorophyll *a*, *b*, and *c* in samples (for additional detail, see Jeffrey and Humphrey (Jeffrey and Humphrey 1975). The protocol applied in the present study is modified from methods for measuring seawater chlorophyll (Sterman 1988); here, periphyton from a known surface area (one side of a standard microscope slide; 18.75cm^2) was scraped and extracted rather than phytoplankton from a known volume of seawater. In this study, settled communities of field-collected periphyton were not monocultures

and it was important to control for surface area sampled rather than attempting to perform cell counts.

$$\frac{\mu g\ chl\ a}{mL\ extract} = 11.85\ A_{664} - 1.54A_{647} - 0.08A_{630} \qquad \text{Equation 4.1}$$

RESULTS

Macrobiota community composition varies between sites

Westside Preserve and Cattle Point differed statistically in their community composition, with Cattle Point dominated by animals (animal:phototroph =1.76 $\pm$ 0.35) and Westside Preserve dominated by phototrophs (animal:phototroph = 0.91 $\pm$ 0.23). Macrobiota structure, as surveyed in vertical transects from the horizontal experimental transect at 0m MLLW to the top of the habitable intertidal zone showed strong differentiation by site (**Figure 4.2**). In multivariate analysis of macrobiota communities, where vertical transects represent single sample units, clustering of samples by site is significantly different from random (ANOSIM R = 0.467, $p < 0.001$). Clustering of sites is strongest on NMDS Axis 1, with Cattle Point samples filling ordination space on the negative side of Axis 1, and Westside Preserve samples filling ordination space on the positive end of Axis 1. Of the ten macrobiota with most strongly negative scores ($\leq$ -0.14) on Axis 1, seven are faunal taxa (**Table 4.B.1**). In direct contrast, of the ten taxa with most strongly positive scores ($\geq$ 0.13) on Axis 1, seven are algal taxa (**Supplementary Table 4.B.1**). There is no clustering by experimental treatment (ammonium, control) within this ordination (**Figure 4.2**; ANOSIM R = 0.003, p = 0.439), which confirms a lack of unintentional placement bias in distribiton of ammonium dispensers across the 100m horizontal transect at each site.

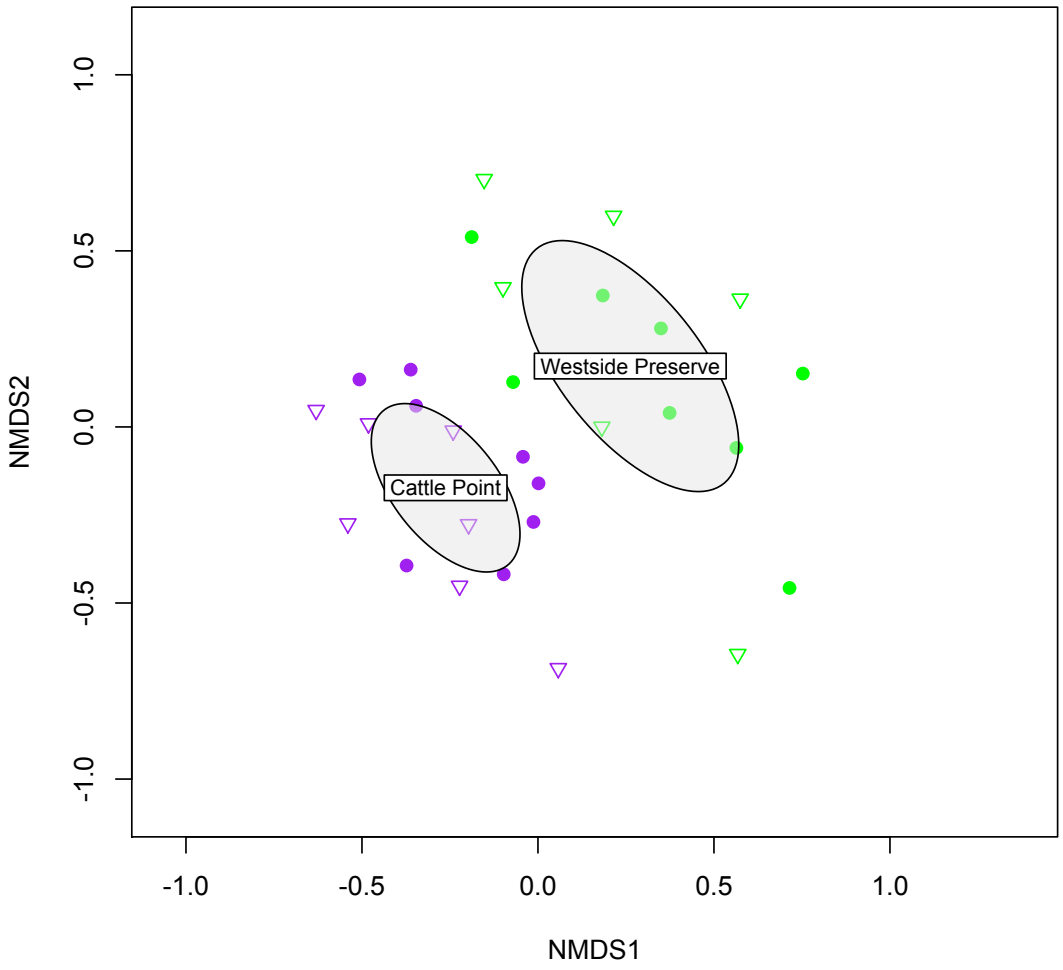

Figure 4.2. NMDS ordination of macrobiota community vertical transect samples in species space (Bray-Curtis distance). Plotted data are community surveys (vertical transects perpendicular to the ocean on habitable intertidal substrate above 0m MLLW emergent hard substrate, with inhabitant attached to rock recorded each 25cm). Use of Bray-Curtis distance accounts for relative abundance of taxa within samples. Points are colored by site type (green = Westside Preserve, purple = Cattle Point), and shape-coded by treatment type (closed circle = Control, open triangle = Field Ammonium Dispenser).

Capability of microbial community to utilize ambient seawater nitrogen

Incubation (4 h) of field-incubated BioBall-associated microbial communities (Control treatment) in ambient seawater in 4.5L mesocosms revealed utilization and transformation of DIN that differed by site. Ammonium increased by 0.5-2 μM in mesocosms containing field-cultured BioBalls, though this trend was insignificant at $p \leq 0.05$ (**Figure 4.3a**; two-way

ANOVA, Time point $F_{1, 8} = 0.284$, $p = 0.169$;). A stronger trend in ammonium concentration increase from Cattle Point BioBalls is in line with the previously observed high site-wide faunal concentration at this site (**Figure 4.2**). Nitrite, the first product of nitrification, can only be produced from microbial activity. After the 4 h incubation, we observed a 0.15 μM mean increase in nitrite concentration in mesocosms containing Cattle Point BioBalls, with no change in mesocosms containing Westside Preserve BioBalls (**Figure 4.3b;** two-way ANOVA, Site $F_{1, 8} = 26.955$, $p < 0.001$, Time point $F_{1, 8} = 7.363$, $p = 0.027$, Site x Time point $F_{1, 8} = 11.236$, $p = 0.010$), suggesting presence of an ammonium-adapted microbial community of nitrifiers at Cattle Point that is absent at Westside Preserve. This process requires oxygen, and so a drawdown of dissolved oxygen paired with elevated nitrite can bolster evidence of microbial nitrification. In these same mesocosms, we observed increased dissolved oxygen (DO) in the presence of BioBalls from both sites, but net production over 4h was lower in mesocosms containing Cattle Point BioBalls (**Figure 4.3d**). Finally, we measured a borderline significant interactive effect between site and incubation time point in nitrate concentration (two-way ANOVA, Site $F_{1, 8} = 0.414$, $p = 0.538$, Time point $F_{1, 8} = 0.660$, $p = 0.440$, Site x Time point $F_{1, 8} = 4.026$, $p = 0.080$). Nitrate is the secondary product of nitrification, but is also the most abundant form of DIN available to coastal marine primary producers. A 3 μM decrease in mean nitrate concentration in mesocosms containing Westside Preserve BioBalls could indicate drawdown of nitrate by photosynthetic members of the biofilm community, while 1 μM mean increase in nitrate concentration in mesocosms containing Cattle Point BioBalls could indicate production of nitrate by a nitrifying microbial community.

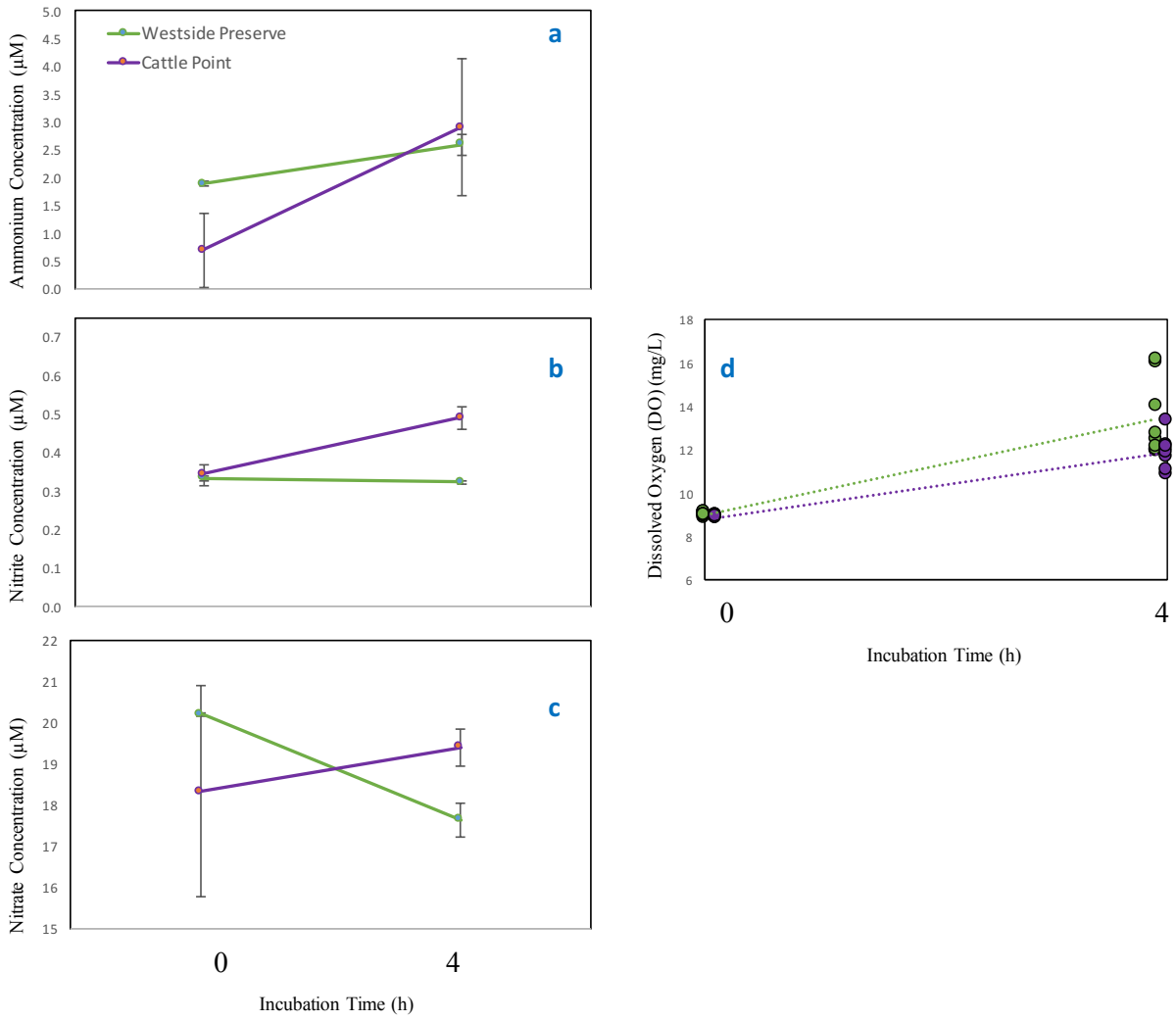

Figure 4.3. Functional capacity of microbial biofilm community on BioBalls cultivated at Westside Preserve and Cattle Point (May-August 2014) to utilize ambient DIN in seawater (**a-c**), and correlation of microbial biofilm incubation with net DO (**d**). For DIN measurements, plotted values are mean concentrations (µM) +/- SE, read at 0h (n = 2) and 4h (n = 4) during 4h incubation in 4.5L ambient seawater mesocosms. For DO measurements, plotted values are raw DO concentration readings (mg/L), read at 0h and 4h during 4h incubation in 4.5L ambient seawater mesocosms (points are jittered on x-axis for clarity).

Predictions for local advection of experimentally elevated nutrients

Dissolution data from plaster blocks deployed at both Westside Preserve and Cattle Point revealed intrasite variability in water flow at both sites (**Figure 4.4**). At both sites, measurements of mass lost from plaster blocks per deployment had a spread of about 10%. However, among the

eight plaster blocks installed at each site over four deployments, proportion of plaster mass lost within a 24h period was higher at nearly all points along the 100m horizontal transect at Cattle Point than at Westside Preserve (**Figure 4.4a**). Indeed, when we collapsed all eight individual installation points per site across all four deployments periods (24h each), proportional plaster loss was consistently higher at Cattle Point than at Westside Preserve (**Figure 4.4b**; Welch's two-sample t-test, $t = 3.576$, $p < 0.001$), indicating that flow is higher at Cattle Point than at Westside Preserve.

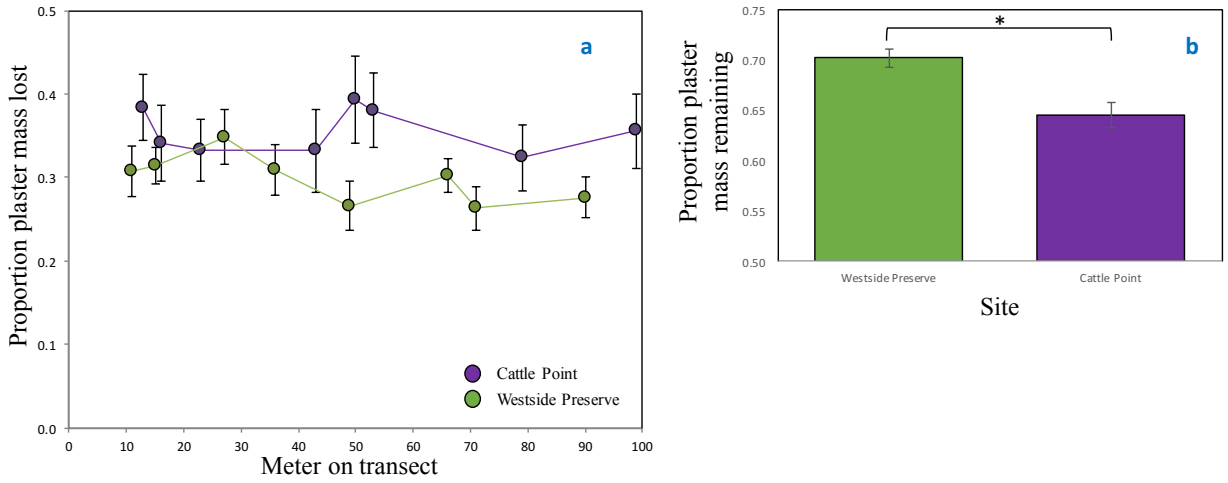

Figure 4.4. Measurement of mass change in plaster dissolution blocks to quantify water motion differences between sites Westside Preserve and Cattle Point. a) Mean proportion of plaster mass lost at each ammonium dispenser location at each site. b) Mean proportion of plaster mass remaining at each site after 24h deployments, with significant Welch's 2-sample t-test result indicated.

Verifying effectiveness of experimental nutrient enhancement

We verified that ammonium addition was a pressed treatment at both sites by comparing amount of ammonium diffused from freshly deployed and field-aged agarose nutrient dispensers in the laboratory. Freshly prepared nutrient dispensers elevated seawater in 4.5L containers from ambient ammonium concentration (~1 µM) to over 1000 µM (**Figure 4.5a**). Dispensers that had been deployed at Westside Preserve for 14 days elevated seawater ammonium concentration in

4.5L containers to 52.65 +/- 16.70 μM (**Figure 4.5a**). Dispensers that had been deployed at Cattle Point for the same 14 day period elevated ammonium concentration in 4.5L seawater containers to only 17.01 +/- 7.63 μM (**Figure 4.5a**). This uneven amount of ammonium remaining in agarose dispensers at the conclusion of 14 days of deployment indicates that diffusion rate was higher at Cattle Point than at Westside Preserve (Welch 2-sample t-test t = 1.93, p = 0.083).

Seawater samples collected from immediately above freshly deployed (0 days) and field-aged (14 days) agarose nutrient dispensers allowed us to determine *in situ* diffusion level at each field site. Here, we found a weakly significant interactive effect between time point (fresh versus spent agar) and site (Westside Preserve, Cattle Point) (**Figure 4.5b**; Time point $F_{1, 27} = 3.890$, p = 0.059, Site $F_{1, 27} = 8.772$, p = 0.006, Time point x Site $F_{1, 27} = 3.799$, p = 0.062). Although ammonium concentration was higher above fresh dispensers than spent dispensers at both sites, we measured higher ammonium diffusion above fresh agar at Cattle Point, and higher remaining ammonium diffusion above spent agar at Westside Preserve. Because sampling was performed immediately adjacent to the dispensers, seawater ammonium concentreation values here are descriptive of the diffusion boundary layer and higher water movement elevates detection of ammonium.

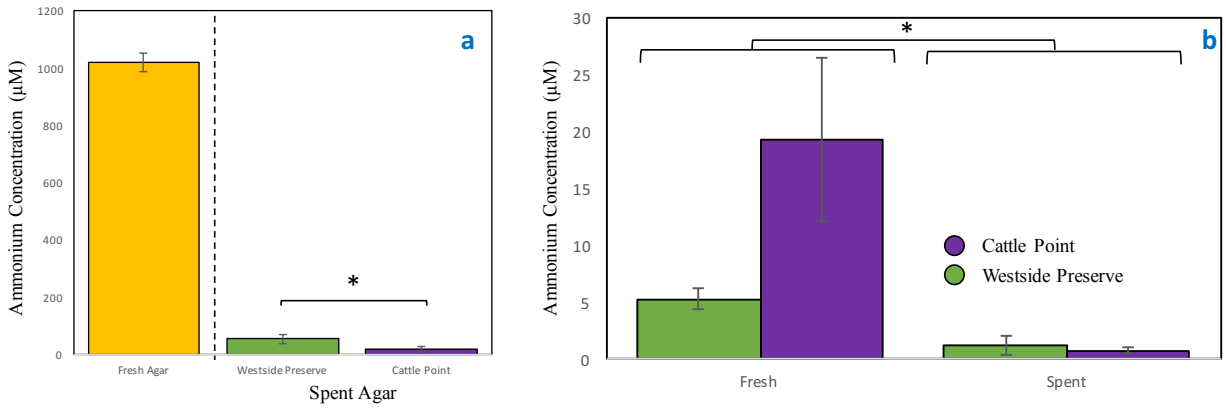

Figure 4.5. Elevation of seawater ammonium concentration associated with fresh and 'spent' agarose ammonium dispensers in **a**) controlled laboratory setting (4.5L mesocosms with 3h incubation) and **b**) *in situ* in the field. Significant differences between site identity are indicated with asterisks.

Seawater DIN concentrations in tide pools at both Westside Preserve and Cattle Point were elevated compared with oceanic water immediately adjacent to the rocky intertidal zone (**Figure 4.6**). Ammonium dispensers created tide pool-like [NH_4^+] conditions (5-10 µM at Westside Preserve and 15-25 µM at Cattle Point; **Figure 4.6a**, **Table 4.1**). Nitrite, which reaches concentrations up to four times higher in tide pools than in ambient coastal seawater due to 'closed system' nitrification activities, was not influenced by experimental ammonium addition (**Figure 4.6b**, **Table 4.1**). Nitrate concentration was higher from all seawater sources at Westside Preserve than Cattle Point. Within Westside Preserve samples, lower nitrate concentration was measured within tide pools than from either emergent source (**Figure 4.6c**, **Table 4.1**).

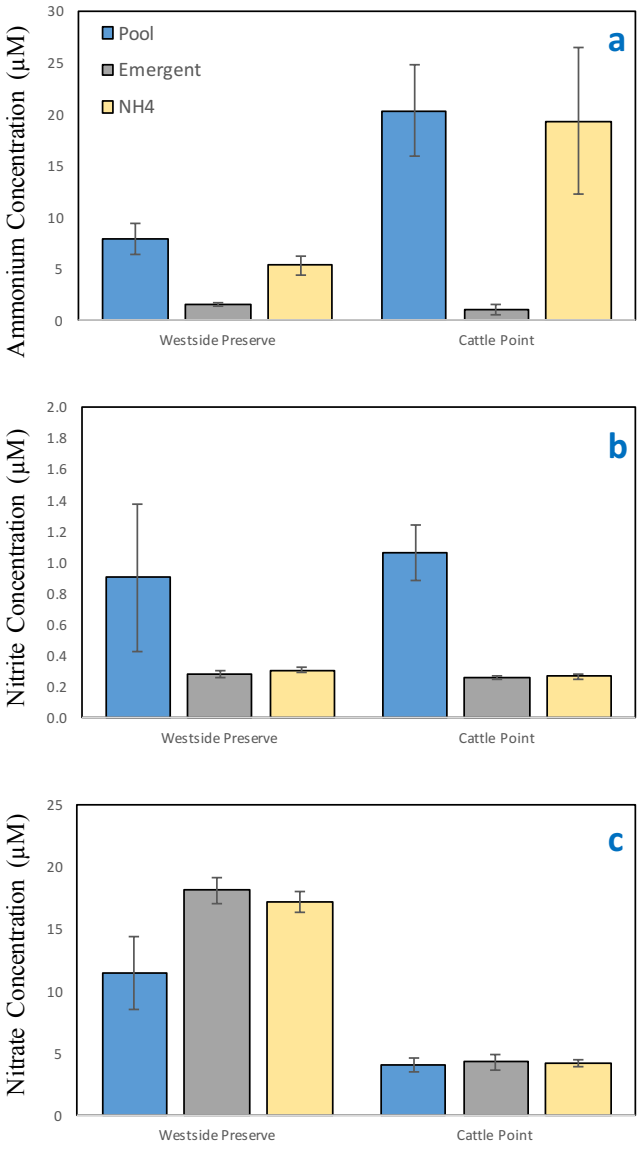

Figure 4.6. Mean seawater nitrogen nutrient concentrations (µM) of samples collected from three seawater sources at 0m MLLW (Tide pools, Emergent Control, Emergent Ammonium Addition) at the start of the experimental period (14-15 May 2014) (**Table 4.1**).

Table 4.1. Two-way ANOVA results from analysis of mean seawater DIN concentrations of samples collected from three seawater sources at 0m MLLW (Tide Pools, Emergent Control, Emergent Ammonium Addition) at the start of the experimental period (14-15 May 2014) (**Figure 4.6**).

	$[NH_4^+]$	$[NO_2^-]$	$[NO_3^-]$
Site	$F_{1, 26} = 7.224$ **p = 0.012**	$F_{1, 26} = 0.026$ p = 0.872	$F_{1, 26} = 115.807$ **p < 0.001**
Seawater Source	$F_{2, 26} = 2.677$ p = 0.088	$F_{2, 26} = 8.459$ **p = 0.001**	$F_{2, 26} = 3.881$ **p = 0.036**
Site x Seawater Source	$F_{2, 26} = 0.930$ p = 0.407	$F_{2, 26} = 0.162$ p = 0.851	$F_{2, 26} = 3.237$ p = 0.056

Reflection of ammonium availability in microbial community structure and function

Microbial community structure responded to experimental ammonium addition, but only at Westside Preserve. PCoA ordinations on weighted UniFrac distances of microbial community samples collected from Westside Preserve showed differentiation among source locations (tide pool, emergent rock control, emergent rock ammonium dispenser) (**Figure 4.7a**; ANOSIM R = 0.445, p = 0.002); unmanipulated emergent rock-associated microbial communities clustered separately from the ammonium addition treatment-associated communities. Further, dispensers drove microbial assemblages to more closely resemble tide pool-associated microbial communities than unmanipulated emergent rock-associated communities do; source locations cluster separately across PC1, with experimental ammonium addition treatment-associated communities falling between 'tide pool' and 'control.' Among Cattle Point samples, though, microbial communities were not differentiated by source location at the $p \leq 0.05$ level (**Figure 4.7b**; ANOSIM R = 0.162, p = 0.074).

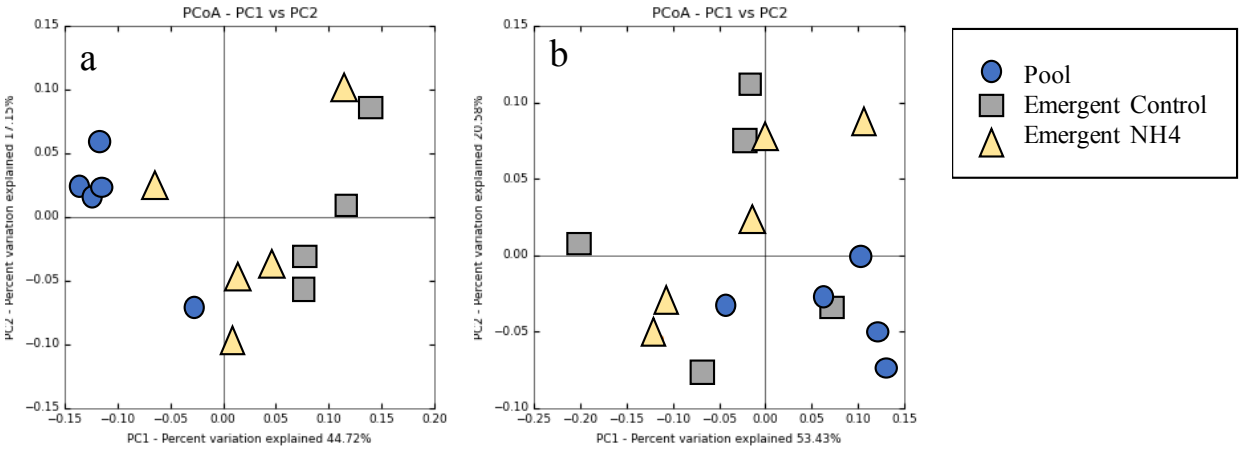

Figure 4.7. Ordination of BioBall-associated microbial samples based on weighted phylogenetic dissimilarity in community composition (UniFrac). Ordinations are based on pairwise weighted UniFrac distance between samples, and sample points are colored by BioBall source location. PCoAs of microbial communities, rarified to even depth, from a) Westside Preserve (depth = 11,945 sequences) and b) Cattle Point (depth = 15,130 sequences) emergent rock control and ammonium dispenser treatments, with corresponding pools included.

Random forest supervised learning identified distinct microbial communities associated with each source at Westside Preserve, but not at Cattle Point. At Westside Preserve, random forest models were successful at determining which source a microbial sample was taken from, correctly classifying samples more than 3 times as effectively as one would expect by chance (**Table 4.2**), which indicates consistent differentiation in the microbial communities of these three different source locations. Cattle Point OTUs did not yield robust classification to source location by the random forest supervised learning model (**Table 4.2**).

Table 4.2. Summary of predictive accuracy of random forest supervised learning models in classifying microbial samples to source location type at each study site. Tenfold cross validation models were constructed with 1,000 trees using OTUs from evenly rarified samples as predictors of origin habitat among samples cultured *in situ* at Westside Preserve and Cattle Point separately.

Site	Predicted Category	N	Est. error +/- sd	Baseline error	Baseline error : Observed error
Westside Preserve	Source location	14	0.200+/- 0.274	0.643	**3.214**
Cattle Point	Source location	15	0.900 +/- 0.316	0.667	0.741

Within the full set of L6 (genus-level) OTUs from both sites, we observed an increased relative abundance of the nitrifying family Alcaligenaceae (Velusamy and Krishnani 2013) in microbial samples adjacent to field ammonium dispensers at Westside Preserve (Control = 0.00018, Ammonium Dispenser = 0.00033), but a slight decrease in the same comparison at Cattle Point (Control = 0.00022, Ammonium Dispenser = 0.00010). The archaeal nitrifying genus *Nitrosopumilus* occurred at low relative abundance in samples from both treatments (< 0.0001); relative abundance of this taxon was equal between treatments at Westside Preserve, but was four fold higher adjacent to ammonium dispensers than on control emergent rock at Cattle Point. No other taxa with commonly recognized functions in nitrification (**Table 4.A.1**, Pfister, Gilbert, et al. 2014) were identified.

An increase in nitrogen metabolizing genes with experimental ammonium addition occurred at Westside Preserve, but not at Cattle Point (**Figure 4.8**). Genes associated with denitrification were more abundant at Westside Preserve with experimental addition of ammonium, but the opposite effect occurred at at Cattle Point (**Figure 4.8b**; two-way ANOVA, Site x Treatment $F_{1,15} = 8.802$, $p = 0.010$). Borderline significant interactive effects of site and ammonium addition treatment were found in abundance of gene sequences associated with Nitrification (**Figure 4.8a**; two-way ANOVA, Site x Treatment $F_{1,15} = 2.686$, $p = 0.122$),

Assimilatory Nitrate Reduction (**Figure 4.8d**; two-way ANOVA, Site x Treatment $F_{1,15} = 3.653$, $p = 0.075$), and Dissimilatory Nitrate Reduction (**Figure 4.8e**; two-way ANOVA, Site x Treatment $F_{1,15} = 4.369$, $p = 0.054$); for these three metabolisms, mean abundance of metabolism-related gene sequences decreased in response to ammonium addition at Cattle Point, but increased or did not vary with treatment at Westside Preserve.

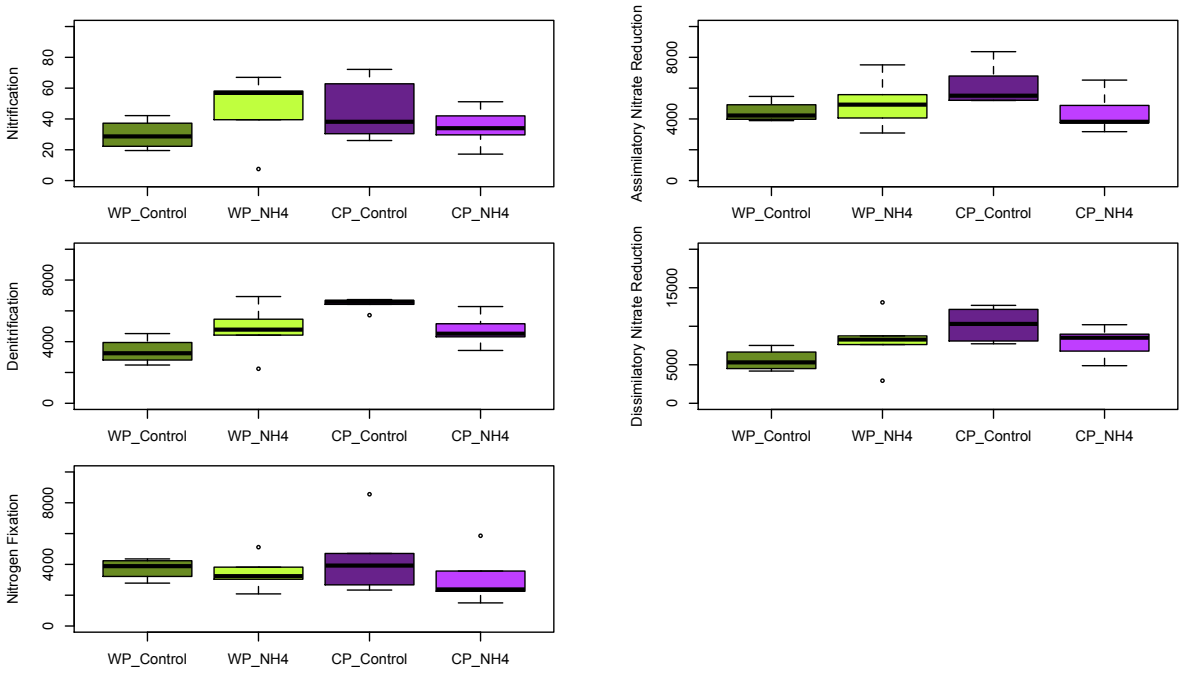

Figure 4.8. Sum counts of gene sequences associated with 5 key nitrogen metabolisms identified within OTU sequence data. Metabolisms of interest are (a) Nitrification, b) Denitrification, c) Nitrogen Fixation, d) Assimilatory Nitrate Reduction, and e) Dissimilatory Nitrate Reduction) within samples from two experimental ammonium addition treatments (Control, NH4) at two sites (Westside Preserve (WP), Cattle Point (CP)). Sum counts were generated by querying the corresponding OTU table for presence of KEGG orthologs (**Table 4.A.2**). Plotted data are untransformed counts.

Experimentally elevated ammonium uptake and assimilation by phototrophs

Use of experimentally elevated ammonium by members of the intertidal algal and photosynthetic microbial community varied by relative longevity of the taxa (or proxy variable) under consideration.

Elemental isotopes measured in low intertidal biofilm, primarily made up of photosynthetic microalgae and microbes, showed both assimilation and utilization of experimentally elevated ammonium (**Figure 4.9**, **Table 4.3**). Percent nitrogen (N) was two-fold higher in biofilm at Westside Preserve in both control and ammonium addition treatment points, but within each site Percent N was 0.5-1% higher adjacent to ammonium dispensers than at control points (**Figure 4.9a**, **Table 4.3**). By virtue of its manufacturing process, experimentally added ammonium chloride (NH_4Cl) is isotopically light; uptake of our NH_4Cl is detectable in tissue. Here, 0.5‰ lighter isotopic N signature is measured in biofilm adjacent to ammonium dispensers than at control points at both sites (**Figure 4.9b**, **Table 4.3**). Neither percent carbon (C) nor $\delta^{13}C$ showed a treatment effect, but did exhibit a strong between-site pattern. Westside Preserve biofilm was 15 points higher in %C, and was 2-4‰ higher in $\delta^{13}C$ than biofilm from Cattle Point (**Figure 4.9c,d**, **Table 4.3**). Elemental carbon to nitrogen ratio did not vary by treatment or site (**Figure 4.9e**, **Table 4.3**).

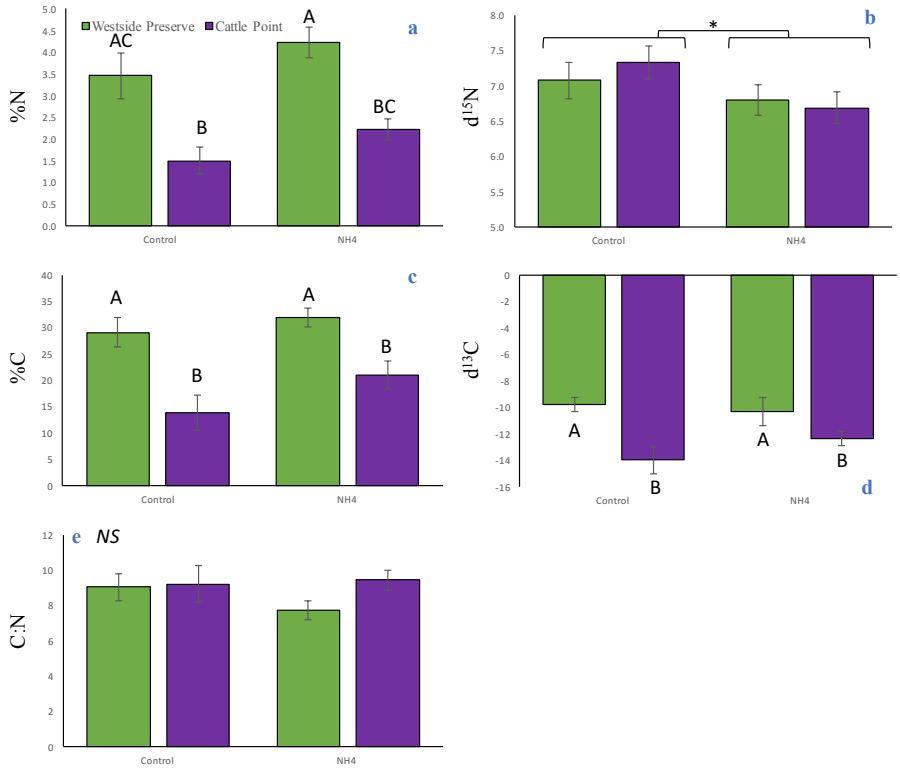

Figure 4.9. Stable isotopes of nitrogen (N) and carbon (C) measured in rock-associated biofilm adjacent to field ammonium dispensers and at control points at Westside Preserve and Cattle Point (N = 4 treatment^{-1} site^{-1}. Samples plotted here were collected at end of the 3-month experimental period (8-9 August 2014).

Table 4.3. Two-way ANOVA results from biofilm elemental isotope analyses. Biofilm was collected from standard-size microscope slides epoxied to rocky substrate adjacent to Control and Ammonium Addition points on the experimental horizontal transect at experimental takedown in August 2014.

	Percent N	**δ^{15}N**	**Percent C**	**δ^{13}C**	**C:N**
Site	$F_{1, 27} = 30.888$ **$p < 0.001$**	$F_{1, 27} = 0.123$ $p = 0.729$	$F_{1, 27} = 23.950$ **$p < 0.001$**	$F_{1, 27} = 12.915$ **$p = 0.001$**	$F_{1, 27} = 1.684$ $p = 0.205$
Treatment	$F_{1, 27} = 4.173$ **$p = 0.051$**	$F_{1, 27} = 3.975$ **$p = 0.056$**	$F_{1, 27} = 3.401$ $p = 0.076$	$F_{1, 27} = 0.447$ $p = 0.510$	$F_{1, 27} = 0.493$ $p = 0.489$
Site x Treatment	$F_{1, 27} = 0.006$ $p = 0.940$	$F_{1, 27} = 0.594$ $p = 0.448$	$F_{1, 27} = 0.636$ $p = 0.432$	$F_{1, 27} = 1.596$ $p = 0.217$	$F_{1, 27} = 1.015$ $p = 0.323$

Elemental isotopes in *Saccharina* tissue showed no response to experimental ammonium addition or other site-level parameters (**Figure 4.10**, **Table 4.4a**), but there is evidence of a functional response to large-scale regional oceanography. When we collapsed treatments and performed a two-way ANOVA on the factors site (Westside Preserve, Cattle Point) and time point (early in the experimental period (May 2014, N = 5 individuals $site^{-1}$), post experimental period (August 2014, N = 8 individuals $treatment^{-1}$ $site^{-1}$)), we detected time point patterning in tissue percent N, $\delta^{15}N$, $\delta^{13}C$, and C:N (**Figure 4.10**, **Table 4.4b**). Percent N in *Saccharina* tissue declined by an average of 1% in new growth of tracked individuals (**Figure 4.10a**), regardless of experimental treatment, indicating utilization of accumulated nitrogen during the growing season. This interpretation is bolstered by a 2 unit increase in C:N ratio among tracked *Saccharina* individuals across the summer season (**Figure 4.10e**). Among these same individuals, the $\delta^{15}N$ value in new growth tissue increased by 0.5-1‰ (**Figure 4.10b**), reflecting increased uptake of the heavier isotope of nitrogen.

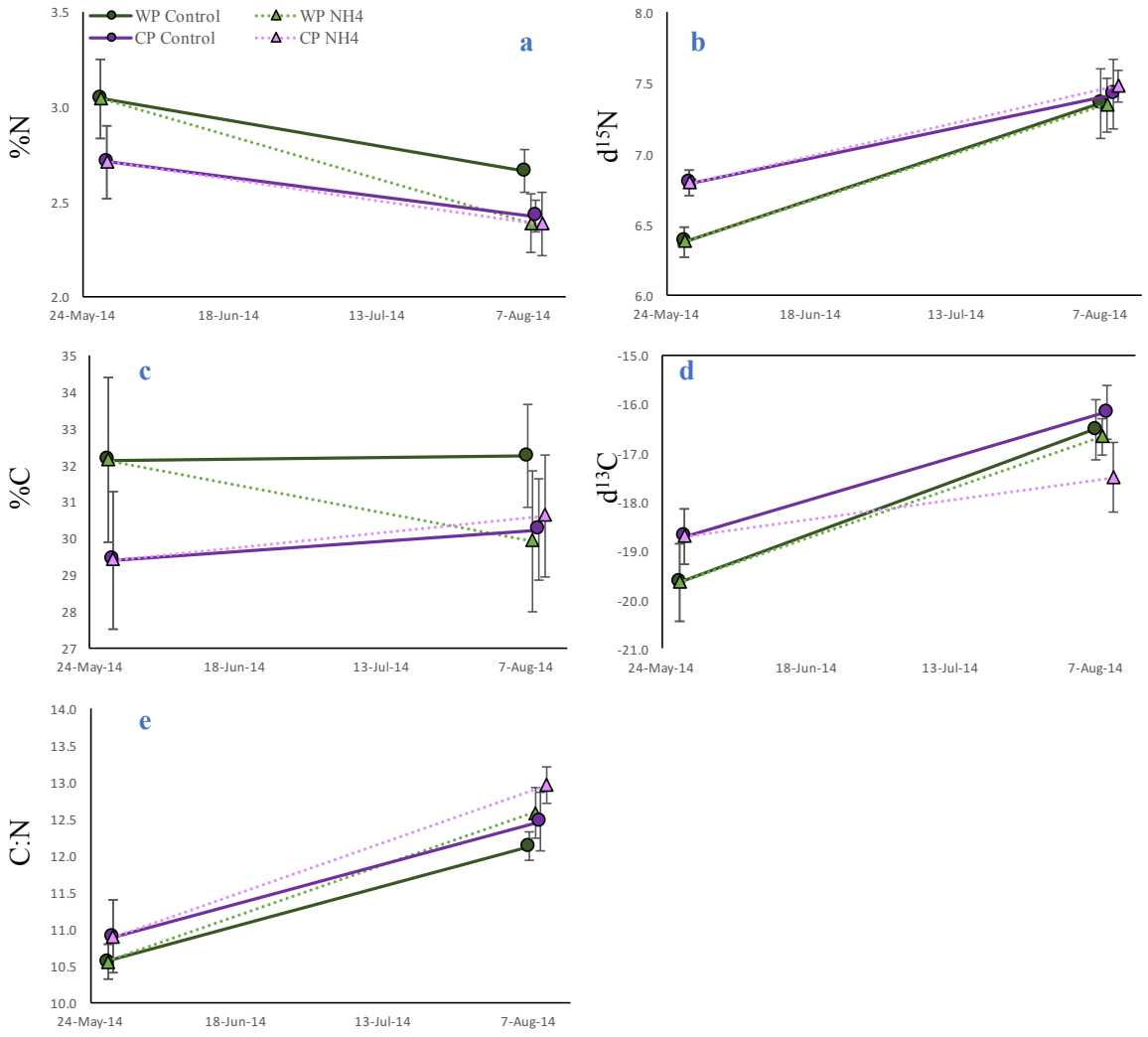

Figure 4.10. Stable isotopes of nitrogen (N) and carbon (C) measured in *Saccharina* tissue adjacent to field ammonium dispensers (triangle symbols) and at control points (circle symbols) at Westside Preserve and Cattle Point. Samples plotted here were collected near the start (27-28 May 2014) and end of the 3-month experimental period (8-9 August 2014). 'Final' symbols (August 2014) are jittered on the x-axis for clarity.

Table 4.4. Two-way ANOVA results from *Saccharina* elemental isotope analyses **a**) on individuals sampled at two sites and two treatment regimes at the end of the experimental period (August 2014), and **b)** on individuals sampled at two sites and two time points during the summer period (May 2014 and August 2014) with experimental treatments lumped. All *Saccharina* tissue was collected from new growth of a single kelp individual per experimental control and ammonium dispenser point on the experimental horizontal transect at each site.

a.

	Percent N	**$\delta^{15}N$**	**Percent C**	**$\delta^{13}C$**	**C:N**
Site	$F_{1, 27} = 0.829$ $p = 0.371$	$F_{1, 27} = 0.204$ $p = 0.655$	$F_{1, 27} = 0.172$ $p = 0.682$	$F_{1, 27} = 0.115$ $p = 0.737$	$F_{1, 27} = 1.279$ $p = 0.268$
Treatment	$F_{1, 27} = 1.492$ $p = 0.232$	$F_{1, 27} = 0.012$ $p = 0.914$	$F_{1, 27} = 0.398$ $p = 0.533$	$F_{1, 27} = 1.597$ $p = 0.217$	$F_{1, 27} = 2.479$ $p = 0.127$
Site x Treatment	$F_{1, 27} = 0.800$ $p = 0.379$	$F_{1, 27} = 0.027$ $p = 0.871$	$F_{1, 27} = 0.708$ $p = 0.408$	$F_{1, 27} = 1.074$ $p = 0.309$	$F_{1, 27} = 0.003$ $p = 0.958$

b.

	Percent N	**$\delta^{15}N$**	**Percent C**	**$\delta^{13}C$**	**C:N**
Site	$F_{1, 37} = 1.899$ $p = 0.177$	$F_{1, 37} = 1.028$ $p = 0.317$	$F_{1, 37} = 0.705$ $p = 0.407$	$F_{1, 37} = 0.011$ $p = 0.916$	$F_{1, 37} = 1.423$ $p = 0.268$
Time point	$F_{1, 37} = 8.629$ **$p = 0.006$**	$F_{1, 37} = 18.867$ **$p < 0.001$**	$F_{1, 37} = 0.000$ $p = 0.988$	$F_{1, 37} = 18.500$ **$p < 0.001$**	$F_{1, 37} = 33.443$ **$p < 0.001$**
Site x Time point	$F_{1, 37} = 0.568$ $p = 0.456$	$F_{1, 37} = 0.727$ $p = 0.399$	$F_{1, 37} = 0.405$ $p = 0.528$	$F_{1, 37} = 0.956$ $p = 0.335$	$F_{1, 37} = 0.000$ $p = 0.998$

Within two months of observation across the 2014 summer season, benthic biofilm chlorophyll *a* concentration was higher at Westside Preserve than at Cattle Point (**Figure 4.11**, **Table 4.5**). However, chlorophyll *a* was never affected by experimental ammonium treatment. When chlorophyll *a* concentrations were analyzed as independent responses via three separate Two-Way ANOVA tests, the magnitude of this between-site difference increased over the course of the summer, from no difference in the June 2014 samples to a doubling between sites in August 2014 samples (**Table 4.5**). Repeated measures two-way ANOVA on these dates, which incorporated sample identity as an error term, revealed sample month as a significant correlate with Chlorophyll *a* at Cattle Point (**Figure 4.11b**; Repeated Measures Two-Way ANOVA $F_{1, 41} = 3.205$, $p = 0.05$). At Westside Preserve, this same statistical analysis revealed month as a borderline significant correlate with Chlorophyll *a* (**Figure 4.11a**; Repeated Measures Two-Way ANOVA: Month $F_{1, 39} = 2.420$, $p = 0.10$, Treatment *NS*, Month * Treatment *NS*).

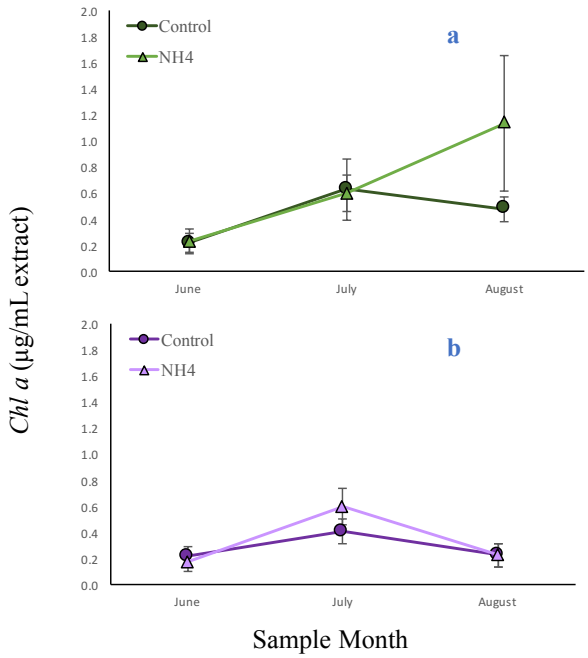

Figure 4.11. Chlorophyll *a* concentration extracted from swabs of standard-size microscope slides adjacent to field ammonium dispensers (triangle symbols) and control points (circle symbols) at a) Westside Preserve and b) Cattle Point at three time points in 2014: 11-12 June, 10-11 July, and 8-9 August.

Table 4.5. Two-way ANOVA results from biofilm chlorophyll a concentration analyses. Biofilm was swabbed from standard-size microscope slides epoxied to rocky substrate adjacent to control and ammonium dispenser points on the experimental horizontal transect.

	June 2014	**July 2014**	**August 2014**
Site	$F_{1, 26} = 0.470$ $p = 0.499$	$F_{1, 28} = 2.422$ $p = 0.131$	$F_{1, 28} = 5.285$ **$p = 0.029$**
Treatment	$F_{1, 26} = 0.009$ $p = 0.926$	$F_{1, 28} = 0.122$ $p = 0.729$	$F_{1, 28} = 1.867$ $p = 0.183$
Site x Treatment	$F_{1, 26} = 0.001$ $p = 0.975$	$F_{1, 28} = 0.023$ $p = 0.881$	$F_{1, 28} = 1.144$ $p = 0.294$

DISCUSSION

Our ammonium addition treatment was uneven between sites, with higher diffusion from Cattle Point experimental ammonium dispensers (**Figure 4.5**) due to increased water motion (**Figure 4.4**). Analysis of biotic responses at paired sites, which differed in macrobiotic community composition (**Figure 4.2**) and water motion (**Figure 4.4**), revealed site-dependent ammonium use by multiple autotrophic members of the lower intertidal community.

Ambient biofilm communities from Westside Preserve and Cattle Point demonstrated distinct nitrogen-processing capabilities when incubated in ambient local seawater in a closed system (**Figure 3**). Most notably, mesocosms containing BioBall-associated biofilm cultured at Cattle Point developed elevated nitrite concentration over the 3h incubation, while mesocosms containing Westside Preserve-cultured biofilm showed no such increase (**Figure 4.3b**). Because nitrite comes from microbial oxidation of ammonium present in seawater, the benthos at Cattle Point showed a functional metabolic response with ammonium availability. Indeed, Cattle Point and Westside Preserve had strongly distinct macrobiota community structure, with greater animal abundance at Cattle Point (**Figure 4.2**). The abundant animal cover of the rocky substrate at Cattle Point translates to elevated estimates of nitrogen regeneration via excretory products

(ammonium, urea); elevated water motion at Cattle Point (**Figure 4.4**) implies that much of this locally regenerated nitrogen is advected quickly, underscoring the importance of a rapidly-responding biofilm community.

Agarose ammonium dispensers deployed fresh every 12-14 days delivered a pressed nutrient addition treatment at both sites, as shown by measurably elevated ammonium concentration in *in situ* seawater above 'spent' agar on the day of dispenser swap (**Figure 4.5**). Although not measured directly, we infer that ammonium treatment decay rate was not identical between sites; the increased ammonium remaining in agar at Westside Preserve at the end of the deployment period than in agar at Cattle Point is consistent with higher rate of plaster dissolution at Cattle Point compared to Westside Preserve (**Figure 4.4**). These local water flow data indicate that advection of ammonium from the dispensers at Cattle Point was higher than at Westside Preserve, creating a steeper nutrient gradient between the ambient seawater and the agar, which resulted in faster ammonium diffusion rates, and also suggests that oceanic nutrient delivery to the intertidal autotroph community was higher at this higher flow site.

Our treatment goal for experimental elevation of ammonium was to achieve concentrations that are naturally only reached in tide pools at these sites. Tide pools and emergent rock at Westside Preserve, Cattle Point, and other nearby field sites host distinct microbial communities, and ammonium concentration is significantly correlated with this dichotomy (Chapter III). In the current study, agarose dispensers successfully created pool-like ammonium concentrations matching natural conditions at each site (**Figure 4.6a**). Tide pools hold higher faunal abundance than emergent rock (Chapter III); these animals provide nutrient stress amelioration to tide pool phototrophs that are otherwise isolated from oceanic water

column nutrients for up to 87% of the time in the high intertidal, integrated over an entire year (Bracken 2004; Bracken and Nielsen 2004a).

BioBall-associated microbial communities (**Figure 4.7**) and microalgal components of biofilm (**Figure 9**) show a positive response to locally elevated ammonium, but primarily at Westside Preserve where oceanic water motion is lower (**Figure 4.4**). Different water flow between sites lead to different nutrient advection/supply (**Figure 4.5**, **Figure 4.6**) that translates to multiple biotic groups.

If animal regenerated ammonium is a driving factor in determining microbial community structure in this rocky intertidal system, then our experimental addition of ammonium should have driven community structure to resemble that in high ammonium tide pools. The experimental ammonium elevation treatment applied at Westside Preserve yielded statistically distinct microbial community structures associated with BioBalls installed in tide pools, on emergent rock, and on emergent rock adjacent to dispensers (**Figure 4.7**). Further, Westside Preserve microbial communities associated with ammonium dispensers clustered between unmanipulated emergent rock and tide pool communities in PCoA ordination space (**Figure 4.7a**), suggesting that our treatment did drive microbial community structure toward a pool environment for benthic-associated microbial communities. The experimental ammonium elevation treatment did not have this strong effect at Cattle Point, though, where water motion was higher and therefore expected to have diluted experimentally added ammonium more quickly.

Time-integrated elemental nutrient isotope signals in phototroph tissue allow us to conclude that experimental ammonium uptake by these primary producers was context dependent. Locally delivered experimental ammonium on emergent rock was assimilated by

biofilm (**Figure 4.9**), but not by the kelp (*Saccharina*) (**Figure 4.10**). Biofilm microalgae are characterized by rapid colonization and turnover (Thompson *et al.* 2004), meaning that this biotic guild is strongly responsive to local conditions. Although elemental analysis of *Saccharina* did not indicate that our ammonium treatment had an effect at either site, the strong seasonal effect in isotope ratios suggests a seasonal pattern of nutrient supply. Among tracked *Saccharina* individuals, the $\delta^{15}N$ isotopic ratio in new growth tissue increased by 0.5-1‰ over the three study months (**Figure 4.10b**), reflecting increased uptake of the heavier isotope of nitrogen, and thus evidence of a regionally shifting nitrogen source from oceanic upwelled nitrate to locally regenerated ammonium (Pfister *et al.* 2014a). This lack of experimentally elevated ammonium treatment effect in kelp suggests that emergent macrophytes may not respond to supply in a highly turbulent system (e.g. Pfister & Van Alstyne 2003), while rapidly growing microbiota (microbes and microalgae) do (e.g. Pfister et al. 2010). Despite evidence of experimentally elevated ammonium effect on tissue nitrogen content in benthic biofilm (**Figure 4.9**), the seasonally developing site effect and lack of ammonium treatment effect within chlorophyll *a* data indicate regional parameters beyond ammonium availability drive standing crop nutrient use in the phototrophic biofilm community (**Figure 4.11**, **Table 4.5**).

Broadly, our findings demonstrate differential use of locally generated ammonium by macroalgae (*Saccharina*), microalgae (photosynthetic components of biofilm), and microbes. Elemental analysis in *Saccharina* tissue indicated a seasonal nutrient uptake pattern consistent with known nitrogen regeneration that occurs regionally (Dugdale and Goering 1967), with no evidence of uptake of locally experimentally elevated ammonium (Pfister and Van Alstyne 2003). Because *Saccharina* typically grows on emergent rock, it could realistically show

preference for nitrate delivered via oceanic water column (not measured here), not ammonium delivered by faunal tide pool inhabitants (see Bracken & Stachowicz (2006)).

There is evidence that both photosynthetic and microbial components of the benthic biofilm have the capacity to access and utilize locally delivered ammonium. Given that nitrogen is a limiting nutrient in temperate coastal systems, our findings set a stage for a potential competitive interaction between these guilds, and a sensible next step beyond the current study would be a controlled experimental analysis of the microbial-microalgal interaction in terms of *in situ* use of experimentally elevated ammonium in an explicit way, by measuring these same variables in the shade. A shade treatment can strongly limit photosynthetic components of the benthic biofilm (Chapter II, Kavanaugh et al. 2009), thus allowing measurement of the microbial response in the absence of direct competitors. This would allow the current study to align with a companion laboratory mesocosm study (Chapter II), demonstrating algal-microbial competition for ammonium.

Coastal marine systems are undergoing accelerated harvest of animals that play nitrogen recycling roles (Worm *et al.* 2006; Maranger *et al.* 2008); as such, studies like this one that tease apart interacting effects of nitrogen processing community components such as biofilm (microbes and microalgae) and macroalgae are of critical importance in forecasting nitrogen-related changes on an ecosystem scale (Moulton *et al.* 2016). Intertidal marine habitats have provided a setting for pioneering research in community ecology. Integrating elemental nutrient uptake and assimilation across phototrophic and microbial community components with extensive preexisting knowledge of rocky intertidal ecosystem dynamics can be used to develop an understanding of the role altered nutrient availability might play in shaping the interactions and observed patterns in this system. By incorporating elemental nutrient analysis in the the

study of algal-microbial interaction in terms of nutrient availability, we can develop an ability to better predict the consequences of human induced changes in nutrient cycles in this habitat.

ACKNOWLEDGMENTS

This work was supported by an LTREB (DEB 09.19420, Earth Microbiome Project, University of Chicago Committee on Evolutionary Biology Hinds Fund, Friday Harbor Laboratories Graduate Fellowships, and an EPA STAR Graduate Fellowship. We thank the San Juan County Land Bank and the University of Washington Friday Harbor Marine Laboratories for access to field sites, K. Biederbeck, N. Rivlin, H. Hayford, A. Henry, and the Spring Street International School Inland Ocean Studies Summer Program for field assistance, J. Hampton-Marcell and S. Owens for sequencing assistance, G. Olack for stable isotope analysis assistance, and J. Gilbert, G. Dwyer, J.T. Wootton, and M. Coleman for helpful comments on research design, analysis, and the manuscript.

Appendix 4A: Microbial taxa and genes associated with N-metabolism.

Table 4.A.1. Microbial genera associated with nitrification (table segment reproduced from Pfister, Gilbert, et al. 2014)

Nitrification
Alcaligenes
Nitrobacter
Nitrococcus
Nitrolancetus
Nitrosococcus
Nitrosolobos
Nitrosopumilus
Nitrosovibrio
Nitrospina
Nitrospira
Nitrotoga
Paracoccus

Table 4.A.2. Gene orthologs identified as having functional roles in specific nitrogen metabolism categories. Orthologs were retrieved from the KEGG database nitrogen metabolism pathway map.

Nitrogen Metabolism	**Corresponding KEGG Orthologs**
Nitrification	K10944, K10945, K10946, K10535
Denitrification	K00370, K00371, K00374, K00373, K02567, K02568, K00368, K15864, K04561, K02305, K15877, K00376
Nitrogen Fixation	K02588, K02586, K02591, K00531
Assimilatory Nitrate Reduction	K00367, K10534, K00372, K00360, K00366, K17877
Dessimilatory Nitrate Reduction	K00370, K00371, K00374, K00373, K02567, K02568, K00362, K00363, K03385, K15876

Appendix 4B: Correlations of macrobiota with multivariate axes.

Table 4.B.1. Correlations (r^2) of surveyed macrobiota with NMDS axes 1 and 2 (**Figure 4.2**). The analysis yielding these data was performed using the Bray-Curtis distance metric, meaning that correlation of taxa with axes is based on abundance within the sample unit.

	MDS1	**MDS2**
Costaria costata	-0.34	-0.17
Pollicipes polymerus	-0.34	-0.17
Halosaccion glandiforme	-0.33	-0.04
Green sponge	-0.32	0.02
Cryptosiphonia woodii	-0.29	-0.10
Mytilus californianus	-0.20	-0.07
Anthopleura elegantissima	-0.15	-0.09
Littorina scutulata	-0.14	-0.09
Semibalanus cariosus	-0.14	-0.05
Chthalamus dalli	-0.14	-0.15
Nucella lamellosa	-0.13	-0.21
Nemertean worm	-0.13	-0.10
Cryptopleura ruprechtiana	-0.12	-0.17
Hermit crab	-0.12	-0.17
Orange sponge	-0.12	-0.17
Leathesia difformis	-0.12	0.22
Lottia pelta	-0.12	-0.04
Egregia menziesii	-0.11	-0.28
Articulated coralline algae	-0.10	0.04
Searlesia dira	-0.10	0.44
Eudistyla vancouveri	-0.09	-0.23
Neorhodomela oregona	-0.08	-0.27
Odonthalia floccosa	-0.08	-0.21
Katharina tunicata	-0.07	0.13
Mopalia muscosa	-0.07	-0.17
Balanus glandula	-0.06	0.01
Phyllospadix scouleri	-0.06	-0.02
Purple sponge	-0.06	-0.26
Mazzaella splendens	-0.05	-0.27
Cladophora columbiana	-0.04	-0.08
Nucella canaliculata	-0.04	-0.03
Prionitis sternbergii	-0.04	-0.08
Microcladia borealis	-0.04	-0.03

Table 4.B.1. *Continued*.

	MDS1	**MDS2**
Lottia digitalis	-0.03	0.03
Mastocarpus crust	-0.03	-0.08
Calliostoma canaliculatum	-0.01	-0.17
Saccharina sessile	0.01	0.01
Crustose coralline algae	0.02	0.04
Mastocarpus upright	0.03	-0.13
Tectura scutum	0.03	0.01
Desmarestia ligulata	0.04	-0.43
Desmarestia viridis	0.04	-0.43
Littorina sitkana	0.04	-0.10
Fucus gardneri	0.05	0.01
Barnacle recruit	0.06	0.10
Endocladia muricata	0.09	0.01
Strongylocentrotus droebachiensis	0.11	0.00
Dodecaceria fewksi	0.11	0.00
Urticina crassicornis	0.13	0.38
Pugettia gracilis	0.15	-0.33
Red crust aglae	0.15	-0.16
Diadora aspera	0.18	0.07
Porphyra sp.	0.20	-0.02
Ulva sp.	0.25	-0.03
Alaria sp.	0.36	-0.41
Acrosiphonia coalita	0.42	-0.33
Urospira sp.	0.45	-0.29
Mazaella cornucopia	0.47	0.10

CHAPTER V

MICROBIAL ASSOCIATIONS WITH MACROBIOTA IN COASTAL ECOSYSTEMS: PATTERNS AND IMPLICATIONS FOR NITROGEN CYCLING[1]

ABSTRACT

Although macrobiota can have significant effects on nitrogen cycling via excretion by macrofauna and assimilation by macroflora, many macrobiota also host or facilitate microbial taxa responsible for nitrogen transformations. This is an area of expanding interest in coastal marine systems, where nitrogen is a limiting nutrient. Our understanding of the diversity of microbes associated with coastal marine animals and macrophytes is increasing, and recent studies indicate that the microbiomes of macrobiota may directly contribute to nitrogen cycling. We review the roles that macrobiota play in coastal nitrogen cycling, appraise current understanding of macrobial-microbial associations in terms of nitrogen processing, and suggest implications for coastal ecosystem function as animals are harvested and foundational habitat is lost or degraded. Given the biodiversity of microbial associates of macrobiota, we advocate increased research into the functional consequences of these associations for the coastal nitrogen cycle.

DRIVERS OF COASTAL NITROGEN

Nitrogen is often a limiting nutrient in coastal marine systems, but human activities have doubled the availability of this nutrient over the past century, particularly via fertilizer production

[1] This review paper was written in collaboration with Dr. Mark A. Altabet (University of Massachusetts Dartmouth), Dr. J. Michael Beman (University of California Merced), Dr. Linda A. Deegan (Marine Biological Laboratory), Meaghan K. Lyons, Dr. James A. Nelson (University of Louisiana Lafayette), And Dr. Catherine Pfister (University of Chicago). It previously appeared in *Frontiers in Ecology and the Environment*, 2016, Volume 14, Issue 4, pages 200-208, and is reprinted here with permission from Wiley Publishing.

to sustain increases in agriculture (Galloway *et al.* 1995). In coastal ecosystems receiving anthropogenic nitrogen, excess nitrogen can fuel harmful algal blooms, and respiration of produced organic material depletes dissolved oxygen, potentially leading to hypoxia (Howarth *et al.* 2011) However, coastal ecosystems (estuaries, marshes, reefs, and the nearshore pelagic ocean) are also well-known sites of nitrogen removal via microbial activity. This removal attenuates the land-sea flux of nitrogen and can ameliorate the effects of nitrogen pollution in coastal regions. At the same time, newly recognized forms of microbial nitrogen metabolism (e.g. anammox, conversion of nitrite and ammonium directly into gaseous nitrogen; Table 5.1), and the identification of new microbial contributors (e.g. Archaea; Könneke *et al.* 2005) have increased our appreciation of the complexity of coastal nitrogen cycling. In open waters, microbial transformations of the marine nitrogen cycle are governed by water column light and oxygen gradients, and "new" nitrogen is primarily supplied by upwelling and biological nitrogen fixation (Figure 5.1, Table 5.1). However, coastal systems also host a diversity of macrobiota (multicellular flora and fauna) that contribute to nitrogen cycling through nitrogen production, retention, and removal (e.g. Nelson *et al.* 2013). Further, macrobiota can locally change oxygen concentrations via metabolic activities, thus promoting a range of nitrogen metabolisms over a scale of only μm to mm (Figure 5.2, Figure 5.3, Table 5.1). It is apparent that macro-fauna and –flora host microbial communities that are capable of a diversity of nitrogen metabolisms (Figure 5.2, Figure 5.3), though our understanding remains nascent. As the distribution and abundance of marine macrobiota change rapidly due to harvest, invasions, habitat fragmentation, pollution, local disturbance, and global climate change, the effects of these changes on associated microbial diversity and nitrogen cycling functions are unknowns in coastal biogeochemistry and ecology. *Here, we evaluate the current understanding of the role of microbial associations with macrobiota*

in coastal nitrogen processing, highlighting where these associations could be significant at an ecosystem level.

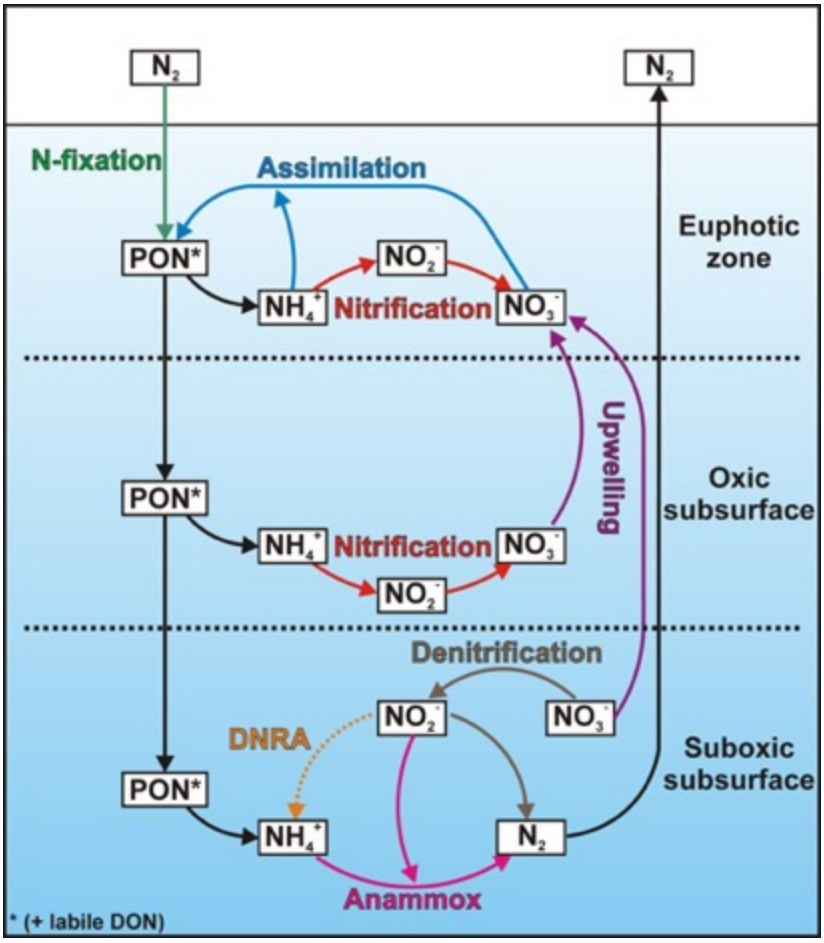

Figure 5.1. A schematic diagram of three different environments in the ocean. In the euphotic zone, aerobic processes and assimilation dominate, and nitrogen inputs come from mainly upwelling and mixing of nitrate from deeper depths. Where light is limiting but the environment remains oxic, aerobic nitrogen transformations occur. Where suboxic conditions exist, anaerobic nitrogen transformations dominate. Oxygen levels can depend on the metabolic activities of animals and thus may influence the dominant nitrogen metabolisms. (PON: Particulate organic nitrogen, DON: Dissolved organic nitrogen). For additional detail, see Capone *et al.* (2008).

Table 5.1. Key microbial nitrogen metabolisms in the coastal ocean

Nitrogen Metabolism	Definition
Anammox	**AN**aerobic **AMM**onium **OX**idation; chemoautotrophic organisms from the bacterial phylum Planctomycetes convert nitrite and ammonium directly into gaseous nitrogen (N_2).
Denitrification	Heterotrophic facultative anaerobic bacteria reduce nitrates (NO_3^-) and nitrites (NO_2^-) to ultimately produce gaseous nitrogen (N_2) via intermediate gaseous nitrogen oxide intermediates (NO and N_2O).
DNRA	**D**issimilatory **N**itrate **R**eduction to **A**mmonium; reduction of nitrate to ammonium via nitrite intermediate by microbial organisms.
Nitrification	A two-step transformation by bacteria and archaea where ammonium (NH_4^+) is oxidized to nitrite (NO_2^-) and nitrite is further oxidized to nitrate (NO_3^-).
Nitrogen Fixation	Atmospheric elemental nitrogen (N_2) is converted into biologically available forms (e.g. ammonium; NH_4^+).

Although nitrogen is a key element in amino acids and therefore critical to all life on earth, the nitrogen cycle has multiple links (e.g. nitrogen fixation, nitrification, denitrification, DNRA, anammox; Table 5.1) carried out primarily or exclusively by microorganisms. Bacterial and archaeal roles in nitrogen transformations are increasingly known, and it has recently become apparent that associations with macrobiota enhance these transformations. Indeed, review of the macrobiota-associated nitrogen transformations indicates that every link in the nitrogen cycle has identifiable microbe-macrobiota associations in the natural environment that can alter the rate of nitrogen cycling (Figure 5.2, Figure 5.3, Table 5.3). We highlight this rapidly emerging area of interaction between microbes, animals, and macrophytes (seaweeds and marine plants).

Figure 5.2. Marine macrofauna (invertebrates and vertebrates) locally alter the surrounding seawater oxygen levels, promoting diverse nitrogen-metabolizing processes. Several faunal organisms that harbor microbial communities with known roles in enhancing specific nitrogen metabolisms illustrate the potential for animals to influence microbial diversity and function.

A. In the **Remineralization** process, organic molecules (particulate organic nitrogen (PON); dissolved organic nitrogen (DON)) are transformed into inorganic forms (Ammonium (NH_4^+)), typically via biological activity (i.e. faunal excretion). Pinfish (*Lagodon rhomboides*), by moving from nearshore seagrass habitat to offshore waters, export nitrogen in excretion at a rate greater than the sum of local river and submarine groundwater discharge (Nelson *et al.* 2013) (*Lagodon rhomboides* illustration used with permission of the artist, Diane Peebles).

B. Nitrification, the sequential oxidation of ammonia (NH_3) or ammonium (NH_4^+) to nitrite (NO_2^-) and subsequently to nitrate (NO_3^-), is performed by specific groups of nitrifying bacteria and Achaea. Ammonium (NH_4^+) is both the primary N-excretion product of marine invertebrates and the required substrate for nitrification in high oxygen environments. Consequently, high rates of nitrification have been measured in association with sessile marine invertebrates such as *Mytilus galloprovincialis* (Welsh and Castadelli 2004) (closely related *Mytilus trossulus* pictured; photo provided by J.T. Wootton).

Figure 5.2. *Continued*.

C. Organisms from the bacterial phylum Planctomycetes are capable of converting nitrite (NO_2^+) and ammonium (NH_4^+) directly into gaseous nitrogen (N_2) in a process called **Anammox** (**AN**aerobic **AMM**onium **Ox**idation). This microbially-driven low-oxygen process has been measured in association with sponge tissue, as evidenced by depletion of NH_4^+ and NO_2^- paired with production of gaseous N_2 in airtight vials containing the sponge *Geodia barretti* (Hoffmann *et al.* 2009), (*Geodia barretti* photo provided by H.T. Rapp).

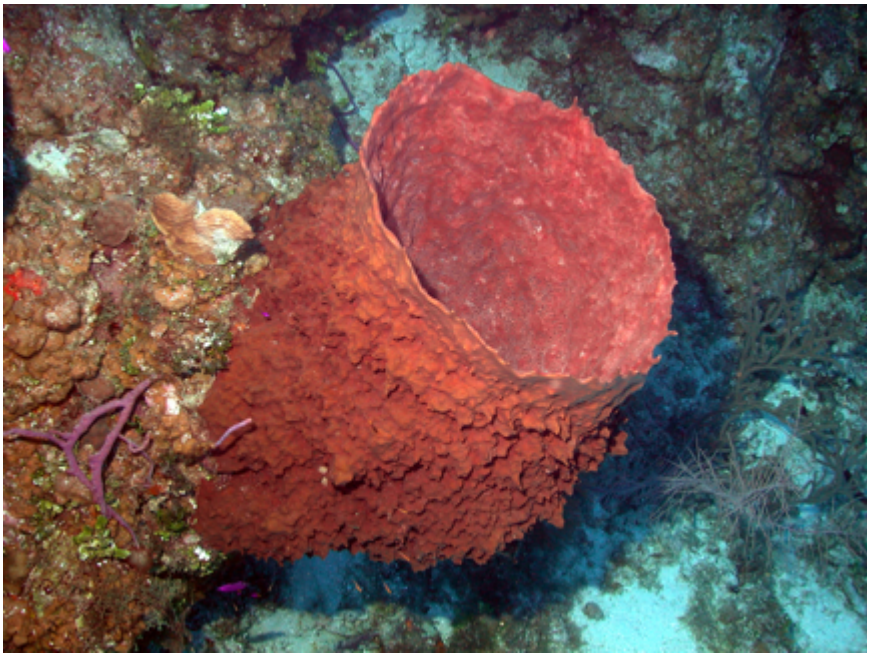

D. In the process of **Denitrification**, nitrate (NO_3^-) is converted to nitrogenous gases (NO, N_2O, or N_2), and biologically available nutrient nitrogen is lost from an ecosystem. Sponges have been shown to be net sinks of nitrate, providing evidence that denitrification is an important process in association with these organisms in cases where the host sponge slows or stops pumping and tissue becomes hypoxic/anoxic (Fiore *et al.* 2010) (*Xestospongia muta* photo provided by M. Lesser).

Figure 5.3. Like macrofauna (Figure 5.2), marine macroflora (seaweeds and plants) differentially promote microbial nitrogen-metabolizing associates and processes via alteration of local seawater oxygen levels.

A. Uptake of nitrogen in biologically available forms is commonly measured in marine macroflora (seaweeds and seagrasses). For example, the Pacific Northwest intertidal seaweed *Prionitis sternbergii* assimilates invertebrate-excreted ammonium (NH_4^+) from local seawater, which is converted into amino acids (Pather *et al.* 2014) (*Prionitis sternbergii* photo by C. Pfister).

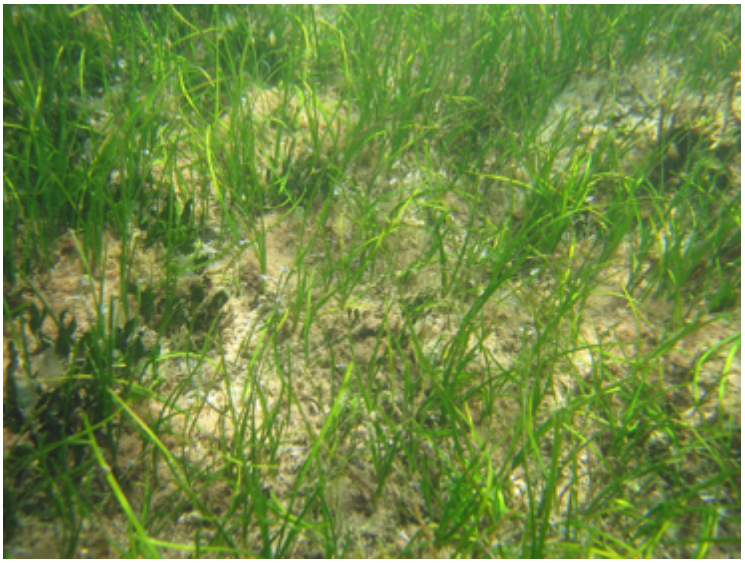

B. Elemental nitrogen gas (N_2) is abundant in the Earth's atmosphere, but this form is inaccessible to most primary producers. **Nitrogen fixation**, the process by which nitrogen gas is reduced into biologically available nitrogen compounds (e.g. ammonia, NH_3), is known to occur at high rates in rhizospheric sediments of seagrasses as a function of plant-bacteria interactions (Welsh 2000) (*Cymodocea nodosa* photo by J. Lloret).

Macrobiota can locally transform the environment in ways that favor particular microbial activities. First, macrobiota can serve as a predictable and comparatively resource-rich surface for microbial populations, especially for those environments where water motion is constant and solid substrate is limited. Thus, the surfaces of macrobiota can be a renewing physical resource for microbial colonization. This is in contrast with soft sediment environments where the mud-sand matrix is persistent, providing a stable spatial structure for a microbial population (Laverock *et al.* 2011).

A second key role specific to macrofauna is as a source of regenerated nitrogen as urea or ammonium, which has been shown to be quantitatively important to productivity in a range of marine systems (Gilbert *et al.* 1982; Bracken 2004; Roman and McCarthy 2010). A significant role for animal excretion (production of nitrogen-containing compounds (ammonium, urea) as byproducts of metabolic processes) is demonstrated across diverse taxa, from zooplankton (Dugdale and Goering 1967; Saba *et al.* 2011) to whales (Roman and McCarthy 2010). Though this nitrogen is ultimately derived from nitrogen uptake lower in the food chain, its availability as ammonium, a comparatively more accessible form of dissolved inorganic nitrogen (DIN) for microbes, means that animals and their aggregations contribute to biogeochemical hotspots in aquatic systems— especially in biogenic habitats such as reefs and kelp beds (Allgeier *et al.* 2013)— and ameliorate nutrient limitation. Further, filter feeders can locally concentrate nitrogen from filtering particulate organic nitrogen (PON) from a large volume of water (Pather *et al.* 2014). Animal aggregations can deliver 5 to 177-fold increases in nitrogen loading over anthropogenic nitrogen delivery, even in areas of high human influence (Allgeier *et al.* 2013). Similarly, large marine mammals transport and concentrate oceanic nitrogen near the sea surface through release of large fecal plumes at feeding areas. The contribution of marine mammals (estimated to be

2.3×10^4 tonnes N yr^{-1}) exceeds the combined inputs from all rivers in the Gulf of Maine system (Roman and McCarthy 2010). Mussel aggregations in coastal areas have been shown to augment ammonium concentrations (Aquilino *et al.* 2009), and are associated with increased nitrogen processing (Pfister *et al.* 2014a). Small nekton in saltmarsh intertidal pools increased nitrogen concentrations 17-109% over pools without nekton in southeastern US saltmarshes (Galloway *et al.* 1995). The relatively low energetic cost to macrophytes of using ammonium as a dissolved inorganic nitrogen source may increase the significance of animal contributions. In sum, in nitrogen-limited coastal systems, animals can have a significant and positive effect on coastal productivity (Figure 5.2).

MACROBIOTA AS MICROBIAL NITROGEN CYCLING HOTSPOTS

Diversity of marine microbiota-macrobiota associations

The number of described microbial associations with macrobiota in the coastal ocean has expanded rapidly in recent years and now covers a diversity of marine taxa, including invertebrates (Table 5.2), macrophytes (Supplementary Table 5.1), and vertebrates (Supplementary Table 5.2). These studies indicate broad phylogenetic diversity of microbial taxa hosted on and within macrobiota, and there is emerging evidence of selection for or promotion of particular microorganisms by macrobiota (Sunagawa *et al.* 2010; Apprill *et al.* 2014) when compared to surrounding seawater. For example, marine macrophytes enhance local microbial diversity relative to surrounding unvegetated sediments (Delille *et al.* 1996), and new microbial taxa have been discovered in association with seagrass (Lucas-Elío *et al.* 2011). Distinct microbial communities are found on the surface of seagrass leaves (Törnblom and Søndergaard 1999), roots and rhizomes (Nielsen *et al.* 2001), and in the rhizosphere (Shieh *et al.* 1989). Selection for particular microbes

by macrobiota is demonstrated by some macrobiotic species hosting a shared ‘core’ microbiome (collection of microorganisms in a shared location) among individuals; for example, humpback whales from different ocean basins have whale species-specific skin microbiomes despite geographic isolation (Apprill *et al.* 2014).

Table 5.2. Marine invertebrates with described microbial associates.

Invertebrate Host	Location of Microbiome	Method of Genomic Analysis	Dominant group(s) in microbiome	Habitat	Host trophic mode	Host life history	Host longevity	Criteria for examining host specificity	Selected Reference(s)
 Coral (*Acropora millepora*)	Coral fragments	Amplicon sequencing	Alpha-Proteobacteria	Reef	Primary consumer	Sessile	Decades	Distinct microbial assemblages inshore vs mid-reef.	(Rohwer *et al.* 2002)(Lema *et al.* 2014) *Photo provided by D. Bourne.*
 Zoanthid (*Palythoa austaliae*)	Zoanthid tissue	16S rRNA pyrosequencing	Proteobacteria, Chloroflexi, Actinobacteria	Reef	Primary producer/ filter feeder	Sessile	Decades	NA	(Sun *et al.* 2014) *Photo by C. Pfister.*
 Sponges (*Halichondria panicea, Haliclona oculata, Haliclona xena*)	Sponge tissue	Bacterial and archeal 16S rRNA pyrosequencing	Proteobacteria	Estuary	Filter feeder	Sessile	A few years	Sponge species-specific classes of Proteobacreria.	(Webster and Taylor 2012)(Naim *et al.* 2014) *Photo provided by D. Sipkema.*
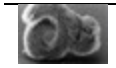 Nematode (*Eubostrichus dianae*)	Entire surface of worm	16S rDNA restriction cutting	Cytophagas, sulfate-reducing bacteria, gamma Proteobacteria, and caulobacters	Benthic sediment	Detritivore	Motile	A few weeks	High microbial diversity on small spatial scale.	(Polz *et al.* 1999) *Photo provided by M. Polz*
 California Mussel (*Mytilus californianus*)	Mussel shell	Shotgun metagenomics,	Cyanobacteria, Alpha- and Gamma-Proteobacteria	Rocky intertidal	Filter feeder	Sessile	Several years	Microbial assemblage similar between pool, emergent mussels	(Pfister *et al.* 2010) *Photo provided by JT Wootton.*

Understudied functions of marine microbiota-macrobiotia associations

Within this overall microbial diversity, a small but growing number of studies have shown unique microbe-macrobiota associations involving known microbial nitrogen cycling taxa (Table 5.3). In some cases, it is possible to identify these organisms by 16S rRNA gene sequencing, because certain families have defined and specific nitrogen-cycling roles. This is true for nitrogen-fixing and anammox bacteria, as well as nitrifying archaea and bacteria (Francis *et al.* 2007; Zehr and Kudela 2011). In contrast, some nitrogen-cycling processes are sustained by a wide diversity of microbial groups and are considered 'broad' processes: denitrification, for instance, is performed by microorganisms from all three domains of life (Archaea, Bacteria, Eukaryota) (Zumft 1997). For these processes, metagenomics— in which a mixture of primarily microbial genetic material is recovered directly from environmental samples (rather than isolates) and sequenced— has provided insight into host-associated microbial functional diversity. This is particularly powerful when paired with nitrogen cycling rate measurements, and can be used to determine linkages between a species of macrobiota, their hosted microbes, and nitrogen cycling. For example, Ribes *et al.* (2012) showed that, among three sponge species, two host diverse microbial communities and had high nitrification and ammonium uptake rates, while the third species hosts a low microbial diversity community with low measured nitrogen uptake rate. Though the two sponge species hosting a high diversity of microbes both demonstrated rapid nitrogen metabolism, the microbial communities associated with each species were distinct (Ribes *et al.* 2012). The potential 'functional convergence' of these microbial communities was supported by metagenomic analyses, which showed that genes for different enzymes in the denitrification pathways were present in both microbial communities, although the taxonomic composition differed (Fan *et al.* 2012).

Though the microbial associates of macrobiota continue to be described, example associations between macrobiota and their nitrogen-cycling microbial associates (Figure 5.2, Figure 5.3, Table 5.3) demonstrate that they can result in either nitrogen loss or fixation. Nitrogen loss occurs via denitrification (Heisterkamp *et al.* 2013), while animal excretion of ammonium may accelerate nitrogen loss through anammox (Bianchi *et al.* 2014). Animals also host known nitrogen fixers (Fiore *et al.* 2010). This indicates that macrobes can act as direct conduits of nitrogen flux to and from coastal ecosystems. To date, tropical corals and sponges are the best-studied macrobiota (e.g. Knowlton and Rohwer 2003), and corals are viewed as 'holobionts' consisting of the coral animal, its photosynthetic symbionts, and coral-associated bacteria and archaea (Rohwer *et al.* 2002) that interact through linked carbon and nitrogen cycling. Sponges appear to harbor specific bacteria (the *Poribacteria*) that include known microbial nitrogen cyclers. Tropical demosponges, for example, are associated with microbial nitrification rates that are three orders of magnitude more than surrounding seawater (Diaz and Ward 1997). When coupled with high water pumping rates (up to 0.27 cm^3 seawater cm^{-3} sponge sec^{-1} (Reiswig 1974)), these sponges are substantial contributors to nitrogen processing in local seawater nutrient profiles, where concentrations of nitrate are typically at the nanomolar level (Southwell *et al.* 2008). Sponges are similarly important for carbon cycling on reefs (de Goeij *et al.* 2013), showing dissolved organic carbon (DOC) cycling rates that equal those of plankton in the water column, and demonstrating how the carbon and nitrogen cycles can be linked by animal activity. Marine animals like these are effective integrators, concentrators, and processors of relatively large volumes of seawater and its chemical and biological constituents.

A key way in which sessile animals promote a diverse array of nitrogen metabolisms is by generating strong oxygen gradients through their respiration. Due to photosynthetic symbionts at

the interface between the animal and surrounding seawater, sponge and coral surfaces are highly zoned with respect to oxygen, and, accordingly, host nitrifying microbes at the oxygenated surface and denitrifying taxa at the deeper, anoxic areas (Fiore *et al.* 2010). Shelled marine invertebrates also have sharp gradients in oxygen, with values varying from 0 to 1200 μM over a scale of less than 3 mm from gut to shell (Heisterkamp *et al.* 2013). In a review of animal effects on nitrification and denitrification in soft sediment communities, the presence of animals increased nitrification by a factor of 3.0 and denitrification by a factor of 2.4. Further, we expect that nitrogen fixation by microbial populations is favored under low oxygen conditions (nitrogenase enzyme is inactivated by O_2), while near-anoxic conditions can drive anaerobic nitrogen loss processes (denitrification and anammox), assuming nitrate is available. The removal of biologically available nitrogen could result in the production of nitrous oxide (an intermediate for denitrification), as demonstrated within anoxic guts of diverse animal taxa (Stief *et al.* 2009). Production of this ozone-destroying greenhouse gas was highest in filter- and deposit-feeders—groups that could increase in abundance with coastal eutrophication (nutrient enrichment) (Murray *et al.* 2015). Macrophytes too affect oxygen gradients through photosynthesis and respiration. Although microbial associations with marine macroflora are only just beginning to be described (e.g. Miranda *et al.* 2013), there is great potential for macrophyte-microbial interactions via shared resources such as carbon and nitrogen.

Positive ecological roles of macrobiota as hosts for microbial function

Although species diversity in marine systems can affect ecosystem function (Worm *et al.* 2006), these systems are also home to species that play particularly crucial foundational, dominant, or keystone roles (Paine 1966; Power *et al.* 1996; Estes *et al.* 2011). Across multiple ecosystems,

keystone species are identified as those with effects on a community trait (e.g. species diversity) that are disproportionate to their abundance, including seastars and sea otters. Abundant species with structural importance are termed foundational species, and are represented in marine systems by seagrasses, algae, and mussels that have significant community effects, often via habitat provision. Ecologically dominant species are those with higher abundance than that of competitors within an ecosystem, with or without relatively higher impact on ecosystem dynamics. Due to their documented importance in terms of abundance or ecosystem-level influence, we expect foundation species, keystone species, and ecological dominants to be particularly important with regards to the nitrogen cycle. Shallow coastal marine foundational habitats such as coral reefs, marsh grasses, seagrasses, mangroves, and mussel beds facilitate existence of other species and provide ecosystem services (e.g. Bracken 2004), as well as host microbial nutrient processing (Welsh 2000; Rosenberg *et al.* 2007). Although information is limited on the effects of foundation species loss on microbial communities in marine habitats, work in terrestrial ecosystems shows major negative consequences for ecosystem structure (Ellison *et al.* 2005), and thus related microbial community function. Worldwide, foundation species, as well as ecological dominants, are experiencing rapid decline as a result of harvesting, pollution, and global environmental change (Orth *et al.* 2006), but are also the target of restoration efforts. Because foundation species likely serve as critical hosts for microbial contributors to nitrogen cycling, it is necessary to understand whether the microbiome shapes the functional outcome of restoration.

If particular animal or macrophyte species are capable of enhancing nitrogen metabolisms, then we ask if any of these macrobiota have disproportionate effects. Hence, *are there foundation species, keystone species, or ecological dominants with respect to the metabolism of nitrogen in coastal marine ecosystems?* Are there foundation species, keystone species, or ecological

dominants with respect to the metabolism of nitrogen in coastal marine ecosystems? If so, are these the macrobes alone, or in organisms in tandem with their microbiomes? Certainly foundation species could have a correspondingly greater impact in nitrogen transformations due to the surface area they provide via thalli in the case of macrophytes, or the shells, skin, and carapaces of animals. The shell area of animals has been shown to harbor from 50 to 94% of the observed nitrogen function (e.g. bivalves (Welsh and Castadelli 2004; Heisterkamp *et al.* 2013)), suggesting that abundance and body/thallus size scales directly with contribution to microbial activity.

Microbiota-macrobiota associations as novel avenues for species interaction

In addition to our need to understand direct fitness linkages between host macrobiota and microbial communities, it is important to consider how interactions could indirectly affect other species. Indirect effects have been an important focus in ecological research for more than two decades (Wootton 1994), and the new appreciation for microbial diversity and function explores novel ways in which species interact. For example, ammonium excreted by polychaete worms is utilized by surrounding algae, but also supplies nitrifying bacteria that provide nitrate to these primary producers (Heisterkamp *et al.* 2012). Benthic-regenerated nitrogen enters the water column, based on estimates that as much as half of the nutrients used by phytoplankton in the coastal ocean are produced in coastal sediments (Jørgensen 1983). Similarly, the metabolic activities of schooling fishes concentrate nitrogen through remineralization and enhance nitrogen locally for other species, including primary producers (Durbin and Durbin 1998). In the case of seagrasses, which often play the role of a foundation species, alterations to the forms of nitrogen available are expected throughout the community. For example, nitrogen fixation is enhanced in the seagrass rhizosphere (Welsh *et al.* 1996), representing concentrated 'new' nitrogen for the

seagrass, as well as for other species (Duarte *et al.* 2005). Not only does nutrient remineralization by animals enhance microbial metabolisms (Welsh and Castadelli 2004), it also increases eukaryotic access to nitrogen (Bracken 2004). Whether eukaryotes compete with bacterial and archaeal microbes for this animal regenerated nitrogen remains to be determined.

HYPOTHESES TO FURTHER OUR UNDERSTANDING OF NITROGEN-BASED MICROBIAL FUNCTION IN THE COASTAL OCEAN

Concerns about how marine ecosystems will respond to continued animal harvest and loss of habitat-forming foundation species (e.g. seagrasses and corals), while anthropogenic nitrogen inputs increase, require that we extend current efforts to understand the functional role of microbe-macrobiota associations. We offer four hypotheses worthy of inquiry in the future study of these associations in coastal nitrogen cycling. While our examples come from the nitrogen-limited coastal ocean, the hypotheses listed below are broadly applicable to nutrient cycling by macrobiota in all ecosystems.

Hypothesis 1*: Macrobiota select for a microbiome composed of nitrogen-cycling microbes*

The specificity of microbial communities with their animal and macrophyte hosts remains underexplored. If microbial interactions with animal or macrophyte hosts are highly specialized, then continued loss of macrobiota will affect microbial diversity and the range of microbial functions. For those macrobiota whose microbiomes have been sequenced in tandem with surrounding seawater, unique taxa occur in association with the host. In a study of tide pool mussels, anemones, and a seaweed, multiple microbial taxa collected from within macrobiotic tissues were absent from the water column (Pfister *et al.* 2014b). Similarly, sponges host distinct

microbial taxa when compared to surrounding seawater (Hentschel *et al.* 2002). However, we need an increased understanding of whether microbial taxa have obligate relationships with host macrobiota. Targeted manipulative experiments and biogeographic studies will reveal host-microbe specificity.

If macrobiota represent an inert physical surface for biofilms, then we expect associated microbes to have a cosmopolitan distribution among different hosts. If, however, hosts exert different selection pressures via resource availability, then high beta-diversity is expected, including the evolution of distinct microbial assemblages among hosts. We know little about whether similar animal or macrophyte taxa host similar microbial assemblages. A study of several macrobiota substrates in rocky intertidal environments showed that each hosted unique microbial taxa, verifying association specificity (Pfister *et al.* 2014b), and strong differentiation of microbial communities between co-occurring species of coral again suggests specificity in microbe-macrobiota relationships (Sunagawa *et al.* 2010).

Hypothesis 2*: Nitrogen-cycling microbial associates provide benefits to macrobiota*

The microbial diversity hosted by macrophytes and animals (Table 2, Supplementary Tables 1, 2) motivates investigation into whether microbes affect host fitness, or if hosts are indifferent to these colonists. Of the diversity of microbial taxa associated with macrobiota, it is yet unclear how quantitatively significant nitrogen cyclers are, and whether macrobiota benefit as well. Mussel studies suggest that microbial uptake may ameliorate ammonium accumulation to levels that could be toxic to animals. Although California mussel excretion rates and densities should theoretically result in mmol L^{-1} local ammonium concentrations (Pfister *et al.* 2010), only

1.26 umol L^{-1} concentrations have been measured above mussel beds (Aquilino *et al.* 2009), suggesting that a combination of advection and uptake decrease ammonium concentrations from millimolar to micromolar levels. In mussel aquaculture, animals have been observed to neither contribute nor deplete nitrogen locally, despite locally dense animal populations (Asmus and Asmus 1991), suggesting uptake by microbes and photosynthetic organisms is quantitatively important.

Hypothesis 3*: Microbiota-macrobiota associations broaden microbial nitrogen-cycling function*

Examples of microbial taxa in association with macrobiota are accumulating rapidly (Table 5.2, Supplementary Tables 5.1, 5.2), and there is strong evidence that microbial metabolisms are enhanced via microbial-animal associations (Table 5.3). Because we expect greater diversity and rates of nitrogen metabolisms in association with animals and macrophytes, macrobiota likely numerically concentrate existing nitrogen functions, enhance the range of energetically possible functions, or both. The strong gradients in oxygen along the surface of animal tissues or the thallus of an alga, and within tissues and digestive tracts, suggest that metabolic activities of macrobiota allow a range of oxidative states, and thus may promote multiple nitrogen metabolisms in proximity to macrobiota (Figure 5.2, Figure 5.3). Whether direct microbial associations or an alteration of the resources available to microbes in the immediate vicinity of the animal are responsible for these functional consequences remains to be determined.

Table 5.3. Nitrogen cycling processes demonstrated to occur in association with macrobiota, and their ecological significance.

Nitrogen cycling process	Macrobiota association(s)	Insight from association	Quantifying the effect	Reference(s)
Nitrification	Corals, sponges, bivalves, benthic crustaceans, benthic polychaetes	Microbes can compete with zooxanthellae for N.	Benthic macrobiota-associated nitrification rates are 3-fold higher than background rates.	Corredor *et al.* 1988; Wafar *et al.* 1990; Diaz and Ward 1997; Hentschel *et al.* 2002; Fiore *et al.* 2010
Denitrification/ anammox	Corals, sponges, bivalves, benthic crustaceans, benthic polychaetes	Animals generate low oxygen microsites that allow anaerobic N cycling to occur.	On average, benthic macrobiota-associated denitrification rates are 2.4-fold higher than background.	Hoffmann *et al.* 2009; Fiore *et al.* 2010; Pfister *et al.* 2010; Heisterkamp *et al.* 2013
Nitrous oxide production	Bivalves and molluscs	Animals generate low oxygen microsites that allow anaerobic N cycling to occur.	Animals may increase N_2O emissions by 32-103%; extremely high N_2O yields relative to overall N cycling (ca. 50%).	Stief *et al.* 2009; Heisterkamp *et al.* 2013
Nitrogen regeneration and transport	Zooplankton	Animals provide ammonium for annamox.	Association enhances oceanic N loss via anammox by 27-40%.	Bianchi *et al.* 2014
Nitrogen fixation	Corals, sea urchins, shipworms, sponges	Animals generate low oxygen microsites that facilitate this process; may be of particular importance in symbioses.	N-fixation is elevated relative to background rates in sediments and water.	Lesser *et al.* 2004; Fiore *et al.* 2010; Cardini *et al.* 2014

Other aspects of macrobiotic life histories could also determine the importance of microbe-macrobiota relationships and the traits of the associated microbes that colonize macrobiota. Organisms that move or migrate translocate microbes and nitrogen with them. Long-lived species with persistent structural components (e.g. shells or stipes) could select for stable, persistent microbial assemblages, while non-equilibrial microbial communities might be associated with fast-growing, rapidly senescing macrobiota.

Hypothesis 4*: Novel ecological links among macrobiota are facilitated by microbial nitrogen-cycling function*

Little is known about whether microbial associations can determine the outcome of interactions with their host macrobiota. Symbionts vary in the fitness benefits they impart to hosts (Lema *et al.* 2012), suggesting that microbial communities may have the capability to mediate interactions among macrobiota individuals and species. Microbial presence can alter the attractiveness and palatability of prey and therefore the attack rate upon macrofaunal species, altering consumer fitness (Burkepile *et al.* 2006). The above relationships motivate a more complete understanding of how and when microbes affect the interactions of macrobiota and impart a fitness advantage to one species at the expense of the other.

Macrobiota-microbial relationships could also generate positive interactions through nitrogen cycling. For example, a microbiome that locally reduces otherwise toxic levels of ammonium provides benefits for the host species as well as surrounding species. Because animals and macrophytes locally change oxygen levels through respiration and photosynthesis, host macrobiota could favor particular microbial taxa and metabolisms, at the benefit or detriment of neighboring species. For example, the photosynthetic production of oxygen by macroalgae and

seagrasses could favor the oxidative process of nitrification, in turn benefitting host animals by local consumption of ammonium. Conversely, concentration of nitrogen and carbon by microbiota creates microbial hotspots of production, respiration, and nitrogen cycling that could subsequently affect the fitness of other microbiota.

IMPLICTIONS FOR COASTAL ECOSYSTEM FUNCTION

Natural nitrogen inputs and cycling are likely changing as macrobiotic diversity and biomass decline in many aquatic ecosystems (Worm *et al.* 2006), part of a larger pattern of global 'defaunation' (Dirzo *et al.* 2014) and habitat loss. It is widely acknowledged that human activities have greatly reduced large consumer biomass (Worm *et al.* 2006), yet we know little about how their loss has affected nutrient cycling and retention—although there is likely a prominent role via lost excretion products (Croll *et al.* 2005). If macrobiota host microbial communities with important roles in nitrogen-cycling, then animal and macrophyte loss will be accompanied by the alteration of nitrogen processing in marine ecosystems. This wide-scale loss in macrobiota-enhanced nitrogen processing will likely coincide with increased anthropogenic nitrogen loading to coastal ecosystems. The many associations between microbes and macrobiota have been identified as a 'new imperative for the life sciences' (McFall-Ngai *et al.* 2013); it is thus timely to ask to what degree microbes in association with macrobiota are important components of the coastal marine nitrogen cycle and what is their role in ameliorating eutrophication. Given the range of human activities that affect the distribution and abundances of macrobiota and inputs of nitrogen to coastal ecosystems, these functional relationships deserve increased research scrutiny in order to advance mechanistic understanding of their contribution to ecosystem processes and their implications for coastal ecosystem function and restoration.

ACKNOWLEDGEMENTS

This work stems from a breakout group discussion at the September 2014 Coastal Nitrogen Synthesis Charrette (CNSC), a workshop funded by the University of Chicago-Marine Biological Laboratories (MBL) affiliation. We are grateful to MBL for hosting the workshop, and to other workshop participants (N. Bouskill, J. Bowen, M. Coleman, A. Giblin, J. Gilbert, M. Sogin, J. Vallino, B. Ward) for fruitful discussions and constructive feedback.

Appendix 5A: Macrobiota with known microbial associates.

Table 5.A.1. Marine macroflora with known microbial associates.

Macroflora type	Location of Microbiome	Method of Genomic Analysis	Dominant group(s) in microbiome	Habitat	Host trophic mode	Host life history	Host longevity	Criteria for examining host specificity	Reference
Neptune grass (*Posidonia oceanica*)	Leaves, roots and internal parts of rhizomes	16S rRNA sequencing	*Marinomonas*	Seagrass meadows	Primary producer	Sessile	Centuries	Novel species associated with *P. oceanica*	Espinosa *et al.* 2010
Dwarf eelgrass (*Zostera noltii*)	Rhizosphere	NA (N-fixation and S-reduction rates)	N-fixing sulphate-reducing bacteria	Seagrass meadows	Primary producer	Sessile	Decades to centuries	NA	Welsh *et al.* 1996
Common eelgrass (*Zostera marina*)	Roots	Bacterial isolations	*Vibrio* spp. and *Photobacterium* spp.	Seagrass meadows	Primary producer	Sessile	Decades to centuries	NA	Shieh *et al.* 1989
Giant kelp (*Macrocystis pyrifera*)	Surface	16S rRNA 454 pyrosequencing	Alpha- and Gamma-Proteobacteria and Bacteriodetes	Kelp forests	Primary producer	Sessile	A few years	Kelp and adjacent seawater host distinct assemblages .	Michelou *et al.* 2013
Intertidal algae (*Fucus vesiculosus, Gracilaria vermiculophylla, Ulva intenstinalis*)	Surface	Denaturing gradient gel electrophoresis (DGGE)	Alpha-proteobacteria Rhodobacterales (*F. vesiculosus*), Rhizobiales (*G. vermiculophylla U. intenstinalis*)	Fjord	Primary producer	Sessile	Several years	Distinct communities on each alga, seasonal within-species community differences	Lachnit *et al.* 2011

Supplementary Table 5.A.2. Marine vertebrates with known microbial associates.

Vertebrate Host	Location of Microbiome	Method of Genomic Analysis	Dominant group (s) in microbiome	Habitat	Host trophic mode	Host life history	Host longevity	Criteria for examining host specificity	Reference
Cornetfish *(Fistularia commersonii)*	Epidermal mucus	Scanning electron microscopy and bacterial isolations	*Pseudomonas*	Reef	Secondary consumer	Motile	A few years	NA	Bernadsky and Rosenberg 1992
Chum salmon *(Oncorhynchus kisutch)*	Epidermal mucus	PCR on cultured isolations	*Photobacterium phosphoreum*	River	Secondary consumer	Motile	A few years	NA	Budsberg *et al.* 2003
Red snapper (*Lutjanus campechanus*)	Fish slime	16S rRNA sequencing	Proteobacteria, esp. *Vibrio* and *Photobacterium*	Coastal pelagic	Secondary consumer	Motile	Several decades	NA	Arias *et al.* 2013
Humpback whale *(Megaptera novaeangliae*)	Skin biopsies and freshly sloughed skin	SSU rRNA 454 pyrosequencing	Flabobacteria (*Tenacibaculum*) and Gamma-proteobacteria (*Pyschrobacter*)	Pelagic	Filter feeder	Motile	Several decades	Skin assemblage varied geographically and with metabolic state.	Apprill *et al.* 2014

LITERATURE CITED

Allgeier JE, Yeager LA, and Layman CA. 2013. Consumers regulate nutrient limitation regimes and primary production in seagrass ecosystems. *Ecology* **94**: 521–9.

Amin SA, Parker MS, and Armbrust EV. 2012. Interactions between diatoms and bacteria. *Microbiol Mol Biol Rev* **76**: 667–84.

Apprill A, Robbins J, Eren AM, *et al.* 2014. Humpback whale populations share a core skin bacterial community: Towards a health index for marine mammals? *PLoS ONE* **9**: e90785.

Aquilino KM, Bracken ME, Faubel MN, and Stachowicz JJ. 2009. Local-scale nutrient regeneration facilitates seaweed growth on wave-exposed rocky shores in an upwelling system. *Limnol Oceanogr* **54**: 309–17.

Arias C, Koenders K, and Larsen A. 2013. Predominant bacteria associated with red snapper from the northern Gulf of Mexico. *J Aquat Anim Health* **25**: 281–9.

Asmus RM and Asmus H. 1991. Mussel beds: limiting or promoting phytoplankton? *J Exp Mar Biol Ecol* **148**: 215–32.

Bardgett RD, Lovell RD, Hobbs PJ, and Jarvis SC. 1999. Seasonal changes in soil microbial communities along a fertility gradient of temperate grasslands. *Soil Biol Biochem* **31**: 1021–30.

Bell EC. 1995. Environmental and morphological influences on thallus temperature and desiccation of the intertidal alga Mastocarpus papillatus Kützing. *J Exp Mar Biol Ecol* **191**: 29–55.

Bernadsky G and Rosenberg E. 1992. Drag-reducing properties of bacteria from the skin mucus of the cornetfish (Fistularia commersonii). *Microb Ecol* **24**: 63–76.

Bianchi D, Babbin AR, and Galbraith ED. 2014. Enhancement of anammox by the excretion of diel vertical migrators. *Proc Natl Acad Sci* **111**: 15653–8.

Bode A, Varela MM, Teira E, *et al.* 2004. Planktonic carbon and nitrogen cycling off northwest Spain: variations in production of particulate and dissolved organic pools. *Aquat Microb Ecol* **37**: 95–107.

Bowen JL, Morrison HG, Hobbie JE, and Sogin ML. 2012. Salt marsh sediment diversity: a test of the variability of the rare biosphere among environmental replicates. *ISME J* **6**: 2014–23.

Bowen JL, Ward BB, Morrison HG, *et al.* 2011. Microbial community composition in sediments resists perturbation by nutrient enrichment. *ISME J* **5**: 1540–8.

Bracken ME. 2004. Invertebrate-mediated nutrient loading increased growth of an intertidal macroalga. *J Phycol* **40**: 1032–41.

Bracken ME and Nielsen KJ. 2004a. Diversity of intertidal macroalgae increases with nitrogen loading by invertebrates. *Ecology* **85**: 2828–36.

Bracken ME and Nielsen KJ. 2004b. Diversity of intertidal macroalgae increases with nitrogen loading by invertebrates. *Ecology* **85**: 2828–36.

Bracken MES and Stachowicz JJ. 2006. Seaweed diversity enhances nitrogen uptake via complementary use of nitrate and ammonium. *Ecology* **87**: 2397–403.

Budsberg KJ, Wimpee CF, and Braddock JF. 2003. Isolation and identification of Photobacterium phosphoreum from an unexpected niche: migrating salmon. *Appl Environ Microbiol* **69**: 6938–42.

Burkepile DE, Parker JD, Woodson CB, *et al.* 2006. Chemically mediated competition between microbes and animals: microbes as consumers in food webs. *Ecology* **87**: 2821–31.

Capone DG, Bronk DA, Mulholland MR, and Carpenter EJ. 2008. Nitrogen in the marine environment. Academic Press.

Caporaso JG, Bittinger K, Bushman FD, *et al.* 2010a. PyNAST: a flexible tool for aligning sequences to a template alignment. *Bioinformatics* **26**: 266–7.

Caporaso JG, Kuczynski J, Stombaugh J, *et al.* 2010b. QIIME allows analysis of high-throughput community sequencing data. *Nat Methods* **7**: 335–6.

Caporaso JG, Lauber CL, Walters WA, *et al.* 2012a. Ultra-high-throughput microbial community analysis on the Illumina HiSeq and MiSeq platforms. *ISME J* **6**: 1621–4.

Caporaso JG, Paszkiewicz K, Field D, *et al.* 2012b. The Western English Channel contains a persistent microbial seed bank. *ISME J* **6**: 1089–93.

Cardini U, Bednarz VN, Foster RA, and Wild C. 2014. Benthic N2 fixation in coral reefs and the potential effects of human-induced environmental change. *Ecol Evol* **4**: 1706–27.

Carpenter SR, Caraco NF, Correll DL, *et al.* 1998. Nonpoint pollution of surface waters with phosphorus and nitrogen. *Ecol Appl* **8**: 559–68.

Castenholz RW. 1961. The effect of grazing on marine littoral diatom populations. *Ecology* **42**: 783–94.

Chamberlain SA, Bronstein JL, and Rudgers JA. 2014. How context dependent are species interactions? *Ecol Lett* **17**: 881–90.

Chavez FP, Pennington JT, Castro CG, *et al.* 2002. Biological and chemical consequences of the 1997–1998 El Niño in central California waters. *Prog Oceanogr* **54**: 205–32.

Cohen JE. 1997. Population, economics, environment and culture: an introduction to human carrying capacity. *J Appl Ecol* **34**: 1325–33.

Cohen RA and Fong P. 2004. Nitrogen uptake and assimilation in Enteromorpha intestinalis (L.) Link (Chlorophyta): using 15N to determine preference during simultaneous pulses of nitrate and ammonium. *J Exp Mar Biol Ecol* **309**: 67–77.

Connell JH. 1961a. Effects of competition, predation by Thais lapillus, and other factors on natural populations of the barnacle Balanus balanoides. *Ecol Monogr* **31**: 61–104.

Connell JH. 1961b. The influence of interspecific competition and other factors on the distribution of the barnacle Chthamalus stellatus. *Ecology* **42**: 710–23.

Corredor J, Wilkinson CC, Vicente V, *et al.* 1988. Nitrate release by Caribbean reef sponges. *Limnol Oceanogr* **33**: 114–20.

Corwith HL and Wheeler PA. 2002. El Nino related variations in nutrient and chlorophyll distributions off Oregon. *Prog Oceanogr* **54**: 361–80.

Croll DA, Maron JL, Estes JA, *et al.* 2005. Introduced predators transform subarctic islands from grassland to tundra. *Science* **307**: 1959–61.

Dayton P. 1970. Competition, predation, and community structure: The allocation and subsequent utilization of space in a rocky intertidal community. Ph.D. thesis. Univ of Washington, Seattle.

Dayton PK. 1971. Competition, disturbance, and community organization: the provision and subsequent utilization of space in a rocky intertidal community. *Ecol Monogr* **41**: 351–89.

Delille D, Canon C, and Windeshausen F. 1996. Comparison of planktonic and benthic bacterial communities associated with a Mediterranean *Posidonia* seagrass system. *Bot Mar* **39**: 239–50.

Diaz MC and Ward BB. 1997. Sponge-mediated nitrification in tropical benthic communities. *Mar Ecol Prog Ser* **156**: 97–107.

Díez B, Bauer K, and Bergman B. 2007. Epilithic cyanobacterial communities of a marine tropical beach rock (Heron Island, Great Barrier Reef): diversity and diazotrophy. *Appl Environ Microbiol* **73**: 3656–68.

Dirzo R, Young HS, Galetti M, *et al.* 2014. Defaunation in the Anthropocene. *Science* **345**: 401–6.

Dortch Q. 1990. The interaction between ammonium and nitrate uptake in phytoplankton. *Mar Ecol Prog Ser Oldendorf* **61**: 183–201.

Doughty CE, Roman J, Faurby S, *et al.* 2015. Global nutrient transport in a world of giants. *Proc Natl Acad Sci*: 201502549.

Duarte CM, Holmer M, and Marbà N. 2005. Plant–Microbe Interactions in Seagrass Meadows. In: Kristensen E, Haese RR, Kostka JE (Eds). Interactions Between Macro- and Microorganisms in Marine Sediments. American Geophysical Union.

Dugdale RC and Goering JJ. 1967. Uptake of new and regenerated forms of nitrogen in primary productivity. *Limnol Ocean* **12**: 196–206.

Durbin AG and Durbin EG. 1998. Effects of menhaden predation of plankton populations in Narragansett Bay, Rhode Island. *Estuaries* **21**: 449–65.

Ellison AM, Bank MS, Clinton BD, *et al.* 2005. Loss of foundation species: consequences for the structure and dynamics of forested ecosystems. *Front Ecol Environ* **3**: 479–86.

Elser JJ, Andersen T, Baron JS, *et al.* 2009. Shifts in lake N: P stoichiometry and nutrient limitation driven by atmospheric nitrogen deposition. *science* **326**: 835–7.

Englert F. 1992. Reef biological filtration device. Google Patents.

Espinosa E, Marco-Noales E, Gómez D, *et al.* 2010. Taxonomic study of Marinomonas strains isolated from the seagrass Posidonia oceanica, with descriptions of Marinomonas balearica sp. nov. and Marinomonas pollencensis sp. nov. *Int J Syst Evol Microbiol* **60**: 93–8.

Estes JA, Terborgh J, Brashares JS, *et al.* 2011. Trophic downgrading of planet Earth. *science* **333**: 301–6.

Fan L, Reynolds D, Liu M, *et al.* 2012. Functional equivalence and evolutionary convergence in complex communities of microbial sponge symbionts. *Proc Natl Acad Sci* **109**: E1878–87.

Fiore CL, Jarett JK, Olson ND, and Lesser MP. 2010. Nitrogen fixation and nitrogen transformations in marine symbioses. *Trends Microbiol* **18**: 455–63.

Fowler D, Coyle M, Skiba U, *et al.* 2013. The global nitrogen cycle in the twenty-first century. *Philos Trans R Soc B Biol Sci* **368**: 20130164.

Francis CA, Beman JM, and Kuypers MMM. 2007. New processes and players in the nitrogen cycle: the microbial ecology of anaerobic and archaeal ammonia oxidation. *ISME J* **1**: 19–27.

Frost PC and Elser JJ. 2002a. Effects of light and nutrients on the net accumulation and elemental composition of epilithon in boreal lakes. *Freshw Biol* **47**: 173–83.

Frost PC and Elser JJ. 2002b. Growth responses of littoral mayflies to the phosphorus content of their food. *Ecol Lett* **5**: 232–40.

Fujita RM, Wheeler PA, and Edwards RL. 1989. Assessment of macroalgal nitrogen limitation in a seasonal upwelling region.

Galloway JN, Dentener FJ, Capone DG, *et al.* 2004. Nitrogen cycles: past, present, and future. *Biogeochemistry* **70**: 153–226.

Galloway JN, Schlesinger WH, Levy H, *et al.* 1995. Nitrogen fixation: Anthropogenic enhancement-environmental response. *Glob Biogeochem Cycles* **9**: 235–52.

Galloway JN, Townsend AR, Erisman JW, *et al.* 2008. Transformation of the nitrogen cycle: recent trends, questions, and potential solutions. *Science* **320**: 889–92.

Gibbons SM, Caporaso JG, Pirrung M, *et al.* 2013. Evidence for a persistent microbial seed bank throughout the global ocean. *Proc Natl Acad Sci* **110**: 4651–5.

Gilbert JA, Jansson JK, and Knight R. 2014. The Earth Microbiome project: successes and aspirations. *BMC Biol* **12**: 69.

Gilbert PM, Lipschultz F, McCarthy JJ, and Altabet MA. 1982. Isotope dilution models of uptake and remineralization of ammonium by marine plankton. *Limnol Oceanogr* **27**: 639–50.

Goeij JM de, Oevelen D van, Vermeij MJA, *et al.* 2013. Surviving in a marine desert: The sponge loop retains resources within coral reefs. *Science* **342**: 108–10.

Golléty C and Crowe TP. 2013. Contribution of biofilm to ecosystem functioning in rock pools with different macroalgal assemblages. *Mar Ecol Prog Ser* **482**: 69–79.

Gower JC. 1975. Generalized procrustes analysis. *Psychometrika* **40**: 33–51.

Hamasaki K, Taniguchi A, Tada Y, *et al.* 2007. Actively Growing Bacteria in the Inland Sea of Japan, Identified by Combined Bromodeoxyuridine Immunocapture and Denaturing Gradient Gel Electrophoresis. *Appl Environ Microbiol* **73**: 2787–98.

Hanisak MD. 1979. Nitrogen limitation of Codium fragile ssp. tomentosoides as determined by tissue analysis. *Mar Biol* **50**: 333–7.

Harley CD. 2002. Light availability indirectly limits herbivore growth and abundance in a high rocky intertidal community during the winter. *Limnol Oceanogr* **47**: 1217–22.

Harrison PJ, Mackas DL, Frost BW, *et al.* 1994. An assessment of nutrients, plankton and some pollutants in the water column of Juan de Fuca Strait, Strait of Georgia and Puget Sound, and their transboundary transport. *Can Tech Rep Fish Aquat Sci Tech Can Sci Halieut Aquat TECH REP FISH AQUAT SCI 1994*.

Heisterkamp IM, Kamp A, Schramm AT, *et al.* 2012. Indirect control of the intracellular nitrate pool of intertidal sediment by the polychaete Hediste diversicolor. *Mar Ecol Prog Ser* **445**: 181–92.

Heisterkamp IM, Schramm A, Larsen LH, *et al.* 2013. Shell biofilm-associated nitrous oxide production in marine molluscs: processes, precursors and relative importance. *Environ Microbiol* **15**: 1943–55.

Hentschel U, Hopke J, Horn M, *et al.* 2002. Molecular evidence for a uniform microbial community in sponges from different oceans. *Appl Environ Microbiol* **68**: 4431–40.

Herbert RA. 1999. Nitrogen cycling in coastal marine ecosystems. *FEMS Microbiol Rev* **23**: 563–90.

Hillebrand H and Sommer U. 2000. Effect of continuous nutrient enrichment on microalgae colonizing hard substrates. *Hydrobiologia* **426**: 185–92.

Hill AS and Hawkins SJ. 1991. Seasonal and spatial variation of epilithic micro algal distribution and abundance and its ingestion by Patella vulgata on a moderately exposed rocky shore. *J Mar Biol Assoc U K* **71**: 403–23.

Hoffmann F, Radax R, Woebken D, *et al.* 2009. Complex nitrogen cycling in the sponge Geodia barretti. *Environ Microbiol* **11**: 2228–43.

Holt RD. 1984. Spatial heterogeneity, indirect interactions, and the coexistence of prey species. *Am Nat*: 377–406.

Howarth RW. 1988. Nutrient limitation of net primary production in marine ecosystems. *Annu Rev Ecol Syst*: 89–110.

Howarth RW. 2008. Coastal nitrogen pollution: a review of sources and trends globally and regionally. *Harmful Algae* **8**: 14–20.

Howarth R, Chan F, Conley DJ, *et al.* 2011. Coupled biogeochemical cycles: eutrophication and hypoxia in temperate estuaries and coastal marine ecosystems. *Front Ecol Environ* **9**: 18–26.

Howarth RW and Marino R. 2006. Nitrogen as the limiting nutrient for eutrophication in coastal marine ecosystems: Evolving views over three decades. *Limnol Oceanogr* **51**: 364–76.

Hutchinson GE. 1965. The ecological theater and the evolutionary play. Yale University Press.

Jackson JB, Kirby MX, Berger WH, *et al.* 2001. Historical overfishing and the recent collapse of coastal ecosystems. *Science* **293**: 629–37.

Jeffrey S t and Humphrey GF. 1975. New spectrophotometric equations for determining chlorophylls a, b, c1 and c2 in higher plants, algae and natural phytoplankton. *Biochem Physiol Pflanz BPP*.

Jenkins SR, Arenas F, Arrontes J, *et al.* 2001. European-scale analysis of seasonal variability in limpet grazing activity and microalgal abundance. *Mar Ecol Prog Ser* **211**: 193–203.

Jensen SL and Muller-Parker G. 1994. Inorganic nutrient fluxes in anemone-dominated tide pools.

Jørgensen BB. 1983. Processes at the sediment-water interface. *Major Biogeochem Cycles Their Interact* **21**: 477–509.

Kanehisa M, Sato Y, Kawashima M, *et al.* 2016. KEGG as a reference resource for gene and protein annotation. *Nucleic Acids Res* **44**: D457–62.

Kavanaugh MT, Nielsen KJ, Chan FT, *et al.* 2009. Experimental assessment of the effects of shade on an intertidal kelp: Do phytoplankton blooms inhibit growth of open coast macroalgae? *Limnol Oceanogr* **54**: 276–88.

Kim T-W, Lee K, Najjar RG, *et al.* 2011. Increasing N abundance in the northwestern Pacific Ocean due to atmospheric nitrogen deposition. *Science* **334**: 505–9.

Knowlton N and Rohwer F. 2003. Multispecies microbial mutualisms on coral reefs: the host as a habitat. *Am Nat* **162**: S51–62.

Könneke M, Bernhard AE, José R, *et al.* 2005. Isolation of an autotrophic ammonia-oxidizing marine archaeon. *Nature* **437**: 543–6.

Könneke M, Schubert DM, Brown PC, *et al.* 2014. Ammonia-oxidizing archaea use the most energy-efficient aerobic pathway for CO2 fixation. *Proc Natl Acad Sci* **111**: 8239–44.

Kruskal JB. 1964. Multidimensional scaling by optimizing goodness of fit to a nonmetric hypothesis. *Psychometrika* **29**: 1–27.

Kuzyakov Y and Xu X. 2013. Competition between roots and microorganisms for nitrogen: mechanisms and ecological relevance. *New Phytol* **198**: 656–69.

Lachnit T, Meske D, Wahl M, *et al.* 2011. Epibacterial community patterns on marine macroalgae are host-specific but temporally variable. *Environ Microbiol* **13**: 655–65.

Lamontagne I, Cardinal A, and Fortier L. 1989. Environmental forcing versus endogenous control of photosynthesis in intertidal epilithic microalgae. *Mar Ecol Prog Ser MESEDT* **51**.

Langille MG, Zaneveld J, Caporaso JG, *et al.* 2013. Predictive functional profiling of microbial communities using 16S rRNA marker gene sequences. *Nat Biotechnol* **31**: 814–21.

Laverock B, Gilbert J, Tait K, *et al.* 2011. Bioturbation: impact on the marine nitrogen cycle. *Biochem Soc Trans* **39**: 315.

Lema KA, Willis BL, and Bourne DG. 2012. Corals form characteristic associations with symbiotic nitrogen-fixing bacteria. *Appl Environ Microbiol* **78**: 3136–44.

Lennon JT and Jones SE. 2011. Microbial seed banks: the ecological and evolutionary implications of dormancy. *Nat Rev Microbiol* **9**: 119–30.

Lesser MP, Mazel CH, Gorbunov MY, and Falkowski PG. 2004. Discovery of symbiotic nitrogen-fixing cyanobacteria in corals. *Science* **305**: 997–1000.

Lozupone C, Lladser ME, Knights D, *et al.* 2011. UniFrac: an effective distance metric for microbial community comparison. *ISME J* **5**: 169.

Lubchenco J and Gaines SD. 1981. A unified approach to marine plant-herbivore interactions. I. Populations and communities. *Annu Rev Ecol Syst* **12**: 405–37.

Lucas-Elío P, Marco-Noales E, Espinosa E, *et al.* 2011. Marinomonas alcarazii sp. nov., M. rhizomae sp. nov., M. foliarum sp. nov., M. posidonica sp. nov. and M. aquiplantarum sp. nov., isolated from the microbiota of the seagrass Posidonia oceanica. *Int J Syst Evol Microbiol* **61**: 2191–6.

Magalhães CM, Bordalo AA, and Wiebe WJ. 2003. Intertidal biofilms on rocky substratum can play a major role in estuarine carbon and nutrient dynamics. *Mar Ecol Prog Ser* **258**: 275–81.

Maranger R, Caraco N, Duhamel J, and Amyot M. 2008. Nitrogen transfer from sea to land via commercial fisheries. *Nat Geosci* **1**: 111–2.

Martens-Habbena W, Berube PM, Urakawa H, *et al.* 2009. Ammonia oxidation kinetics determine niche separation of nitrifying Archaea and Bacteria. *Nature* **461**: 976–9.

McCune B, Grace JB, and Urban DL. 2002. Analysis of ecological communities. MjM software design Gleneden Beach, OR.

McFall-Ngai M, Hadfield MG, Bosch TC, *et al.* 2013. Animals in a bacterial world, a new imperative for the life sciences. *Proc Natl Acad Sci* **110**: 3229–36.

McIlvin MR and Altabet MA. 2005. Chemical conversion of nitrate and nitrite to nitrous oxide for nitrogen and oxygen isotopic analysis in freshwater and seawater. *Anal Chem* **77**: 5589–95.

McNaughton SJ. 1979. Grazing as an optimization process: grass-ungulate relationships in the Serengeti. *Am Nat*: 691–703.

McNaughton SJ. 1985. Ecology of a grazing ecosystem: the Serengeti. *Ecol Monogr* **55**: 259–94.

Menge BA. 1972. Foraging strategy of a starfish in relation to actual prey availability and environmental predictability. *Ecol Monogr*: 25–50.

Menge BA. 1974. Effect of wave action and competition on brooding and reproductive effort in the seastar, Leptasterias hexactis. *Ecology*: 84–93.

Menge BA. 1995. Indirect effects in marine rocky intertidal interaction webs: patterns and importance. *Ecol Monogr* **65**: 21–74.

Menge BA, Daley BA, Wheeler PA, *et al.* 1997. Benthic–pelagic links and rocky intertidal communities: Bottom-up effects on top-down control? *Proc Natl Acad Sci* **94**: 14530–5.

Menge BA, Farrell TM, Oison AM, *et al.* 1993. Algal recruitment and the maintenance of a plant mosaic in the low intertidal region on the Oregon coast. *J Exp Mar Biol Ecol* **170**: 91–116.

Menge JL and Menge BA. 1974. Role of resource allocation, aggression and spatial heterogeneity in coexistence of two competing intertidal starfish. *Ecol Monogr*: 189–209.

Michelou VK, Caporaso JG, Knight R, and Palumbi SR. 2013. The Ecology of microbial communities associated with Macrocystis pyrifera. *PLoS ONE* **8**: e67480.

Miller TE. 1994. Direct and indirect species interactions in an early old-field plant community. *Am Nat*: 1007–25.

Miranda LN, Hutchison K, Grossman AR, and Brawley SH. 2013. Diversity and Abundance of the Bacterial Community of the Red Macroalga Porphyra umbilicalis: Did Bacterial Farmers Produce Macroalgae? *PLoS ONE* **8**: e58269.

Moulton OM, Altabet MA, Beman JM, *et al.* 2016. Microbial associations with macrobiota in coastal ecosystems: patterns and implications for nitrogen cycling. *Front Ecol Environ* **14**: 200–8.

Murray RH, Erler DV, and Eyre BD. 2015. Nitrous oxide fluxes in estuarine environments: Response to global change. *Glob Change Biol*: n/a – n/a.

Nagarkar S. 1996. The ecology of intertidal epilithic biofilms with special reference tocyanobacteria. *HKU Theses Online HKUTO*.

Nelson JA, Stallings CD, Landing WM, and Chanton J. 2013. Biomass transfer subsidizes nitrogen to offshore food webs. *Ecosystems* **16**: 1130–8.

Nicotri ME. 1977. Grazing effects of four marine intertidal herbivores on the microflora. *Ecology*: 1020–32.

Nielsen LB, Finster K, Welsh DT, *et al.* 2001. Sulphate reduction and nitrogen fixation rates associated with roots, rhizomes and sediments from Zostera noltii and Spartina maritima meadows. *Environ Microbiol* **3**: 63–71.

Ogilvie BG, Rutter M, and Nedwell DB. 1997. Selection by temperature of nitrate-reducing bacteria from estuarine sediments: species composition and competition for nitrate. *FEMS Microbiol Ecol* **23**: 11–22.

Orth RJ, Carruthers TJB, Dennison WC, *et al.* 2006. A Global Crisis for Seagrass Ecosystems. *BioScience* **56**: 987–96.

Paine RT. 1966. Food web complexity and species diversity. *Am Nat*: 65–75.

Paine RT. 1969. The Pisaster-Tegula interaction: prey patches, predator food preference, and intertidal community structure. *Ecology*: 950–61.

Pather S, Pfister CA, Post DM, and Altabet MA. 2014. Ammonium cycling in the rocky intertidal: Remineralization, removal, and retention. *Limnol Ocean* **59**: 361–72.

Pauly D, Christensen V, Dalsgaard J, *et al.* 1998. Fishing down marine food webs. *Science* **279**: 860–3.

Pfister CA. 2007. Intertidal invertebrates locally enhance primary production. *Ecology* **88**: 1647–53.

Pfister CA, Altabet MA, Pather S, and Dwyer G. 2016. Tracer experiment and model evidence for macrofaunal shaping of microbial nitrogen functions along rocky shores. *Biogeosciences* **13**: 3519.

Pfister CA, Altabet MA, and Post DM. 2014a. Animal Regeneration and microbial retention of nitrogen along coastal rocky shores. *Ecology*.

Pfister CA, Gilbert JA, and Gibbons SM. 2014b. The role of macrobiota in structuring microbial communities along rocky shores. *PeerJ* **2**: e631.

Pfister CA, Meyer F, and Antonopoulos DA. 2010. Metagenomic profiling of a microbial assemblage associated with the california mussel: A node in networks of carbon and nitrogen cycling. *PLoS ONE* **5**: e10518.

Pfister CA and Van Alstyne KL. 2003. An experimental assessment of the effects of nutrient enhancement on the intertidal kelp *Hedophyllum sessile* (Laminariales, Phaophyceae). *J Phycol* **39**: 285–90.

Pfister CA, Wootton JT, and Neufeld CJ. 2007. Relative roles of coastal and oceanic processes in determining physical and chemical characteristics of an intensively sampled nearshore system. *Limnol Oceanogr* **52**: 1767.

Plaganyi EE and Branch GM. 2000. Does the limpet Patella cochlear fertilize its own algal garden? *Mar Ecol Prog Ser* **194**: 113–22.

Power ME, Tilman D, Estes JA, *et al.* 1996. Challenges in the quest for keystones. *BioScience*: 609–20.

Redfield AC. 1934. On the proportions of organic derivatives in sea water and their relation to the composition of plankton. university press of liverpool Liverpool, UK.

Reiswig HM. 1974. Water transport, respiration and energetics of three tropical marine sponges. *J Exp Mar Biol Ecol* **14**: 231–49.

Ribes M, Jiménez E, Yahel G, *et al.* 2012. Functional convergence of microbes associated with temperate marine sponges. *Environ Microbiol* **14**: 1224–39.

Ricciardi A and Rasmussen JB. 1999. Extinction rates of North American freshwater fauna. *Conserv Biol* **13**: 1220–2.

Risgaard-Petersen N, Nicolaisen MH, Revsbech NP, and Lomstein BA. 2004. Competition between ammonia-oxidizing bacteria and benthic microalgae. *Appl Environ Microbiol* **70**: 5528–37.

Rocca JD, Hall EK, Lennon JT, *et al.* 2015. Relationships between protein-encoding gene abundance and corresponding process are commonly assumed yet rarely observed. *ISME J* **9**: 1693–9.

Rohwer F, Seguritan V, Azam F, *et al.* 2002. Diversity and distribution of coral-associated bacteria. *Mar Ecol Prog Ser* **243**: 1–10.

Roman J and McCarthy JJ. 2010. The Whale Pump: Marine mammals enhance primary productivity in a coastal basin. *PLoS ONE* **5**: e13255.

Rosenberg E, Koren O, Reshef L, *et al.* 2007. The role of microorganisms in coral health, disease and evolution. *Nat Rev Microbiol* **5**: 355–62.

Ryther JH, Corwin N, DeBusk TA, and Williams LD. 1981. Nitrogen uptake and storage by the red alga Gracilaria tikvahiae (McLachlan, 1979). *Aquaculture* **26**: 107–15.

Saba GK, Steinberg DK, and Bronk DA. 2011. The relative importance of sloppy feeding, excretion, and fecal pellet leaching in the release of dissolved carbon and nitrogen by Acartia tonsa copepods. *J Exp Mar Biol Ecol* **404**: 47–56.

Shieh WY, Simidu U, and Maruyama Y. 1989. Enumeration and characterization of nitrogen-fixing bacteria in an eelgrass (Zostera marina) bed. *Microb Ecol* **18**: 249–59.

Small C and Cohen JE. 2004. Continental physiography, climate, and the global distribution of human population. *Curr Anthropol* **45**: 269–77.

Small C and Nicholls RJ. 2003. A global analysis of human settlement in coastal zones. *J Coast Res*: 584–99.

Sodhi NS, Koh LP, Brook BW, and Ng PK. 2004. Southeast Asian biodiversity: an impending disaster. *Trends Ecol Evol* **19**: 654–60.

Sogin ML, Morrison HG, Huber JA, *et al.* 2006. Microbial diversity in the deep sea and the underexplored "rare biosphere." *Proc Natl Acad Sci* **103**: 12115–20.

Somero GN. 2002. Thermal Physiology and Vertical Zonation of Intertidal Animals: Optima, Limits, and Costs of Living. *Integr Comp Biol* **42**: 780–9.

Southwell MW, Weisz JB, Martens CS, and Lindquist N. 2008. In situ fluxes of dissolved inorganic nitrogen from the sponge community on Conch Reef, Key Largo, Florida. *Limnol Oceanogr* **53**: 986.

Spencer CP. 1956. The bacterial oxidation of ammonia in the sea. *J Mar Biol Assoc U K* **35**: 621–30.

Sterman NT. 1988. Spectrophotometric and fluorometric chlorophyll analysis. *Exp Phycol Camb Univ Press Camb*: 35–46.

Sterner RW and Elser JJ. 2002. Ecological stoichiometry: the biology of elements from molecules to the biosphere. Princeton University Press.

Sterner R, KILHAM S, JOHNSON F, *et al.* 1996. Factors regulating phytoplankton and zooplankton biomass in temperate rivers. *Limnol Ocean* **41**: 1572–7.

Stief P, Poulsen M, Nielsen LP, *et al.* 2009. Nitrous oxide emission by aquatic macrofauna. *Proc Natl Acad Sci* **11**: 4296–300.

Sunagawa S, Woodley CM, and Medina M. 2010. Threatened corals provide underexplored microbial habitats. *PLoS ONE* **5**: e9554.

Tan EL-Y, Mayer-Pinto M, Johnston EL, and Dafforn KA. 2015. Differences in intertidal microbial assemblages on urban structures and natural rocky reef. *Front Microbiol* **6**.

Taylor R and Rees TAV. 1998. Excretory products of mobile epifauna as a nitrogen source for seaweeds. *Limnol Oceanogr* **43**: 600–6.

Team RC. 2015. R: A Language and Environment for Statistical Computing (R Foundation for Statistical Computing, Vienna, 2012). *URL Http Www R-Proj Org*.

Thompson RC, Norton TA, and Hawkins SJ. 1998. The influence of epilithic microbial films on the settlement of Semibalanus balanoides cyprids–a comparison between laboratory and field experiments. *Hydrobiologia* **375**: 203–16.

Thompson RC, Norton TA, and Hawkins SJ. 2004. Physical stress and biological control regulate the producer-consumer balance in intertidal biofilms. *Ecology* **85**: 1372–82.

Tomasch J, Gohl R, Bunk B, *et al.* 2011. Transcriptional response of the photoheterotrophic marine bacterium Dinoroseobacter shibae to changing light regimes. *ISME J* **5**: 1957–68.

Törnblom E and Søndergaard M. 1999. Seasonal dynamics of bacterial biomass and production on eelgrass Zostera marina leaves. *Mar Ecol Prog Ser* **179**: 231–40.

Torres R, Goñi Miguel A, Voulgaris G, *et al.* 2004. Effects of Low Tide Rainfall on Intertidal Zone Material Cycling. In: Fagherazzi S, Rcorani, Blum LK (Eds). The Ecogeomorphology of Tidal Marshes. American Geophysical Union.

Underwood AJ. 1984. The vertical distribution and seasonal abundance of intertidal microalgae on a rocky shore in New South Wales. *J Exp Mar Biol Ecol* **78**: 199–220.

Underwood AJ and Jernakoff P. 1984. The effects of tidal height, wave-exposure, seasonality and rock-pools on grazing and the distribution of intertidal macroalgae in New South Wales. *J Exp Mar Biol Ecol* **75**: 71–96.

Velusamy K and Krishnani KK. 2013. Heterotrophic nitrifying and oxygen tolerant denitrifying bacteria from greenwater system of coastal aquaculture. *Appl Biochem Biotechnol* **169**: 1978–92.

Vitousek PM. 1984. Litterfall, nutrient cycling, and nutrient limitation in tropical forests. *Ecology* **65**: 285–98.

Vitousek PM, Mooney HA, Lubchenco J, and Melillo JM. 1997. Human domination of Earth's ecosystems. *Science* **277**: 494–9.

Wafar MVM, Wafar S, and David JJ. 1990. Nitrification in reef corals. *Limnol Oceanogr* **35**: 725–30.

Ward BB. 2013. Nitrification. In: Reference Module in Earth Systems and Environmental Sciences. Elsevier.

Welsh DT. 2000. Nitrogen fixation in seagrass meadows: regulation, plant–bacteria interactions and significance to primary productivity. *Ecol Lett* **3**: 58–71.

Welsh DT, Bourgues S, De Wit R, and Herbert RA. 1996. Seasonal variations in nitrogen-fixation (acetylene reduction) and sulphate-reduction rates in the rhizosphere of Zostera noltii: nitrogen fixation by sulphate-reducing bacteria. *Mar Biol* **125**: 619–28.

Welsh DT and Castadelli G. 2004. Bacterial nitrification activity directly associated with isolated benthic marine animals. *Mar Biol* **144**: 1029–37.

Williams GA. 1994. The relationship between shade and molluscan grazing in structuring communities on a moderately-exposed tropical rocky shore. *J Exp Mar Biol Ecol* **178**: 79–95.

Williamson JE and Rees TAV. 1994. Nutritional interaction in an alga-barnacle association. *Oecologia* **99**: 16–20.

Wilson SD and Tilman D. 1991. Component of plant competition along an experimental gradient of nitrogen availability. *Ecology* **72**: 1050–65.

Wilson SD and Tilman D. 1993. Plant competition and resource availability in response to disturbance and fertilization. *Ecology* **74**: 599–611.

Wolt JD. 2004. A meta-evaluation of nitrapyrin agronomic and environmental effectiveness with emphasis on corn production in the Midwestern USA. *Nutr Cycl Agroecosystems* **69**: 23–41.

Wootton JT. 1991. Direct and indirect effects of nutrients on intertidal community structure: variable consequences of seabird guano. *J Exp Mar Biol Ecol* **151**: 139–53.

Wootton JT. 1994. Predicting Direct and Indirect Effects: An Integrated Approach Using Experiments and Path Analysis. *Ecology* **75**: 151–65.

Worm B, Barbier EB, Beaumont N, *et al.* 2006. Impacts of biodiversity loss on ocean ecosystem services. *Science* **314**: 787–90.

Worm B, Lotze HK, and Sommer U. 2000. Coastal food web structure, carbon storage, and nitrogen retention regulated by consumer pressure and nutrient loading. *Limnol Oceanogr* **45**: 339–49.

Zehr JP and Kudela RM. 2011. Nitrogen Cycle of the Open Ocean: From Genes to Ecosystems. *Annu Rev Mar Sci* **3**: 197–225.

Zhang L, Altabet MA, Wu T, and Hadas O. 2007. Sensitive measurement of NH4+ 15N/14N (δ15NH4+) at natural abundance levels in fresh and saltwaters. *Anal Chem* **79**: 5297–303.

Zumft WG. 1997. Cell biology and molecular basis of denitrification. *Microbiol Mol Biol Rev* **61**: 533–616.